

# 6

## POLARIZATION AND MODULATION OF LIGHT

### 6.1 POLARIZATION

#### A. State of Polarization

A propagating electromagnetic (EM) wave has its electric and magnetic fields at right angles to the direction of propagation. If we place a  $z$ -axis along the direction of propagation, then the electric field can be in any direction in the plane perpendicular to the  $z$ -axis. The term **polarization** of an EM wave describes the behavior of the electric field vector in the EM wave as it propagates through a medium. If the oscillations of the electric field at a given point at all times are contained within a well-defined line, then the EM wave is said to be **linearly polarized** as shown in Figure 6.1 (a). The field oscillations and the direction of propagation ( $z$ ) define a plane of polarization (plane of oscillation) so that linear polarization implies a wave that is **plane-polarized**. By contrast, if a beam of light has waves with the  $E$ -field in each wave in a random direction perpendicular to  $z$ , then this light beam is *unpolarized*. A light beam can be linearly polarized by passing the beam through a polarizer, such as a polaroid sheet, a device that only passes electric field oscillations lying on a well-defined plane at right angles to the direction of propagation.

Suppose that we arbitrarily place  $x$ - and  $y$ -axes, and describe the electric field in terms of its components  $E_x$  and  $E_y$  along  $x$  and  $y$ , as defined by an observer receiving the EM wave;  $x$  and  $y$  are perpendicular to each other and the direction of propagation<sup>1</sup> as in Figure 6.1 (a). To find the electric field in the wave at any space and time location, we add  $E_x$  and  $E_y$  *vectorially*. Both  $E_x$  and  $E_y$  can individually be described by a wave equation, which must have the same angular frequency  $\omega$  and propagation constant  $k$ . However, we must include a phase difference  $\phi$  between the two

$$E_x = E_{xo}\cos(\omega t - kz) \quad (6.1.1)$$

and

$$E_y = E_{yo}\cos(\omega t - kz + \phi) \quad (6.1.2)$$

---

<sup>1</sup>The directions of  $x$ - and  $y$ -axes are taken as they would be drawn by an observer receiving the light wave. In this case, the observer ignores the rigid Cartesian directions, which would make the  $x$ -axis point to the left not right in Figure 6.1 (a). The definitions and discussions that follow are actually unaffected by the choice of  $x$  and  $y$  in Figure 6.1 (a).

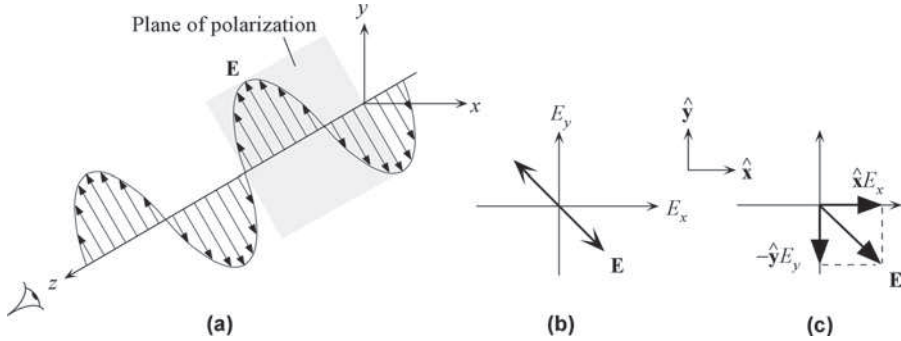


**FIGURE 6.1** (a) A linearly polarized wave has its electric field oscillations defined along a line perpendicular to the direction of propagation,  $z$ . The field vector  $E$  and  $z$  define a plane of polarization. (b) The  $E$ -field oscillations are contained in the plane of polarization. (c) A linearly polarized light at any instant can be represented by the superposition of two fields,  $E_x$  and  $E_y$ , with the right magnitude and phase.

where  $\phi$  is the phase difference between  $E_y$  and  $E_x$ . A phase difference  $\phi$  can arise if one of the components is delayed, and this delay is termed *retardation*.

The linearly polarized wave in Figure 6.1 (a) has the  $E$ -field oscillations at  $-45^\circ$  to the  $x$ -axis as shown in (b). We can generate this field by choosing  $E_{xo} = E_{yo}$  and  $\phi = \pm 180^\circ$  ( $\pm \pi$ ) in Eqs. (6.1.1) and (6.1.2). Put differently,  $E_x$  and  $E_y$  have the same magnitude but they are out of phase by  $180^\circ$ . If  $\hat{x}$  and  $\hat{y}$  are the unit vectors along  $x$  and  $y$ , using  $\phi = \pi$  in Eq. (6.1.2), the field in the wave is

$$\mathbf{E} = \hat{x}E_x + \hat{y}E_y = \hat{x}E_{xo}\cos(\omega t - kz) - \hat{y}E_{yo}\cos(\omega t - kz)$$

or

$$\mathbf{E} = \mathbf{E}_o\cos(\omega t - kz) \quad (6.1.3)$$

where

$$\mathbf{E}_o = \hat{x}E_{xo} - \hat{y}E_{yo} \quad (6.1.4)$$

Equation (6.1.4) describes the vector amplitude in Eq. (6.1.3), and shows that the vector  $\mathbf{E}_o$  is at  $-45^\circ$  to the  $x$ -axis. Equation (6.1.3) describes the propagation of this  $\mathbf{E}_o$  at  $-45^\circ$  along the  $z$ -direction.

There are many choices for the behavior of the electric field besides the simple linear polarization in Figure 6.1 (a). For example, if the magnitude of the field vector  $\mathbf{E}$  remains constant but its tip at a given location on  $z$  traces out a circle by rotating in a clockwise sense with time, as observed by the receiver of the wave, then the wave is said to be **right circularly polarized**,<sup>2</sup> as in Figure 6.2. If the rotation of the tip of  $\mathbf{E}$  is counterclockwise, the wave is said to be **left circularly polarized**. From Eqs. (6.1.1) and (6.1.2), it should be apparent that a right circularly polarized wave has  $E_{xo} = E_{yo} = A$  (an amplitude), and  $\phi = \pi/2$ . This means that

$$E_x = A\cos(\omega t - kz) \quad (6.1.5a)$$

<sup>2</sup>There is a difference in this definition in optics and engineering. The definition here follows that in optics, and it is also prevalent in optoelectronics.

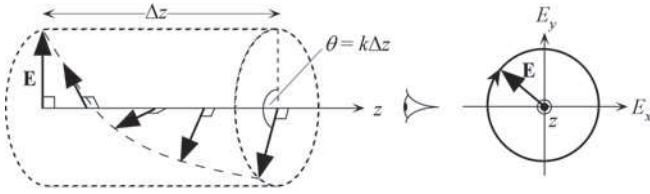


**FIGURE 6.2** A right circularly polarized light. The field vector  $\mathbf{E}$  is always at right angles to  $z$ , rotates clockwise around  $z$  with time, and traces out a full circle over one wavelength of distance propagated.

and

$$E_y = -A \sin(\omega t - kz) \quad (6.1.5b)$$

It is relatively straightforward to show Eqs. (6.1.5a) and (6.1.5b) represent a circle, that is,

$$E_x^2 + E_y^2 = A^2 \quad (6.1.6)$$

as shown in Figure 6.2.

The snapshot of the circularly polarized light in Figure 6.2 shows that over a distance  $\Delta z$ , the field  $\mathbf{E}$  rotates through an angle  $\theta = k\Delta z$ . Linear and circular polarization concepts are summarized in Figure 6.3, where, for simplicity,  $E_{y0} = 1$  has been taken and the corresponding  $E_{x0}$  and  $\phi$  are shown.

An **elliptically polarized**, or elliptic, light has the tip of the  $\mathbf{E}$ -vector trace out an ellipse as the wave propagates through a given location in space. As in circular polarization, light can

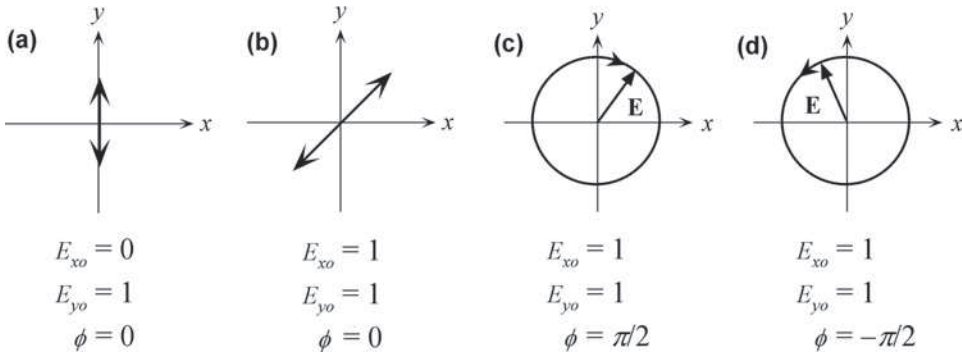


**FIGURE 6.3** (a) and (b) are examples of linearly polarized light. (c) and (d) are right circularly and left circularly polarized light, respectively (as seen when the wave directly approaches a viewer).

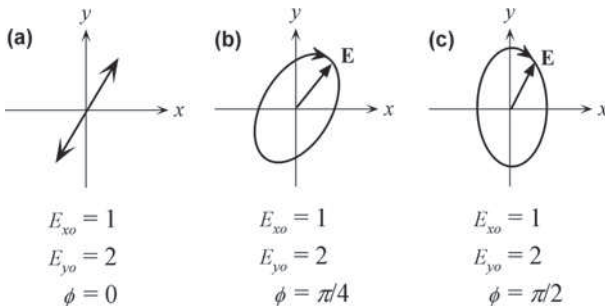


**FIGURE 6.4** (a) Linearly polarized light with  $E_{y0} = 2E_{x0}$  and  $\phi = 0$ . (b) When  $\phi = \pi/4$  ( $45^\circ$ ), the light is right elliptically polarized with a tilted major axis. (c) When  $\phi = \pi/2$  ( $90^\circ$ ), the light is right elliptically polarized. If  $E_{x0}$  and  $E_{y0}$  were equal, this would be right circularly polarized light.

be right and left elliptically polarized depending on clockwise or counterclockwise rotation of the **E**-vector.

Figure 6.4 illustrates how an elliptically polarized light can result for any  $\phi$  *not* equal to any multiple of  $\pi$ , and when  $E_{xo}$  and  $E_{yo}$  are not equal in magnitude. Elliptic light can also be obtained when  $E_{xo} = E_{yo}$  and the phase difference is  $\pm \pi/4$  or  $\pm 3\pi/4$ , *etc.*

### EXAMPLE 6.1.1 Elliptical and circular polarization

Show that if  $E_x = A \cos(\omega t - kz)$  and  $E_y = B \cos(\omega t - kz + \phi)$ , the amplitudes  $A$  and  $B$  are different and the phase difference  $\phi$  is  $\pi/2$ , the wave is elliptically polarized.

#### Solution

From the  $x$  and  $y$  components we have

$$\cos(\omega t - kz) = E_x/A$$

and

$$\cos(\omega t - kz + \pi/2) = -\sin(\omega t - kz) = E_y/B$$

Using  $\sin^2(\omega t - kz) + \cos^2(\omega t - kz) = 1$  we find,

$$\left(\frac{E_x}{A}\right)^2 + \left(\frac{E_y}{B}\right)^2 = 1$$

This is the equation that relates the instantaneous values  $E_x$  and  $E_y$  of the field along  $x$  and  $y$ . The equation is a *circle* when  $A = B$ , as in Figure 6.3 (c) and an *ellipse* when  $A \neq B$  as in Figure 6.4 (c).

Further, at  $z = 0$ , and at  $\omega t = 0$ ,  $E = E_x = A$ . Later when  $\omega t = \pi/2$ ,  $E = E_y = -B$ . Thus, the tip of the electric field rotates in a clockwise sense and the wave is right circularly polarized.

## B. Malus's Law

There are various optical devices that operate on the polarization state of a wave passing through it and thereby modify the polarization state. A linear polarizer will only allow electric field oscillations along some preferred direction, called the **transmission axis**, to pass through the device, as illustrated in Figure 6.5. A *polaroid sheet* is a good example of a commercially available linear polarizer. Dichroic crystals such as tourmaline crystals are good polarizers because they are optically anisotropic and attenuate EM waves with fields that are *not* oscillating parallel to a particular axis, called the transmission axis. The emerging beam from the polarizer has its field oscillations along the transmission axis and therefore it is *linearly polarized*; see Figure 6.5.

Suppose that the linearly polarized light from the polarizer is now incident on a second identical polarizer. Then, by rotating the transmission axis of this second polarizer we can analyze the polarization state of the incident beam; hence the second polarizer is called an **analyzer**. If the transmission axis of the second polarizer is at an angle  $\theta$  to the **E**-field of the incident beam (*i.e.*, to the first polarizer) then only the component  $E \cos \theta$  of the field will be allowed to pass through the analyzer. The irradiance (intensity) of light passing through the analyzer is proportional to the square of the electric field which means that the detected intensity varies as  $(E \cos \theta)^2$ . Since all the electric field will pass when  $\theta = 0$  (**E** parallel to **TA**<sub>2</sub>),

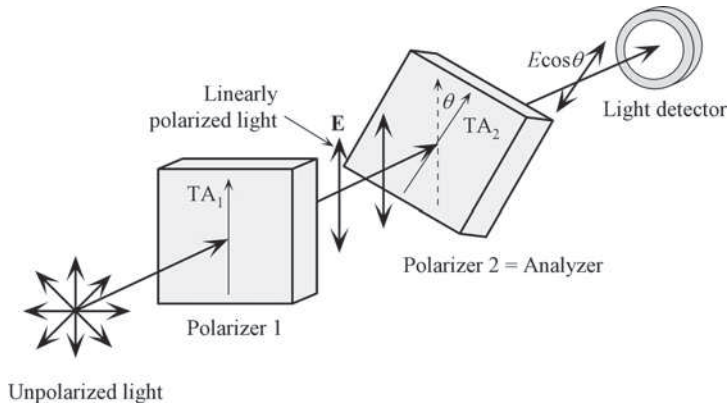


**FIGURE 6.5** Randomly polarized light is incident on Polarizer 1 with a transmission axis  $TA_1$ . Light emerging from Polarizer 1 is linearly polarized with  $E$  along  $TA_1$ , and becomes incident on Polarizer 2 (called the analyzer) with a transmission axis  $TA_2$  at an angle  $\theta$  to  $TA_1$ . A detector measures the intensity of the incident light.  $TA_1$  and  $TA_2$  are perpendicular to the light direction.

this is the maximum irradiance condition. The irradiance (or intensity)  $I$  at any other angle  $\theta$  is then given by **Malus's law**<sup>3</sup>

$$I(\theta) = I(0)\cos^2\theta \quad (6.1.7) \quad \text{Malus's law}$$

Malus's law therefore relates the intensity of a linearly polarized light passing through a polarizer to the angle between the transmission axis and the electric field vector.

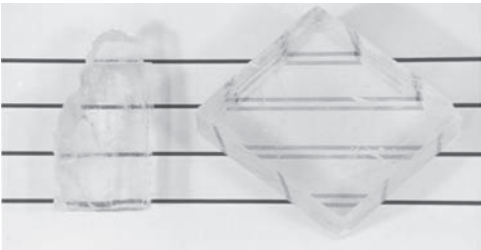
## 6.2 LIGHT PROPAGATION IN AN ANISOTROPIC MEDIUM: BIREFRINGENCE

### A. Optical Anisotropy

An important characteristic of crystals is that many of their properties depend on the crystal direction, that is, crystals are generally anisotropic. The dielectric constant  $\epsilon_r$  depends on electronic polarization, which involves the displacement of electrons with respect to positive atomic nuclei. Electronic polarization depends on the crystal direction inasmuch as it is easier to displace electrons along certain crystal directions. This means that *the refractive index  $n$  of a crystal depends on the direction of the electric field in the propagating light beam*. Consequently, the velocity of light in a crystal depends on the direction of propagation and on the state of its polarization, *i.e.*, the direction of the electric field. Most noncrystalline materials, such as glasses and liquids, and all cubic crystals are **optically isotropic**, that is, the refractive index is the same in all directions. For all classes of crystals excluding cubic structures, the refractive index depends on the propagation direction and the state of polarization. The result of optical anisotropy is that, except along certain special directions, any unpolarized light ray entering such a crystal breaks into two different rays with different polarizations and

<sup>3</sup> $I$  is used for the intensity in this chapter. Etienne-Louis Malus (1775–1812) was a French physicist and an engineer, who studied the polarization properties of light.

**FIGURE 6.6** A line viewed through a cubic sodium chloride (halite) crystal (optically isotropic) and a calcite crystal (optically anisotropic).



phase velocities. When we view an image through a calcite crystal, an optically anisotropic crystal, we see two images, each constituted by light of different polarization passing through the crystal, whereas there is only one image through an optically isotropic crystal as illustrated in Figure 6.6. Optically anisotropic crystals are called **birefringent** because an incident light beam may be *doubly refracted*. There is also a special direction in a birefringent crystal, called the **optic axis**, along which all waves with different polarizations experience the same refractive index or travel with the same phase velocity. A light entering a birefringent crystal along the optic axis does not experience double refraction. Depending on the crystal type, there may be one or two optic axes.

Experiments and theories on most anisotropic crystals, *i.e.*, those with the highest degree of anisotropy, show that we can describe light propagation in terms of *three* refractive indices, called **principal refractive indices**,  $n_1$ ,  $n_2$ , and  $n_3$ , along three mutually orthogonal directions in the crystal, say  $x$ ,  $y$ , and  $z$ , called *principal axes*. These indices correspond to the polarization state of the wave along these axes.

Crystals that have three distinct principal indices also have *two* optic axes and are called **biaxial crystals**. On the other hand, **uniaxial crystals** have two of their principal indices the same ( $n_1 = n_2$ ) and only have *one* optic axis. Table 6.1 summarizes crystal classifications according to optical anisotropy. Uniaxial crystals, such as quartz, that have  $n_3 > n_1$  are called **positive**, and those such as calcite that have  $n_3 < n_1$  are called **negative** uniaxial crystals.

**TABLE 6.1** Principal refractive indices of some optically isotropic and anisotropic crystals (near 589 nm, yellow Na-D line)

Optically isotropic		$n = n_o$		
	Glass (crown)	1.510		
	Diamond	2.417		
	Fluorite (CaF <sub>2</sub> )	1.434		
Uniaxial–Positive		$n_o$	$n_e$	
	Ice	1.309	1.3105	
	Quartz	1.5442	1.5533	
	Rutile (TiO <sub>2</sub> )	2.616	2.903	
Uniaxial–Negative		$n_o$	$n_e$	
	Calcite (CaCO <sub>3</sub> )	1.658	1.486	
	Tourmaline	1.669	1.638	
	Lithium niobate (LiNbO <sub>3</sub> )	2.29	2.20	
Biaxial		$n_1$	$n_2$	$n_3$
	Mica (muscovite)	1.5601	1.5936	1.5977

## B. Uniaxial Crystals and Fresnel's Optical Indicatrix

For our discussions of optical anisotropy, we will consider uniaxial crystals such as calcite and quartz. All experiments and theories lead to the following basic principles<sup>4</sup>

Any EM wave entering an anisotropic crystal splits into two orthogonal linearly polarized waves, which travel with different phase velocities, that is, they experience different refractive indices. These two orthogonally polarized waves in uniaxial crystals are called *ordinary* (*o*) and *extraordinary* (*e*) waves. The *o*-wave has the same phase velocity in all directions and behaves like an ordinary wave in which the field is perpendicular to the phase propagation direction. The *e*-wave has a phase velocity that depends on its direction of propagation and its state of polarization; and the electric field in the *e*-wave is not necessarily perpendicular to the phase propagation direction. These two waves propagate with the same velocity only along a special direction called the **optic axis**. The *o*-wave is always perpendicularly polarized to the optic axis and obeys the usual Snell's law.

The two images observed in Figure 6.6 are due to *o*-waves and *e*-waves being refracted differently so that when they emerge from the crystal they have been separated. Each ray constitutes an image but the optical field directions are orthogonal. This is easily demonstrated by using two polaroid analyzers with their transmission axes at right angles as in Figure 6.7. If we were to view an object along the optic axis of the crystal, we would not see two images because the two rays would experience the same refractive index.

As mentioned above, we can represent the optical properties of a crystal in terms of three refractive indices along three orthogonal axes, the principal axes of the crystal, shown as *x*, *y*, and *z* in Figure 6.8 (a). These are special axes along which the polarization vector and the electric field are parallel. (Put differently, the electric displacement<sup>5</sup> **D** and the electric field **E** vectors are parallel.) The refractive indices along these *x*-, *y*-, and *z*-axes are the principal indices  $n_1$ ,  $n_2$ ,

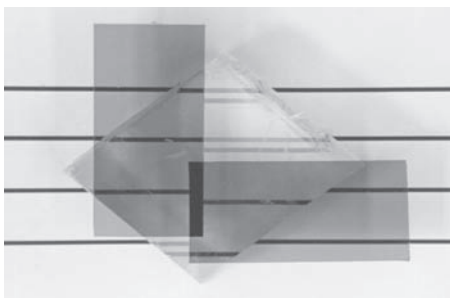


**FIGURE 6.7** Two polaroid analyzers are placed with their transmission axes, along the long edges, at right angles to each other. The ordinary ray, undeflected, goes through the left polarizer, whereas the extraordinary wave, deflected, goes through the right polarizer. The two waves therefore have orthogonal polarizations.

<sup>4</sup>These statements can be proved by solving Maxwell's equations in an anisotropic medium. The discussion of light wave propagation in anisotropic media invariably involves dealing with the displacement vector **D**, which is not always covered in undergraduate curricula.

<sup>5</sup>Electric displacement **D** at any point is defined by  $\mathbf{D} = \epsilon_0 \mathbf{E} + \mathbf{P}$  where **E** is the electric field and **P** is the polarization at that point. In many of the discussions in this chapter we will simply ignore the angle between the electric field **E** and **D**. A readable treatment of EM wave propagation in anisotropic media can be found in G. R. Fowles, *Introduction to Modern Optics*, 2nd Edition (Dover Publications, 1975), Ch. 6.

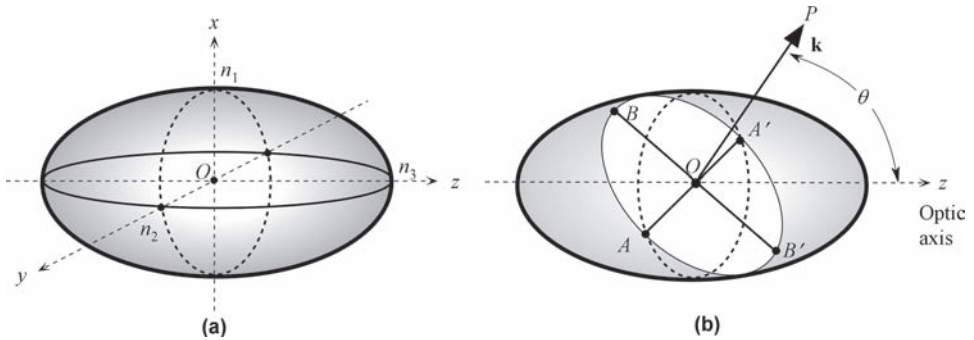


**FIGURE 6.8** (a) Fresnel's ellipsoid (for  $n_1 = n_2 < n_3$ ; quartz). (b) An EM wave propagating along  $OP$  at an angle  $\theta$  to the optic axis.

and  $n_3$ , respectively, for electric field oscillations along these directions (not to be confused with the wave propagation direction). For example, for a wave with a polarization parallel to the  $x$ -axis, the refractive index is  $n_1$ .

The refractive index associated with a particular EM wave in a crystal can be determined by using Fresnel's *refractive index ellipsoid*, called the **optical indicatrix**,<sup>6</sup> which is a refractive index surface placed in the center of the principal axes, as shown in Figure 6.8 (a), where the  $x$ -,  $y$ -, and  $z$ -axes have intercepts  $n_1$ ,  $n_2$ , and  $n_3$ , respectively. If all three indices were the same,  $n_1 = n_2 = n_3 = n_o$ , we would have a spherical surface and all electric field polarization directions would experience the same refractive index  $n_o$ . Such a spherical surface would represent an optically isotropic crystal. For positive uniaxial crystals such as quartz,  $n_1 = n_2 < n_3$ , which is the example in Figure 6.8 (a).

Suppose that we wish to find the refractive indices experienced by a wave traveling with an arbitrary wave vector  $\mathbf{k}$ , which represents the direction of phase propagation. This phase propagation direction is shown as  $OP$  in Figure 6.8 (b) and is at an angle  $\theta$  to the  $z$ -axis. We place a plane perpendicular to  $OP$  and passing through the center  $O$  of the indicatrix. This plane intersects the ellipsoid surface in a curve  $ABA'B'$  which is an *ellipse*. The major ( $BOB'$ ) and minor ( $AOA'$ ) axes of this ellipse determine the field oscillation directions and the refractive indices associated with this wave. Put differently, the original wave is now represented by two orthogonally polarized EM waves.

The line  $AOA'$ , the *minor axis*, corresponds to the polarization of the ordinary wave, and its semiaxis  $OA$  is the refractive index  $n_o = n_2$  of this  $o$ -wave. The electric displacement and the electric field are in the same direction and parallel to  $AOA'$ . If we were to change the direction of  $OP$ , we would always find the same minor axis, *i.e.*,  $n_o$  is either  $n_1$  or  $n_2$  whatever the orientation of  $OP$  (try orientating  $OP$  to be along  $y$  and along  $x$ ). Since  $n_1 = n_2$  for uniaxial crystals [Figure 6.8 (a)], this means that the  $o$ -wave always experiences the same refractive index in all directions. The  $o$ -wave behaves just like an ordinary wave (hence the name).

The line  $BOB'$  in Figure 6.8 (b), the *major axis*, corresponds to the electric displacement field ( $\mathbf{D}$ ) oscillations in the extraordinary wave and its semiaxis  $OB$  is the refractive index  $n_e(\theta)$  of this  $e$ -wave traveling along  $OP$  at an angle  $\theta$  to  $z$ . This refractive index is smaller than  $n_3$  but greater than

<sup>6</sup>There are various names in the literature with various subtle nuances: the *Fresnel ellipsoid*, *optical indicatrix*, *index ellipsoid*, *reciprocal ellipsoid*, *Poinsot ellipsoid*, *ellipsoid of wave normals*.



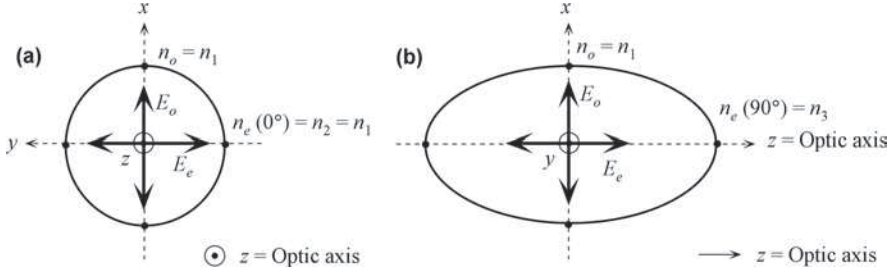


**FIGURE 6.9**  $E_o = E_o$ -wave and  $E_e = E_e$ -wave. (a) Wave propagation along the optic axis. (b) Wave propagation normal to optic axis.

$n_2(=n_o)$ . The  $e$ -wave therefore travels more slowly than the  $o$ -wave in this particular direction and in this crystal. If we change the direction of  $OP$ , we find that the length of the major axis changes with the  $OP$  direction. Thus,  $n_e(\theta)$  depends on the wave direction,  $\theta$ . As apparent,  $n_e = n_o$  when  $OP$  is along the  $z$ -axis, that is, when the wave is traveling along  $z$  as in Figure 6.9 (a). This direction is the **optic axis** and all waves traveling along the optic axis have the same phase velocity whatever their polarization. When the  $e$ -wave is traveling along the  $y$ -axis or along the  $x$ -axis,  $n_e(\theta) = n_3 = n_e$  and the  $e$ -wave has its slowest phase velocity as shown in Figure 6.9 (b). Along any  $OP$  direction that is at an angle  $\theta$  to the optic axis, the  $e$ -wave has a refractive index  $n_e(\theta)$  given by

$$\frac{1}{n_e(\theta)^2} = \frac{\cos^2\theta}{n_o^2} + \frac{\sin^2\theta}{n_e^2} \quad (6.2.1)$$

Refractive  
index  
of the  
 $e$ -wave

Clearly, for  $\theta = 0^\circ$ ,  $n_e(0^\circ) = n_o$  and for  $\theta = 90^\circ$ ,  $n_e(90^\circ) = n_e$ .

The major axis  $BOB'$  in Figure 6.8 (b) determines the  $e$ -wave polarization by defining the direction of the displacement vector  $\mathbf{D}$  and not  $\mathbf{E}$ . Although  $\mathbf{D}$  is perpendicular to  $\mathbf{k}$ , this is not true for  $\mathbf{E}$ . The electric field of the  $e$ -wave is orthogonal to that of the  $o$ -wave and it is in the plane determined by  $\mathbf{k}$  and the optic axis, as discussed below.  $\mathbf{E}$  is orthogonal to  $\mathbf{k}$  when the  $e$ -wave propagates along one of the principal axes.

From the indicatrix, or equivalently from Eq. (6.2.1), we can easily determine the refractive indices of the  $o$ - and  $e$ -waves in any direction and thereby calculate their wave vectors. We can then construct a **wave vector surface** for all the  $o$  and  $e$ -waves in the crystal, as shown for a particular cross-section in Figure 6.10 (a). The distance from the origin  $O$  to any arbitrary point  $P$  on a wave vector surface represents the value of  $\mathbf{k}$  along the direction  $OP$ . Since the  $o$ -wave has the same refractive index in all directions, its wave vector surface will be a sphere of radius  $n_o k_{\text{vacuum}}$ , where  $k_{\text{vacuum}}$  is the wave vector in free space. This is shown as a circle in an “ $xz$ ” cross-section in Figure 6.10 (a). On the other hand, the wave vector of the  $e$ -wave depends on the propagation direction and is given by  $n_e(\theta)k_{\text{vacuum}}$  so its surface is an ellipse in the “ $xz$ ” cross-section in Figure 6.10 (a). Two example wave vectors  $\mathbf{k}_o$  and  $\mathbf{k}_e$  that represent an  $o$ -wave and an  $e$ -wave propagating along arbitrary directions  $OP$  and  $OQ$ , respectively, are illustrated in Figure 6.10 (a) (different directions chosen only for clarity).

The electric field  $\mathbf{E}_o$  of the  $o$ -wave is always orthogonal to its wave vector direction  $\mathbf{k}_o$  and also to the optic axis. This fact is shown as dots on the  $o$ -wave wave vector surface in Figure 6.10 (a) and is highlighted for an arbitrary  $\mathbf{k}_o$  along  $OP$ . Since the electric and magnetic fields in the  $o$ -wave are normal to  $\mathbf{k}_o$ , the  $o$ -wave Poynting vector  $\mathbf{S}_o$ , i.e., the direction of energy flow, is along  $\mathbf{k}_o$ .

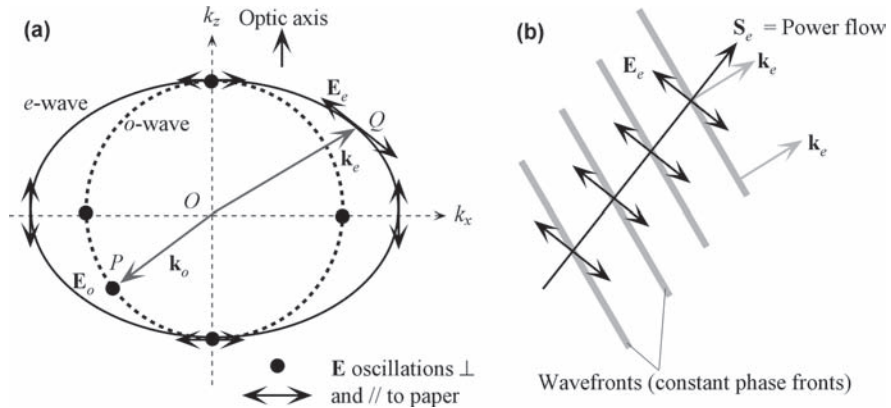


**FIGURE 6.10** (a) Wave vector surface cuts in the  $xz$  plane for  $o$ - and  $e$ -waves. (b) An extraordinary wave in an anisotropic crystal with a  $\mathbf{k}_e$  at an angle to the optic axis. The electric field is not normal to  $\mathbf{k}_e$ . The energy flow (group velocity) is along  $\mathbf{S}_e$ , which is different than  $\mathbf{k}_e$ .

It may be thought that, as in normal EM wave propagation, *i.e.*, as in the  $o$ -wave, the electric field  $\mathbf{E}_e$  in the  $e$ -wave should be normal to the wave vector  $\mathbf{k}_e$ . This is not generally true. The reason is that the polarization of the medium is not parallel to the inducing field in the  $e$ -wave and consequently, the overall electric field  $\mathbf{E}_e$  in the EM wave is *not* at right angles to the phase propagation direction  $\mathbf{k}_e$  as indicated in Figure 6.10 (a). This means that the energy flow (group velocity) and the phase velocity directions are different (a phenomenon called the Poynting vector “walk-off” effect). The energy flow, *i.e.*, the Poynting vector  $\mathbf{S}_e$ , direction is taken as the **ray direction** for the  $e$ -wave so that the wavefronts advance “sideways” as illustrated in Figure 6.10 (b). The group velocity is in the same direction as energy flow ( $\mathbf{S}_e$ ).

### C. Birefringence of Calcite

Consider a calcite crystal ( $\text{CaCO}_3$ ) which is a negative uniaxial crystal and also well-known for its double refraction. When the surfaces of a calcite crystal have been cleaved, *i.e.*, cut along certain crystal planes, the crystal attains a shape that is called a *cleaved form* and the crystal faces are rhombohedrons (parallelogram with angles  $78.08^\circ$  and  $101.92^\circ$ ). A cleaved form of the crystal is called a **calcite rhomb**. A plane of the calcite rhomb that contains the optic axis and is normal to a pair of opposite crystal surfaces is called a **principal section**.

Consider what happens when an unpolarized or natural light enters a calcite crystal at normal incidence and thus also normal to a principal section to this surface, but at an angle to the optic axis as shown in Figure 6.11. The ray breaks into ordinary ( $o$ ) and extraordinary ( $e$ ) waves with mutually orthogonal polarizations. The waves propagate in the plane of the principal section, as this plane also contains the incident light. The  $o$ -wave has its field oscillations perpendicular to the optic axis. It obeys Snell’s law, which means that it enters the crystal undeflected. Thus the direction of  $E$ -field oscillations must come out of the paper so that it is normal to the optic axis and also to the direction of propagation. The field  $E_\perp$  in the  $o$ -ray is shown as dots, oscillating into and out of the paper.

The  $e$ -wave has a polarization orthogonal to the  $o$ -wave and in the principal section (which contains the optic axis and  $\mathbf{k}$ ). The  $e$ -wave polarization is in the plane of the paper, indicated as  $E_\parallel$ , in Figure 6.11. It travels with a different velocity and diverges from the  $o$ -wave.

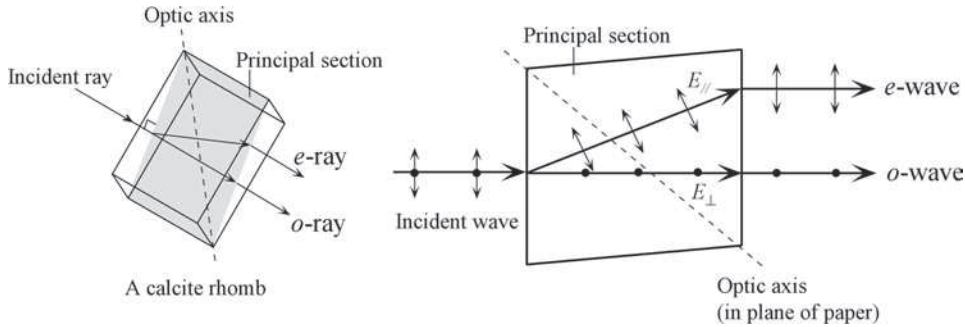


**FIGURE 6.11** An EM wave that is off the optic axis of a calcite crystal splits into two waves called ordinary and extraordinary waves. These waves have orthogonal polarizations and travel with different velocities. The *o*-wave has a polarization that is always perpendicular to the optical axis.

Clearly, the *e*-wave does not obey the usual Snell's law inasmuch as the angle of refraction is not zero. We can determine the *e*-ray direction by noting that the *e*-wave propagates sideways as in Figure 6.10 (b) at right angles to  $E_{\parallel}$ .

If we were to cut a plate from a calcite crystal so that the optic axis (along  $z$ ) would be parallel to two opposite faces of the plate as in Figure 6.12 (a), then a ray entering at normal incidence to one of these faces would not diverge into two separate waves. This is the case illustrated in Figure 6.9 (b), that is, propagation along the  $y$ -direction, except now  $n_e < n_o$ . The *o*- and *e*-waves would travel in the same direction but with different speeds. The waves emerge in the same direction as well, which means that we would not see double refraction. This optical arrangement is used in the construction of various optical retarders and polarizers as discussed below. If we were to cut a plate so that the optic axis was perpendicular to the plate faces as in Figure 6.12 (b), then both the *o*- and *e*-waves would be traveling at the same speed [Figure 6.9 (a)] and along the same direction, which means we would not again see any double refraction.

## D. Dichroism

In addition to the variation in the refractive index, some anisotropic crystals also exhibit **dichroism**, a phenomenon in which the optical absorption in a substance depends on the direction of propagation and the state of polarization of the light beam. A dichroic crystal is an optically anisotropic crystal in which either the *e*-wave or the *o*-wave is heavily attenuated (absorbed). This means that a

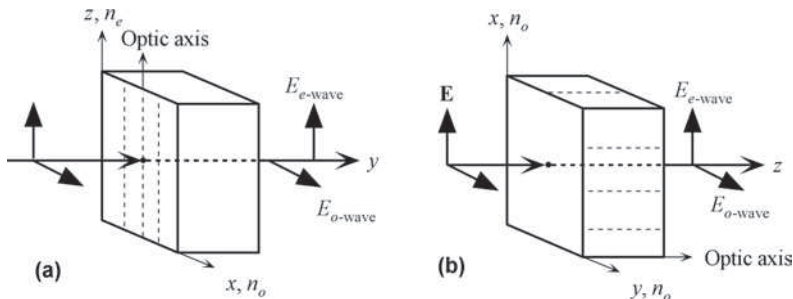


**FIGURE 6.12** (a) A birefringent crystal plate with the optic axis parallel to the plate surfaces. (b) A birefringent crystal plate with the optic axis perpendicular to the plate surfaces.

light wave of arbitrary polarization entering a dichroic crystal emerges with a well-defined polarization because the other orthogonal polarization would have been attenuated. Generally, dichroism depends on the wavelength of light. For example, in a tourmaline (aluminum borosilicate) crystal, the  $o$ -wave is much more heavily absorbed with respect to the  $e$ -wave.

### 6.3 BIREFRINGENT OPTICAL DEVICES

#### A. Retarding Plates

Consider a positive uniaxial crystal plate, such as a quartz ( $n_e > n_o$ ) plate, that has the optic axis (taken along  $z$ ) parallel to the plate faces as in Figure 6.13. Suppose that a *linearly polarized* wave is incident at normal incidence on a plate face. If the field  $\mathbf{E}$  is parallel to the optic axis (shown as  $E_{\parallel}$ ), then this wave will travel through the crystal as an  $e$ -wave with a velocity  $c/n_e$  slower than the  $o$ -wave, since  $n_e > n_o$ . Thus, the optic axis is the “slow axis” for waves polarized parallel to it. If  $\mathbf{E}$  is at right angles to the optic axis (shown as  $E_{\perp}$ ), then this wave will travel with a velocity  $c/n_o$ , which will be the fastest velocity in the crystal. Thus, the axis perpendicular to the optic axis (say  $x$ ) will be the “fast axis” for polarization along this direction. When a light ray enters a crystal at normal incidence to the optic axis and plate surface, as in Figure 6.12 (a), then the  $o$ - and  $e$ -waves travel along the same direction as shown in Figure 6.13. We can of course resolve a linear polarization at an angle  $\alpha$  to  $z$  into  $E_{\perp}$  and  $E_{\parallel}$ . When the light comes out at the opposite face, these two components would have been phase shifted by  $\phi$ . Depending on the initial angle  $\alpha$  of  $\mathbf{E}$  and the length of the crystal, which determines the total phase shift  $\phi$  through the plate, the emerging beam can have its initial linear polarization rotated, or changed into an elliptically or circularly polarized light as summarized in Figure 6.14.

If  $L$  is the thickness of the plate then the  $o$ -wave experiences a phase change  $k_{o\text{-wave}}L$  through the plate, where  $k_{o\text{-wave}}$  is the wave vector of the  $o$ -wave:  $k_{o\text{-wave}} = (2\pi/\lambda)n_o$ , where  $\lambda$  is the free-space wavelength. Similarly, the  $e$ -wave experiences a phase change  $(2\pi/\lambda)n_eL$  through the plate. Thus, the phase difference  $\phi$  between the orthogonal components  $E_{\perp}$  and  $E_{\parallel}$  of the emerging beam is

$$\phi = \frac{2\pi}{\lambda}(n_e - n_o)L \quad (6.3.1)$$

The phase difference  $\phi$  expressed in terms of full wavelengths is called the **retardation** of the plate. For example, a phase difference  $\phi$  of  $180^\circ$  is a half-wavelength retardation.

The polarization of the through beam depends on the crystal type ( $n_e - n_o$ ), and the plate thickness  $L$ . We know that, depending on the phase difference  $\phi$  between the orthogonal

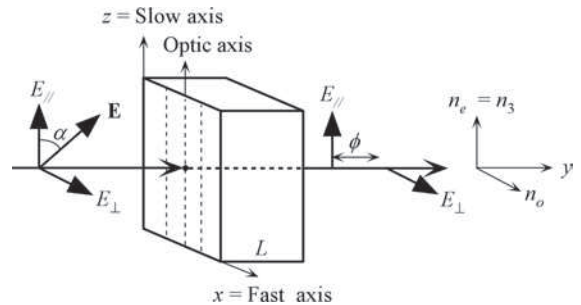


**FIGURE 6.13** A retarder plate. The optic axis is parallel to the plate face. The  $o$ - and  $e$ -waves travel in the same direction but at different speeds.

Relative  
phase  
through  
retarder  
plate

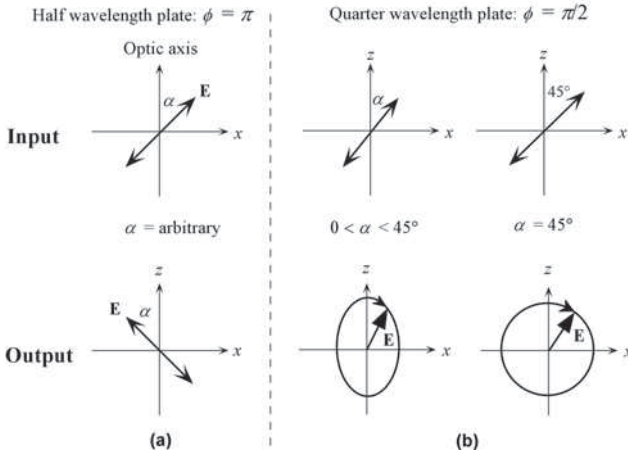


**FIGURE 6.14** Input and output polarizations of light through (a) a half-wavelength plate and (b) through a quarter-wavelength plate.

components of the field, the EM wave can be linearly, circularly, or elliptically polarized as in Figure 6.4.

A **half-wave plate retarder** has a thickness  $L$  such that the phase difference  $\phi$  is  $\pi$  or  $180^\circ$ , corresponding to a half of wavelength ( $\lambda/2$ ) of retardation. The result is that  $E_{\parallel}$  is delayed by  $180^\circ$  with respect to  $E_{\perp}$ . If we add the emerging  $E_{\perp}$  and  $E_{\parallel}$  with this shift  $\phi$ ,  $\mathbf{E}$  would be at an angle  $-\alpha$  to the optic axis and still linearly polarized.  $\mathbf{E}$  has been rotated counterclockwise through  $2\alpha$  as shown in Figure 6.14 (a).

A **quarter-wave plate retarder** has a thickness  $L$  such that the phase difference  $\phi$  is  $\pi/2$  or  $90^\circ$ , corresponding to a quarter of wavelength. If we add the emerging  $E_{\perp}$  and  $E_{\parallel}$  with this shift  $\phi$ , the emerging light will be elliptically polarized if  $0 < \alpha < 45^\circ$  and circularly polarized if  $\alpha = 45^\circ$  as illustrated in Figure 6.14 (b).

### EXAMPLE 6.3.1 Quartz half-wave plate

What should be the thickness of a half-wave quartz plate for a wavelength  $\lambda \approx 590 \text{ nm}$  given the ordinary and extraordinary refractive indices in Table 6.1?

#### Solution

Half-wavelength retardation is a phase difference of  $\pi$  so that from Eq. (6.3.1)

$$\phi = \frac{2\pi}{\lambda}(n_e - n_o)L = \pi$$

giving,

$$L = \frac{\frac{1}{2}\lambda}{(n_e - n_o)} = \frac{\frac{1}{2}(590 \times 10^{-9} \text{ m})}{(1.5533 - 1.5442)} = 32.4 \text{ } \mu\text{m}$$

If we were to repeat the calculation for calcite, we would find about  $1.7 \text{ } \mu\text{m}$  thickness, which is not very practical. Typically mica, quartz, or polymeric substances are used as retarder plates because they have a  $(n_e - n_o)$  difference that is not too large to result in an impractical thickness.

**EXAMPLE 6.3.2 Circular polarization from linear polarization**

Consider a linearly polarized light that is incident on a quarter-wavelength plate as in Figure 6.13, such that the polarization is  $45^\circ$  to the slow axis. Show that the output beam is circularly polarized.

**Solution**

Both the  $x$  and  $z$  components of the electric field emerging from the retarder plate in Figure 6.13 are propagating along the  $y$ -axis with the same  $\cos(\omega t - ky)$  harmonic term after emerging from the crystal but with a phase difference  $\phi$ . We are only interested in adding  $E_x$  and  $E_z$  vectorially at one location so that we can neglect the  $ky$  phase term. We can write the field components along fast ( $x$ ) and slow ( $z$ ) axes as

$$E_x = E_{\perp} \cos(\omega t) \quad E_z = E_{\parallel} \cos(\omega t - \phi)$$

When the incident polarization is at  $45^\circ$ , then  $E_{\parallel} = E_{\perp} = E_o$ . Putting  $\phi = \pi/2$  for a quarter-wave plate, using  $\cos(\omega t - \pi/2) = \sin(\omega t)$ , and then  $\sin^2(\omega t) + \cos^2(\omega t) = 1$ , we find

$$\cos^2(\omega t) + \sin^2(\omega t) = \left(\frac{E_x}{E_o}\right)^2 + \left(\frac{E_z}{E_o}\right)^2 = 1$$

which is the equation of a circle on the  $E_x$  and  $E_z$  axes [Figure 6.14 (b)] with a radius  $E_o$ .

**B. Soleil–Babinet Compensator**

An optical compensator is a device that allows one to control the retardation (*i.e.*, the phase change) of a wave passing through it. In a wave plate retarder such as the half-wave plate, the relative phase change  $\phi$  between the ordinary and extraordinary waves depends on the plate thickness and cannot be changed. In compensators,  $\phi$  is adjustable. The Soleil–Babinet compensator described below is one such optical device that is widely used for controlling and analyzing the polarization state of light.

Consider the optical structure illustrated in Figure 6.15 which has two quartz wedges touching over their large faces to form a “block” of adjustable height  $d$ . Sliding one wedge over the other wedge alters the “thickness”  $d$  of this block. The two-wedge block is placed on a parallel plate quartz slab with a fixed thickness  $D$ . The slab has its optic axis parallel to its surface face. The optic axes in the wedges are parallel but perpendicular to the optic axis of the slab, as indicated in the figure.

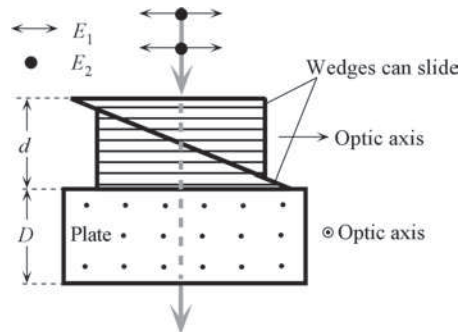


**FIGURE 6.15** Soleil–Babinet compensator.



A Soleil-Babinet compensator. (Courtesy of Thorlabs.)



A Wollaston prism. The actual prism is held inside a cylindrical housing. (Courtesy of Thorlabs.)

Suppose that a linearly polarized light is incident on this compensator at normal incidence. We can represent this light by field oscillations parallel and perpendicular to the optic axis of the two-wedge block; these fields are  $E_1$  and  $E_2$ , respectively. The polarization  $E_1$  travels through the wedges ( $d$ ) experiencing a refractive index  $n_e$  ( $E_1$  is along the optic axis) and then travels through the plate ( $D$ ) experiencing an index  $n_o$  ( $E_1$  is perpendicular to the optic axis). Its phase change is

$$\phi_1 = \frac{2\pi}{\lambda}(n_e d + n_o D)$$

But the  $E_2$ -polarization wave first experiences  $n_o$  through the wedges ( $d$ ) and then  $n_e$  through the plate ( $D$ ) so that its phase change is

$$\phi_2 = \frac{2\pi}{\lambda}(n_o d + n_e D)$$

The phase difference  $\phi (= \phi_2 - \phi_1)$  between the two polarizations is

$$\phi = \frac{2\pi}{\lambda}(n_e - n_o)(D - d) \quad (6.3.2) \quad \text{Soleil-Babinet compensator}$$

It is apparent that, as we can change  $d$  continuously by sliding the wedges (by using a micrometer screw), we can continuously alter the phase difference  $\phi$  from 0 to  $2\pi$ . We can therefore produce a quarter-wave or half-wave plates by simply adjusting this compensator. It should be emphasized that this control occurs over the surface region that corresponds to both the wedges in contact, and in practice this is a narrow region.

### C. Birefringent Prisms

Prisms made from birefringent crystals are useful for producing a highly polarized light wave or polarization splitting of light. The **Wollaston prism** is a polarization splitter in which the split beam has orthogonal polarizations. Two calcite (with  $n_e < n_o$ ) right-angle prisms  $A$  and  $B$  are placed with their diagonal faces touching to form a rectangular block as shown in Figure 6.16. Looking at the cross-section of this block, the optic axis in  $A$  is in the plane of the paper, whereas that in  $B$  comes out of the paper; the two prisms have their optic axes mutually orthogonal. Further, as shown, the optic axes are parallel to the prism sides.



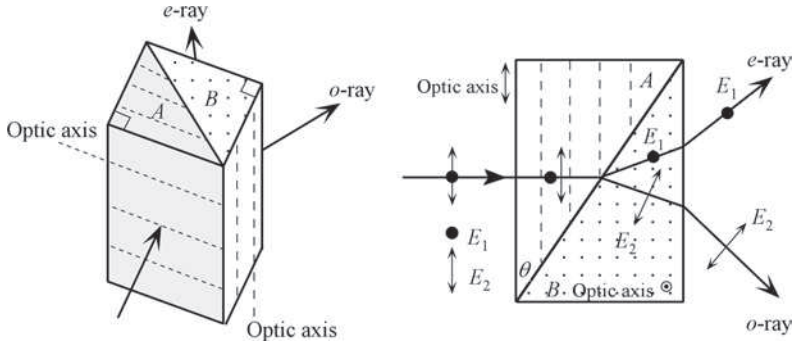


**FIGURE 6.16** The Wollaston prism is a beam polarization splitter.  $E_1$  is orthogonal to the plane of the paper and also to the optic axis of the first prism.  $E_2$  is in the plane of the paper and orthogonal to  $E_1$ . Notice that, in prism A,  $E_1$  is the  $o$ -wave and  $E_2$  is the  $e$ -wave. However, in prism B,  $E_1$  is the  $e$ -wave and  $E_2$  is the  $o$ -wave.

Consider a light wave of arbitrary polarization at normal incidence to prism A. The light beam entering prism A travels in this prism as two orthogonally polarized waves that have fields  $E_1$  and  $E_2$  as in Figure 6.16.  $E_1$  (normal to the plane of paper) is orthogonal to the optic axis and corresponds to  $o$ -waves in A.  $E_2$  (in the plane of the paper) is along the optic axis of A and corresponds to the  $e$ -waves.  $E_1$  has a refractive index  $n_o$  and  $E_2$  has  $n_e$ . However, in prism B,  $E_1$  is the  $e$ -wave. This means that in going through the diagonal interface,  $E_1$  experiences a *decrease* from  $n_o$  to  $n_e$ . On the other hand, the  $e$ -wave in A becomes the  $o$ -wave in B and experiences an *increase* from  $n_e$  to  $n_o$ . Notice that  $E_2$  is now orthogonal to the optic axis in B. These refractive index changes are opposite, which means that the two waves are refracted in opposite directions at the interface, as shown in Figure 6.16. The  $E_1$ -wave moves away from the normal to the diagonal face whereas the  $E_2$ -wave moves closer to this normal. The two orthogonal polarizations are therefore angularly separated out by these oppositely sensed refractions. The divergence angle depends on the prism wedge angle  $\theta$ . Various Wollaston prisms with typical beam splitting angles of 15–45° are commercially available. It is left as an exercise to show that if we rotate the prism about the incident beam by 180°, we would see the two orthogonal polarizations  $E_1$  and  $E_2$  have switched places, and if we use a quartz Wollaston prism, we would find  $E_1$  and  $E_2$  in the figure are again switched.

## 6.4 OPTICAL ACTIVITY AND CIRCULAR BIREFRINGENCE

When a linearly polarized light wave is passed through a quartz crystal along its optic axis, it is observed that the emerging wave has its **E**-vector (plane of polarization) rotated, which is illustrated in Figure 6.17. This rotation increases continuously with the distance traveled through the crystal (about 21.7° per mm of quartz). The rotation of the plane of polarization by a substance is called **optical activity**. In very simple intuitive terms, optical activity occurs in materials in which the electron motions induced by the external electromagnetic field follow spiraling or helical paths (orbits).<sup>7</sup> Electrons flowing in helical paths resemble a current flowing in a coil and thus possess a magnetic moment. The optical field in the light therefore induces

<sup>7</sup>The explanation of optical activity involves examining both induced magnetic and electric dipole moments which will not be described here in detail. See Eugene Hecht, *Optics*, 4th Edition (Addison Wesley, Pearson Education, 2002), Section 8.10, for the discussion of optical activity and the derivation of Eq. (6.4.1).



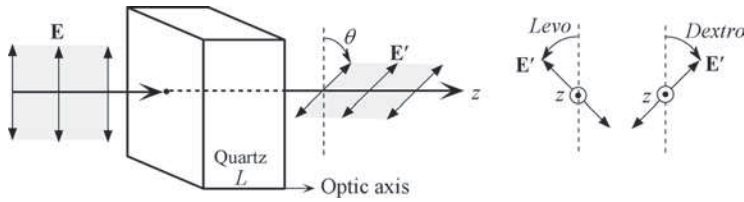


**FIGURE 6.17** An optically active material such as quartz rotates the plane of polarization of the incident wave: The optical field  $\mathbf{E}$  rotates to  $\mathbf{E}'$ . If we reflect the wave back into the material,  $\mathbf{E}'$  rotates back to  $\mathbf{E}$ .

oscillating magnetic moments which can be either parallel or antiparallel to the induced oscillating electric dipoles. Wavelets emitted from these oscillating induced magnetic and electric dipoles interfere to constitute a forward wave that has its optical field rotated either clockwise or counterclockwise.

If  $\theta$  is the angle of rotation, then  $\theta$  is proportional to the distance  $L$  propagated in the optically active medium, as illustrated in Figure 6.17. For an observer receiving the wave through quartz, the rotation of the plane of polarization may be *clockwise* (to the right) or *counterclockwise* (to the left), which are respectively called **dextrorotatory** and **levorotatory** forms of optical activity. The structure of quartz is such that atomic arrangements spiral around the optic axis either in clockwise or counterclockwise sense. Quartz thus occurs in two distinct crystalline forms, right-handed and left-handed, which exhibit dextrorotatory and levorotatory types of optical activity, respectively. Although we used quartz as an example, there are many substances that are optically active, including various biological substances and even some liquid solutions (e.g., corn syrup) that contain various organic molecules with a rotatory power.

The **specific rotatory power** is defined as the extent of rotation per unit of distance traveled in the optically active substance, that is,  $\theta/L$ . Specific rotatory power depends on the wavelength. For example, for quartz this is  $49^\circ \text{ m}^{-1}$  at 400 nm but  $17^\circ \text{ m}^{-1}$  at 650 nm.

Optical activity can be understood in terms of left and right circularly polarized waves traveling at different velocities in the crystal, *i.e.*, experiencing different refractive indices. Due to the helical twisting of the molecular or atomic arrangements in the crystal, the velocity of a circularly polarized wave depends on whether the optical field rotates clockwise or counterclockwise. A vertically polarized light with a field  $\mathbf{E}$  at the input can be thought of as two right- and left-handed circularly polarized waves,  $\mathbf{E}_L$  and  $\mathbf{E}_R$ , that are symmetrical with respect to the  $y$ -axis, *i.e.*, at any instant  $\alpha = \beta$ , as shown in Figure 6.18 ( $\alpha$  and  $\beta$  are  $\omega t$ ). If they travel at the same velocity through the crystal, then they remain symmetrical with respect to the vertical ( $\alpha = \beta$  remains the same) and the resultant is still a vertically polarized light. If, however, these travel at different velocities through a medium, then the output  $\mathbf{E}'_L$  and  $\mathbf{E}'_R$  are no longer symmetrical with respect to the vertical,  $\alpha' \neq \beta'$ , and their resultant is a vector  $\mathbf{E}'$  at an angle  $\theta$  to  $y$ -axis.

Suppose that  $n_R$  and  $n_L$  are the refractive indices experienced by the right- and left-handed circularly polarized light, respectively. After traversing the crystal length  $L$ , the phase difference between the two optical fields  $\mathbf{E}'_L$  and  $\mathbf{E}'_R$  at the output leads to a new optical field  $\mathbf{E}'$ , which corresponds to  $\mathbf{E}$  rotated by  $\theta$ , given by

$$\theta = \frac{\pi}{\lambda}(n_L - n_R)L \quad (6.4.1) \quad \text{Optical activity}$$

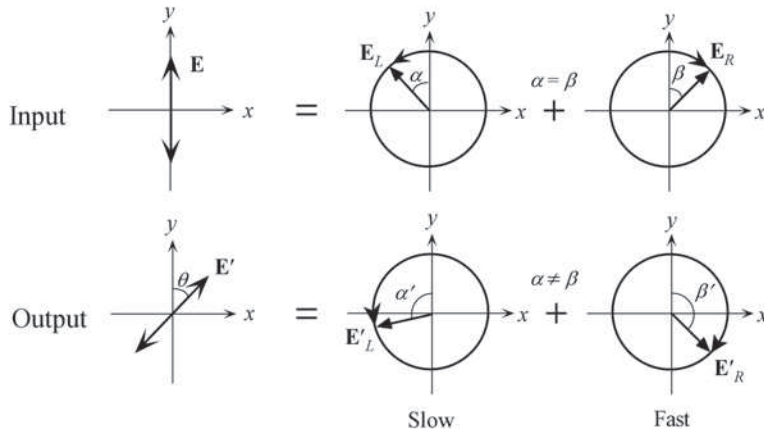


**FIGURE 6.18** Vertically polarized wave at the input can be thought of as two right- and left-handed circularly polarized waves that are symmetrical, *i.e.*, at any instant  $\alpha = \beta$ . If these travel at different velocities through a medium, then at the output they are no longer symmetrical with respect to  $y$ ,  $\alpha' \neq \beta'$ , and the result is a vector  $E'$  at an angle  $\theta$  to  $y$ .

where  $\lambda$  is the free-space wavelength. For a left-handed quartz crystal, and for 589 nm light propagation along the optic axis,  $n_R = 1.54427$  and  $n_L = 1.54420$ , which means  $\theta$  is about  $21.4^\circ$  per mm of crystal.

In a **circularly birefringent** medium, the right- and left-handed circularly polarized waves propagate with different velocities and experience different refractive indices,  $n_R$  and  $n_L$ . Since optically active materials naturally rotate the optical field, it is not unreasonable to expect that a circularly polarized light with its optical field rotating in the same sense as the optical activity will find it easier to travel through the medium. Thus, an optically active medium possesses different refractive indices for right- and left-handed circularly polarized light and exhibits circular birefringence. It should be mentioned that if the direction of the light wave is reversed in Figure 6.17, the ray simply retraces itself and  $E'$  becomes  $E$ .

## 6.5 LIQUID CRYSTAL DISPLAYS

Many flat-panel televisions and computer displays are liquid crystal displays (LCDs) in which liquid crystals cause changes in the polarization of a passing beam of light. **Liquid crystals** (LCs) are materials that have a rod-like molecular structure as shown in Figure 6.19 (a). These molecules, called **mesogens**, have strong dipoles, which means that the whole structure can be easily polarized. LCs essentially have properties that are between those of a liquid phase and those of a crystalline solid phase; *e.g.*, they can flow like a liquid but, at the same time, possess crystalline domains that lead to anisotropic optical properties. A distinct characteristic of the liquid crystal state is the tendency of the mesogens to point along a common axis called the **director**, a preferred common axis in the liquid crystal that results in an orientationally ordered state, as illustrated in Figure 6.19 (b). This behavior is very different than the way in which molecules behave in a normal liquid phase, where there is no intrinsic order. The orientational order in the liquid crystal state lies between that of a normal crystalline solid, *i.e.*, fully ordered periodic structure, and that of a normal liquid, *i.e.*, nearly fully disordered, and hence is given the name **mesogenic state**.

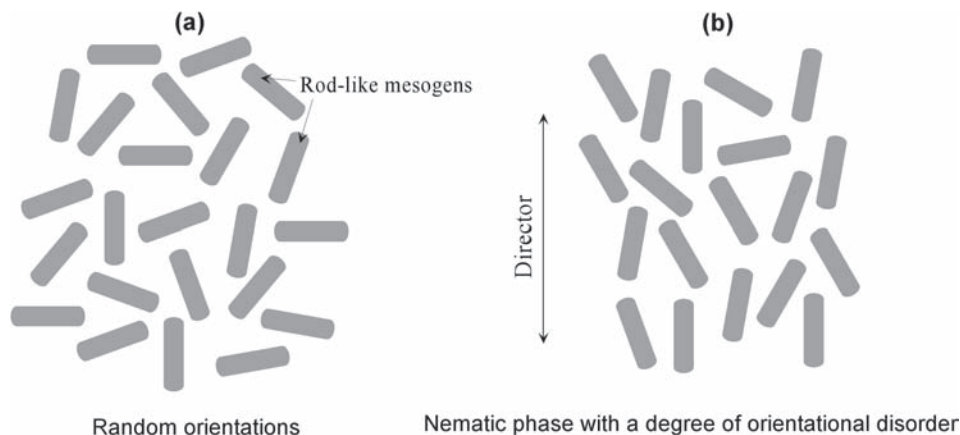


**FIGURE 6.19** Schematic illustration of orientational disorder in a liquid with rod-like mesogens. (a) No order, and rods are randomly oriented. (b) There is a tendency for the rods to align with the *director*, the vertical axis in this example.

The number of mesogens pointing along the director, that is, the *degree of anisotropy*, depends on the temperature because thermally induced random motions of the mesogens act against dipole alignment. The degree of alignment will be a maximum at low temperature and decreases with increasing temperature, until at some critical temperature thermal agitation will result in a state of no net ordering. There are a number of possible liquid crystal phases. We will consider the **nematic phase**, which is characterized by mesogens that have no positional order, but tend to point along the same direction, *i.e.*, along the director. Physical properties of these materials tend to depend sensitively on the degree of alignment, and can be highly *anisotropic* for well-aligned materials. A distinct advantage is that the molecular orientation and hence the optical properties can be controlled by an applied field. The molecules have rod-like shapes with lengths typically in the 20–30 nm range as shown in Figure 6.19 (a).

**Liquid crystal display** is a display that uses a liquid crystal medium whose optical properties can be controlled by an applied field. We can consider it as an LC *light modulator* or a **light valve**. The display has a thin film of *liquid crystal*, *e.g.*, a few microns in thickness, placed between two semitransparent electrically conducting electrodes to form a cell. Most LCDs are based on the **twisted nematic field effect**.<sup>8</sup> In a **twisted nematic liquid crystal cell**, as shown in Figure 6.20 (a), the two electrodes have surfaces that have been treated, *i.e.*, have an orientational layer, to act as directors for the molecules, and the directors are at right angles to each other. Molecules next to the surfaces are forced to align along these surface directors and hence the molecules homogeneously twist through 90° from one electrode to the other. The **twisted nematic liquid crystal** has its molecules arranged in helical structure, and is able to “twist,” or rotate the optical field in the light that passes through it. Two polarizers at the entrance and the exit ends of the cell have their transmission axes at 90° to each other as shown in Figure 6.20 (a). Polarized light thus enters the cell and has its polarization rotated by 90° as it arrives at the exit polarizer. Since this light has its polarization aligned with the

<sup>8</sup> Although a number of researchers have reported interesting observations on the optical properties of liquid crystals, the pioneering work on the twisted nematic LCD has been attributed to Martin Schadt and Wolfgang Helfrich (at Hoffman-LaRoche, Switzerland) in 1970–1971 and James Ferguson (USA) in 1971.

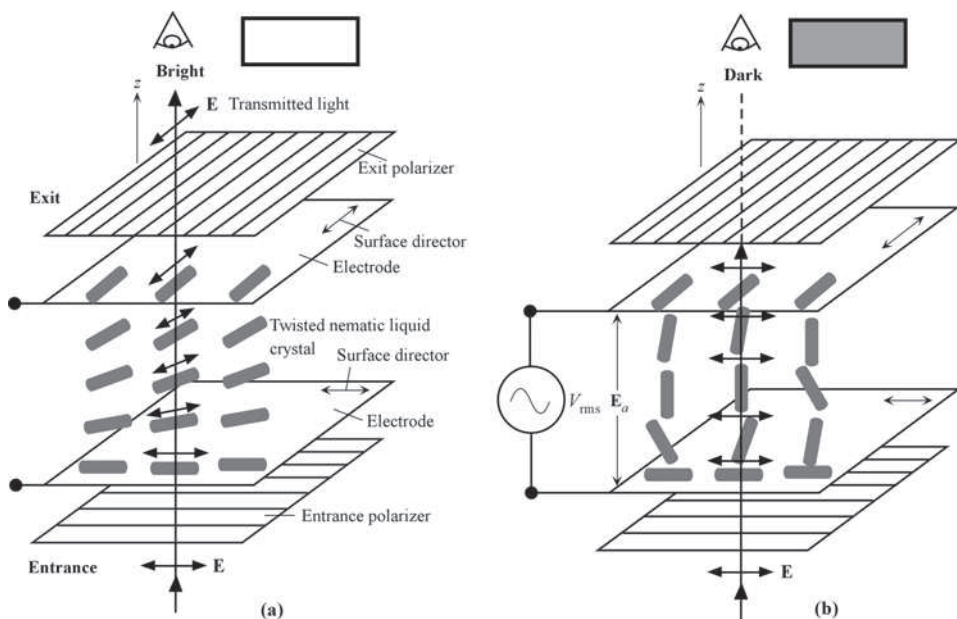


**FIGURE 6.20** Transmission-based LCD. (a) In the absence of a field, the liquid crystal has the twisted nematic phase and the light passing through it has its polarization rotated by  $90^\circ$ . The light is transmitted through both polarizers. The viewer sees a bright image. (b) When a voltage, and hence a field  $E_a$  is applied, the molecules in the liquid crystal align with the field and are unable to rotate the polarization of the light passing through it; light therefore cannot pass through the exit polarizer. The light is extinguished, and the viewer sees a dark image.

transmission axis of the exit polarizer, it passes through. Thus, without an applied field, the light is transmitted and the display is bright.

Suppose that an electric field  $E_a$  is applied by supplying an AC voltage (usually a few volts) to the two electrodes comprising the faces of the cell. The applied field now disturbs the alignment of the molecules in the nematic liquid crystal. The field  $E_a$  acts as an externally imposed director and the molecules align with the field, which results in the twisted molecular arrangement being destroyed. Put differently, the helical structure in Figure 6.20 (a) becomes unwound and we end up with the structure shown in Figure 6.20 (b). The polarization in the light entering the cell is unaffected and therefore the light cannot pass through the exit polarizer. The LCD cell therefore appears dark. In fact, the light transmission can be completely extinguished by applying a suitably large field. If a mirror is placed behind the second polarizer, the display can be operated under reflection instead of transmission.

A reverse switching behavior, that is, switching the LCD from dark (without an applied voltage) to bright (with applied voltage), can be achieved by using *parallel* polarizers at the light entrance and exit. By varying the applied voltage between the threshold for reorientation and the saturation field for unwinding the twisted nematic structure, we can obtain gray-scale modulation. The transparent electrodes are typically indium-tin-oxide, and can be patterned by lithographic techniques into various desirable shapes. More than 50% of TV screens use the LCD technology.

The arrangement in Figure 6.20 indicates that an AC voltage must be applied to the LCD. This is indeed the case and LCDs are always operated with an AC voltage; typical operating frequencies

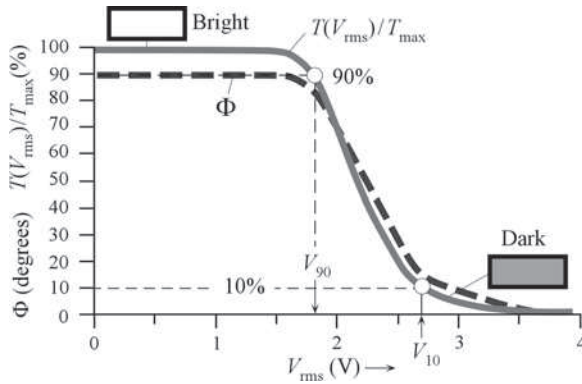


**FIGURE 6.21** Plots of the rotation angle  $\Phi$  of the linearly polarized light vs. the rms voltage  $V_{\text{rms}}$  across an LCD cell, and the normalized transmittance  $T(V_{\text{rms}})/T_{\text{max}}$  (%) vs.  $V_{\text{rms}}$  for a typical twisted nematic liquid crystal cell.

for LCDs are  $\sim 1$  kHz. The reversal of the field does not change the principle of operation because molecules always try to align parallel to the field, which is along either  $+z$  or  $-z$ . In both cases, optical field is not rotated and the through-light is extinguished at the second polarizer. The extent of transmission through an LCD depends on the rms value of the AC voltage. Manufacturers typically provide the transmittance vs. rms voltage characteristics of their LCDs. Figure 6.21 shows how the rotation angle  $\Phi$  of the linearly polarized light through the liquid crystal medium depends on the rms voltage  $V_{\text{rms}}$  across an LCD cell. The normalized transmittance  $T' = T(V_{\text{rms}})/T_{\text{max}}$  is also shown as a function of  $V_{\text{rms}}$ .  $T_{\text{max}}$  is the maximum transmittance under bright transmission conditions so that  $T(V_{\text{rms}})/T_{\text{max}}$  is 100% with no or very small  $V_{\text{rms}}$ .

It is apparent from Figure 6.21 that the rms voltage  $V_{\text{rms}}$  must reach a certain **threshold** value before any effect is seen. A threshold voltage is required to start untwisting the alignment of the mesogens. The rms voltage  $V_{90}$  corresponding to 90% normalized transmittance  $T'$  is usually taken as the **threshold voltage**. The voltage at which  $T'$  has dropped to 10% defines the **saturation voltage**,  $V_{10}$ . LCD response times for turning on (alignment with the applied field) and off (alignment with the surface directors) depend on the properties of the LC, the thickness of the cell, and temperature. At room temperature these turn on and off times are typically in the millisecond time range, with the turn off time usually being longer than the on time. It is faster to align the molecules with the applied field than the time it takes for them to naturally align with the surface directors when the field is turned off.



The light from an LCD display is linearly polarized. A number of square polarizers have been placed on the screen of this laptop computer at different angles until the light is totally extinguished. There are five polarizers placed on the screen at different angles.

It should be apparent that the whole LCD operation is based on three important effects: the optical activity exhibited by the twisted nematic LC structure in which the “twisted mesogens” rotate the optical field; the ability to rotate or align the mesogens in the LC by a sufficiently large applied (external) field; and the use of two polarizers in converting the rotation of the optical field within the medium to an intensity variation.

## 6.6 ELECTRO-OPTIC EFFECTS

### A. Definitions

Electro-optic effects refer to changes in the refractive index of a material induced by the application of an external electric field, which therefore *modulates* the optical properties; the applied field is not the electric field of any light wave, but a separate external field. We can apply such an external field by placing electrodes on opposite faces of a crystal and connecting these electrodes to a battery. The presence of such a field distorts the electron motions in the atoms or molecules of the substance, or distorts the crystal structure, resulting in changes in the optical properties. For example, an applied external field can cause an optically isotropic cubic crystal such as GaAs to become birefringent. In this case, the field induces principal axes and an optic axis. Typically, changes in the refractive index are small. The frequency of the applied field has to be such that the field appears static over the time scale it takes for the medium to change its properties, *i.e.*, respond, as well as for any light to cross the substance. The electro-optic effects are classified according to **first-** and **second-order effects**.

If we were to take the refractive index  $n$  to be a function of the applied electric field  $E$ , that is,  $n = n(E)$ , we can, of course, expand this as a Taylor series in  $E$ . The new refractive index  $n'$  is

Field-induced refractive index

$$n' = n + a_1 E + a_2 E^2 + \dots \quad (6.6.1)$$

where the coefficients  $a_1$  and  $a_2$  are called the **linear electro-optic effect** and **second-order electro-optic effect** coefficients. Although we would expect even higher terms in the expansion in Eq. (6.6.1), these are generally very small and their effects negligible within highest practical fields. The change in  $n$  due to the first  $E$  term is called the **Pockels effect**. The change in  $n$  due to the second  $E^2$  term is called the **Kerr effect**,<sup>9</sup> and the coefficient  $a_2$  is generally written as  $\lambda K$  where  $K$  is called the **Kerr coefficient**. Thus, the two effects are,

Pockels effect

$$\Delta n = a_1 E \quad (6.6.2)$$

and

Kerr effect

$$\Delta n = a_2 E^2 = (\lambda K) E^2 \quad (6.6.3)$$

All materials exhibit the Kerr effect. It may be thought that we will always find some (nonzero) values for  $a_1$  for all materials but this is not true and only certain crystalline materials exhibit the Pockels effect. If we apply a field  $\mathbf{E}$  in one direction and then reverse the field and apply  $-\mathbf{E}$ , then according to Eq. (6.6.2),  $\Delta n$  should change sign. If the refractive index

<sup>9</sup>John Kerr (1824–1907) was a Scottish physicist and faculty member at Free Church Training College for Teachers (1857–1901), Glasgow, where he set up an optics laboratory and demonstrated the Kerr effect (1875).



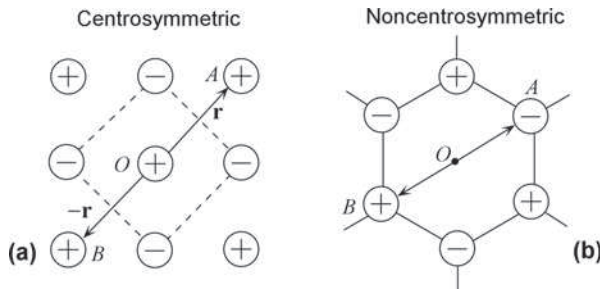


**FIGURE 6.22** (a) A centrosymmetric unit cell (such as NaCl) has a center of symmetry at  $O$ . (b) An example of a noncentrosymmetric unit cell. In this example, the hexagonal unit cell has no center of symmetry.

increases for  $\mathbf{E}$ , it must decrease for  $-\mathbf{E}$ . Reversing the field should *not* lead to an identical effect (the same  $\Delta n$ ). The structure has to respond differently to  $\mathbf{E}$  and  $-\mathbf{E}$ ; there must therefore be some *asymmetry* in the structure to distinguish between  $\mathbf{E}$  and  $-\mathbf{E}$ . In a noncrystalline material,  $\Delta n$  for  $\mathbf{E}$  would be the same as  $\Delta n$  for  $-\mathbf{E}$  as all directions are equivalent in terms of dielectric properties. Thus  $a_1 = 0$  for all noncrystalline materials (such as glasses and liquids). Similarly, if the crystal structure has a center of symmetry, as shown in Figure 6.22 (a), then reversing the field direction has an identical effect and  $a_1$  is again zero. A centrosymmetric crystal is such that if we draw a vector  $\mathbf{r}$  from the center  $O$  to an ion  $A$ , and then invert the vector making it  $-\mathbf{r}$ , we would then find the same type of ion at  $-\mathbf{r}$ , that is,  $A$  and  $B$  in Figure 6.22 (a) are identical ions. On the other hand, the hexagonal crystal in Figure 6.22 (b) is **noncentrosymmetric**. If we draw a vector  $\mathbf{r}$  from  $O$  to  $A$ , and then invert this, we would find a different ion  $B$  at  $-\mathbf{r}$ ;  $A$  and  $B$  are different ions. Only noncentrosymmetric crystals exhibit the Pockels effect. For example, an NaCl crystal is centrosymmetric, and therefore exhibits no Pockels effect. On the other hand, a GaAs crystal is noncentrosymmetric and evinces the Pockels effect under an applied field.

## B. Pockels Effect

The Pockels effect expressed in Eq. (6.6.2) is an oversimplification because in reality we have to consider the effect of an applied field along a particular crystal direction on the refractive index for light with a given propagation direction and polarization. For example, suppose that  $x$ ,  $y$ , and  $z$  are the principal axes of a crystal with refractive indices  $n_1$ ,  $n_2$ , and  $n_3$  along these



*Friedrich Carl Alwin Pockels* (1865–1913), son of Captain Theodore Pockels and Alwine Becker, was born in Vincenza (Italy). He obtained his doctorate from Göttingen University in 1888. From 1900 until 1913 he was a professor of theoretical physics in the Faculty of Sciences and Mathematics at the University of Heidelberg, where he carried out extensive studies on electro-optic properties of crystals—the Pockels effect is the basis of many practical electro-optic modulators. (Courtesy of the Department of Physics and Astronomy, University of Heidelberg, Germany.)

Various KD\*P-based Pockels cells used for  $Q$ -switching in laser applications. Left, half-wave voltage  $V_{\lambda/2}$  of 6.8 kV; right, small,  $V_{\lambda/2} = 6.5$  kV; far right large,  $V_{\lambda/2} = 6.8$  kV. The cells have AR (antireflection coatings), and can be used from 0.4 to 1.1  $\mu\text{m}$ . *Note:* KD\*P is a  $\text{KD}_2\text{PO}_4$  crystal. (Courtesy of Eksma Optics, Vilnius, Lithuania.)



directions. For an optically isotropic crystal, these would be the same, whereas for a uniaxial crystal,  $n_1 = n_2 \neq n_3$  as illustrated in the  $xy$  cross-section in Figure 6.23 (a). Suppose that we suitably apply a voltage across a crystal and thereby apply an external DC field  $E_a$  along the  $z$ -axis. In Pockels effect, the field will modify the optical indicatrix. The exact effect depends on the crystal structure. For example, a crystal like GaAs, optically isotropic with a spherical indicatrix, becomes birefringent, and a crystal like KDP ( $\text{KH}_2\text{PO}_4$ —potassium dihydrogen phosphate), *i.e.*, uniaxial, becomes biaxial. In the case of KDP, the field  $E_a$  along  $z$  rotates the principal axes by  $45^\circ$  about  $z$ , and changes the principal indices as indicated in Figure 6.23 (b). The new principal indices are now  $n'_1$  and  $n'_2$ , which means that the cross-section is now an ellipse. Propagation along the  $z$ -axis under an applied field in Figure 6.23 (b) now occurs with different refractive indices  $n'_1$  and  $n'_2$ . As apparent in Figure 6.23 (b), the applied field induces new principal axes  $x'$ ,  $y'$ , and  $z'$  for this crystal, though in this special case  $z' = z$ . In the case of  $\text{LiNbO}_3$  (lithium niobate), an optoelectronically important uniaxial crystal, a field  $E_a$  along the  $y$ -direction does not significantly rotate the principal axes but rather changes the principal refractive indices  $n_1$  and  $n_2$  (both equal to  $n_o$ ) to  $n'_1$  and  $n'_2$  as illustrated in Figure 6.23 (c).

As an example, consider a wave propagating along the  $z$ -direction (optic axis) in an  $\text{LiNbO}_3$  crystal. This wave will experience the same refractive index ( $n_1 = n_2 = n_o$ ) whatever the polarization, as in Figure 6.23 (a). However, in the presence of an applied field  $E_a$  parallel to the principal  $y$ -axis as in Figure 6.23 (c), the light propagates as two orthogonally polarized waves (parallel to  $x$  and  $y$ ) experiencing different refractive indices  $n'_1$  and  $n'_2$ . The applied field thus *induces a birefringence* for light traveling along the  $z$ -axis. The field-induced rotation of the principal axes in this case, though present, is small and can be neglected. Before the field  $E_a$

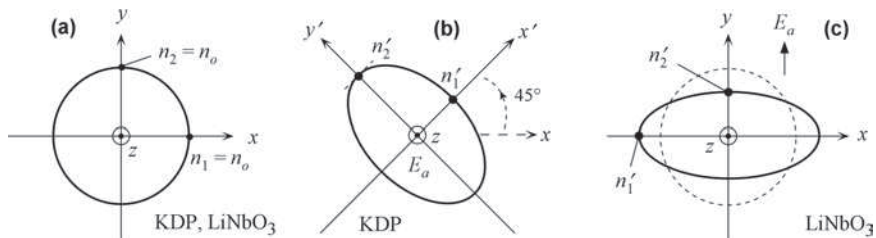


**FIGURE 6.23** (a) Cross-section of the optical indicatrix with no applied field,  $n_1 = n_2 = n_o$ . (b) The applied external field  $E_a$  along  $z$  modifies the optical indicatrix. In a KDP crystal, it rotates the principal axes by  $45^\circ$  to  $x'$  and  $y'$ , and  $n_1$  and  $n_2$  change to  $n'_1$  and  $n'_2$ . (c) Applied field along  $y$  in  $\text{LiNbO}_2$  modifies the indicatrix and changes  $n_1$  and  $n_2$  to  $n'_1$  and  $n'_2$ .



is applied, the refractive indices  $n_1$  and  $n_2$  are both equal to  $n_o$ . The Pockels effect then gives the new refractive indices  $n'_1$  and  $n'_2$  in the presence of  $E_a$  as

$$n'_1 \approx n_1 + \frac{1}{2}n_1^3 r_{22} E_a \quad \text{and} \quad n'_2 \approx n_2 - \frac{1}{2}n_2^3 r_{22} E_a \quad (6.6.4) \quad \text{Pockels effect}$$

where  $r_{22}$  is a constant, called a **Pockels coefficient**, that depends on the crystal structure and the material. The reason for the seemingly unusual subscript notation is that there are more than one constant and these are elements of a tensor that represents the optical response of the crystal to an applied field along a particular direction with respect to the principal axes (the exact theory is more mathematical than intuitive). We therefore have to use the correct Pockels coefficients for the refractive index changes for a given crystal and a given field direction.<sup>10</sup> If the field were along  $z$ , the Pockels coefficient in Eq. (6.6.4) would be  $r_{13}$ .

It is clear that the control of the refractive index by an external applied field (and hence a voltage) is a distinct advantage that enables the phase change through a Pockels crystal to be controlled or modulated; such a **phase modulator** is called a **Pockels cell**. In the **longitudinal Pockels cell phase modulator**, the applied field is in the direction of light propagation, whereas in the **transverse phase modulator**, the applied field is transverse to the direction of light propagation. For light propagation along  $z$ , the longitudinal and transverse effects are illustrated in Figures 6.23 (b) and (c), respectively.

Consider the transverse phase modulator in Figure 6.24. In this example, the applied electric field,  $E_a = V/d$ , is applied parallel to the  $y$ -direction, normal to the direction of light propagation along  $z$ . Suppose that the incident beam is linearly polarized (shown as  $\mathbf{E}$ ), say at  $45^\circ$  to the  $y$ -axis. We can represent the incident light in terms of polarizations  $\mathbf{E}_x$  and  $\mathbf{E}_y$  along the  $x$ - and  $y$ -axes. These components,  $\mathbf{E}_x$  and  $\mathbf{E}_y$ , experience refractive indices  $n'_1$  and  $n'_2$ , respectively. Thus when  $\mathbf{E}_x$  traverses the distance  $L$ , its phase changes by  $\phi_1$ ,

$$\phi_1 = \frac{2\pi n'_1}{\lambda} L = \frac{2\pi L}{\lambda} \left( n_o + \frac{1}{2} n_o^3 r_{22} \frac{V}{d} \right)$$

When the component  $\mathbf{E}_y$  traverses the distance  $L$ , its phase changes by  $\phi_2$ , given by a similar expression except that  $r_{22}$  changes sign. Thus, the phase change  $\Delta\phi$  between the two field components is

$$\Delta\phi = \phi_1 - \phi_2 = \frac{2\pi}{\lambda} n_o^3 r_{22} \frac{L}{d} V \quad (6.6.5) \quad \text{Transverse Pockels effect}$$

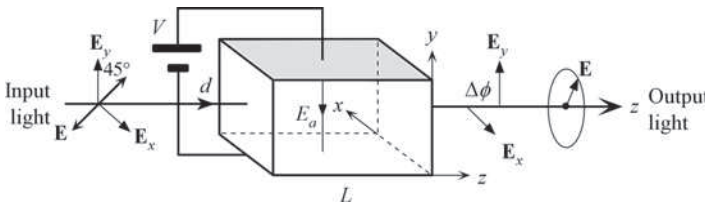


**FIGURE 6.24** Transverse Pockels cell phase modulator. A linearly polarized input light into an electro-optic crystal emerges as a circularly polarized light.

<sup>10</sup>The reader should not be too concerned with the subscripts but simply interpret them as identifying the right Pockels coefficient value for the particular electro-optic problem at hand.



Electro-optic phase modulator using  $\text{LiNbO}_3$ .  
The socket is for the RF modulation input.  
(Courtesy of Thorlabs.)

The applied voltage thus inserts an adjustable phase difference  $\Delta\phi$  between the two field components. The polarization state of output wave can therefore be controlled by the applied voltage and the Pockels cell is a **polarization modulator**. We can change the medium from a quarter-wave to a half-wave plate by simply adjusting  $V$ . The voltage  $V = V_{\lambda/2}$ , the **half-wave voltage**, corresponds to  $\Delta\phi = \pi$  and generates a half-wave plate. The advantage of the transverse Pockels effect is that we can independently reduce  $d$ , and thereby increase the field, and increase the crystal length  $L$ , to build up more phase change;  $\Delta\phi$  is proportional to  $L/d$ . This is not the case in the longitudinal Pockels effect. If  $L$  and  $d$  were the same, typically  $V_{\lambda/2}$  would be a few kilovolts but tailoring  $d/L$  to be much smaller than unity would bring  $V_{\lambda/2}$  down to desirable practical values.

From the polarization modulator in Figure 6.24, we can build an **intensity modulator** by inserting a polarizer  $P$  and an analyzer  $A$  before and after the phase modulator as in Figure 6.25 (a) such that they are cross-polarized, *i.e.*,  $P$  and  $A$  have their transmission axes at  $90^\circ$  to each other. The transmission axis of  $P$  is at  $45^\circ$  to the  $y$ -axis (hence  $A$  also has its transmission axis at  $45^\circ$  to  $y$ ) so that the light entering the crystal has equal  $\mathbf{E}_x$  and  $\mathbf{E}_y$  components. In the absence of an applied voltage, the two components travel with the same refractive index, and polarization output from the crystal is the same as its input. There is no light detected at the detector as  $A$  and  $P$  are at right angles ( $\theta = 90^\circ$  in Malus's law).

An applied voltage inserts a phase difference  $\Delta\phi$  between the two electric field components. The light leaving the crystal now has an elliptical polarization and hence a field component along

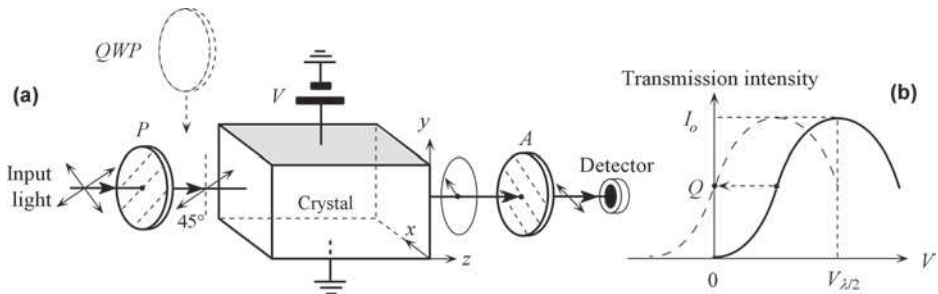


**FIGURE 6.25** (a) A transverse Pockels cell intensity modulator. The polarizer  $P$  and analyzer  $A$  have their transmission axis at right angles and  $P$  polarizes at an angle  $45^\circ$  to  $y$ -axis. (b) Transmission intensity vs. applied voltage characteristics. If a quarter-wave plate ( $QWP$ ) is inserted after  $P$ , the characteristic is shifted to the dashed curve.

the transmission axis of  $A$ . A portion of this light will therefore pass through  $A$  to the detector. The transmitted intensity now depends on the applied voltage  $V$ . The field components at the analyzer will be out of phase by an amount  $\Delta\phi$ . We have to find the total field  $\mathbf{E}$  and the component of this field along the transmission axis of  $A$ . Suppose that  $E_o$  is the amplitude of the wave incident on the crystal face. The amplitudes along  $x$ - and  $y$ -axes will be  $E_o/\sqrt{2}$  each (notice that the  $x$ -component of  $\mathbf{E}$  is along the  $-x$ -direction). The total field  $\mathbf{E}$  at the analyzer is

$$\mathbf{E} = -\hat{\mathbf{x}} \frac{E_o}{\sqrt{2}} \cos(\omega t) + \hat{\mathbf{y}} \frac{E_o}{\sqrt{2}} \cos(\omega t + \Delta\phi)$$

A factor  $\cos(45^\circ)$  of each component passes through  $A$ . We can resolve  $\mathbf{E}_x$  and  $\mathbf{E}_y$  along  $A$ 's transmission axis, then add these components, and finally use a trigonometric identity to obtain the field emerging from  $A$ . The final result is

$$E = E_o \sin\left(\frac{1}{2}\Delta\phi\right) \sin\left(\omega t + \frac{1}{2}\Delta\phi\right)$$

The intensity  $I$  of the detected beam is the square of the term multiplying the sinusoidal time variation, *i.e.*,

$$I = I_o \sin^2\left(\frac{1}{2}\Delta\phi\right) \quad (6.6.6)$$

which can be written as

$$I = I_o \sin^2\left(\frac{\pi}{2} \cdot \frac{V}{V_{\lambda/2}}\right) \quad (6.6.7)$$

Pockels  
intensity  
modulator

where  $I_o$  is the light intensity under full transmission and  $V_{\lambda/2}$  is the voltage that gives a phase change  $\Delta\phi$  of  $\pi$  in Eq. (6.6.5).

An applied voltage of  $V_{\lambda/2}$  is needed to allow full transmission. The transmission characteristics of this modulator is shown in Figure 6.25 (b). In digital electronics, we would switch a light pulse on and off so that the nonlinear dependence of transmission intensity on  $V$  in Eq. (6.6.7) would not be a problem. However, if we wish to obtain a linear modulation between the intensity  $I$  and  $V$  we need to bias this structure about the apparent “linear region” of the curve at half-height. This is done by inserting a quarter-wave plate ( $QWP$ ) after the polarizer  $P$ , as in Figure 6.25 (a), which provides a circularly polarized light as input. The insertion of  $QWP$  means that  $\Delta\phi$  is already shifted by  $\pi/4$  before any applied voltage. The applied voltage then, depending on the sign, increases or decreases  $\Delta\phi$ . The new transmission characteristic is shown as a dashed curve in Figure 6.25 (b). We have, effectively, optically biased the modulator at point  $Q$  on the new characteristics. (Will it matter, if instead, we were to insert the quarter-wave plate before the analyzer<sup>11</sup>?)

<sup>11</sup> The answer is no, since it only serves to introduce a phase change of  $\pi/4$  between  $P$  and  $A$ .

**EXAMPLE 6.6.1 Pockels Cell Modulator**

What should be the aspect ratio  $d/L$  for the transverse lithium niobate ( $\text{LiNbO}_3$ ) phase modulator in Figure 6.24, that will operate at a free-space wavelength of  $1.3\text{ }\mu\text{m}$  and will provide a phase shift  $\Delta\phi$  of  $\pi$  (half wavelength) between the two field components propagating through the crystal for an applied voltage of  $12\text{ V}$ ? At  $\lambda = 1.3\text{ }\mu\text{m}$ ,  $\text{LiNbO}_3$  has  $n_o \approx 2.21$ ,  $r_{22} \approx 5 \times 10^{-12}\text{ m V}^{-1}$ .

**Solution**

From Eq. (6.6.5), putting  $\Delta\phi = \pi$  for the phase difference between the field components  $\mathbf{E}_x$  and  $\mathbf{E}_y$  in Figure 6.24 gives

$$\Delta\phi = \frac{2\pi}{\lambda} n_o^3 r_{22} \frac{L}{d} V_{\lambda/2} = \pi$$

or

$$\frac{d}{L} = \frac{1}{\Delta\phi} \cdot \frac{2\pi}{\lambda} n_o^3 r_{22} V_{\lambda/2} \approx \frac{1}{\pi} \cdot \frac{2\pi}{(1.3 \times 10^{-6})} (2.21)^3 (5 \times 10^{-12}) (12)$$

giving

$$d/L \approx 1 \times 10^{-3}$$

This particular transverse phase modulator has the field applied along the  $y$ -direction and light traveling along the  $z$ -direction as in Figure 6.24. If we were to use the transverse arrangement in which the field is applied along the  $z$ -axis, and the light travels along the  $y$ -axis, the relevant Pockels coefficients would be greater, and the corresponding aspect ratio  $d/L$  would be  $\sim 10^{-2}$ . We cannot arbitrarily set  $d/L$  to any ratio we like for the simple reason that when  $d$  becomes too small, the light will suffer diffraction effects that will prevent it from passing through the device.  $d/L$  ratios  $10^{-3}$ – $10^{-2}$  in practice can be implemented by fabricating an integrated optical device.

**C. Kerr Effect**

Suppose that we apply a strong electric field to an otherwise optically isotropic material such as glass (or liquid). The change in the refractive index will be due to the Kerr effect, a second-order effect. We can arbitrarily set the  $z$ -axis of a Cartesian coordinate system along the applied field as illustrated in Figure 6.26 (a). The applied field distorts the electron motions (orbits)

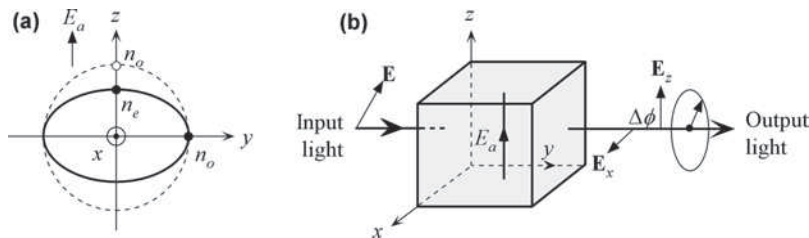


**FIGURE 6.26** (a) An applied electric field, via the Kerr effect, induces birefringence in an otherwise optically isotropic material. (b) A Kerr cell phase modulator.

in the constituent atoms and molecules, including those valence electrons in covalent bonds, in such a way that it becomes more difficult for the electric field in the light wave to displace electrons parallel to the applied field direction. Thus, a light wave with a polarization parallel to the  $z$ -axis will experience a smaller refractive index, reduced from its original value  $n_o$  to  $n_e$ . Light waves with polarizations orthogonal to the  $z$ -axis will experience the same refractive index  $n_o$ . The applied field thus induces birefringence with an optic axis parallel to the applied field direction as shown in Figure 6.26 (a). The material becomes birefringent for waves traveling off the  $z$ -axis.

The polarization modulator and intensity modulator concepts based on the Pockels cell can be extended to the Kerr effect as illustrated in Figure 6.26 (b), which shows a Kerr cell phase modulator. In this case, the applied field again induces birefringence. The phase modulator in Figure 6.26 (b) uses the Kerr effect, whereupon the applied field  $E_a$  along  $z$  induces a refractive index  $n_e$  parallel to the  $z$ -axis, whereas that along the  $x$ -axis will still be  $n_o$ . The light components  $\mathbf{E}_x$  and  $\mathbf{E}_z$  then travel along the material with different velocities and emerge with a phase difference  $\Delta\phi$  resulting in an elliptically polarized light. However, the Kerr effect is small as it is a second-order effect, and therefore only accessible for modulation use at high fields. The advantage, however, is that all materials, including glasses and liquids, exhibit the Kerr effect, and the response time in solids is very short, much less than nanoseconds leading to high modulation frequencies; greater than GHz.

If  $E_a$  is the applied field, then the change in the refractive index for polarization parallel to the applied field, as in Figure 6.26 (a), can be shown to be given by

$$\Delta n = \lambda K E_a^2 \quad (6.6.8) \quad \text{Kerr effect}$$

where  $K$  is the Kerr coefficient. We can now use Eq. (6.6.8) to find the induced phase difference  $\Delta\phi$  and hence relate it to the applied voltage.

Table 6.2 summarizes the Pockels and Kerr coefficients for various materials. The Kerr effect also occurs in anisotropic crystals but the effect there cannot be simply characterized by a single coefficient  $K$ .

**TABLE 6.2 Pockels ( $r$ ) and Kerr ( $K$ ) coefficients in a few selected materials.**  
Values in parentheses for  $r$  are at very high applied field frequencies

Material	Crystal	Indices	Pockels Coefficients ( $\times 10^{-12} \text{ m V}^{-1}$ )	$K (\text{m V}^{-2})$	Comment
LiNbO <sub>3</sub>	Uniaxial	$n_o = 2.286$ $n_e = 2.200$	$r_{13} = 9.6(8.6); r_{33} = 30.9(30.8)$ $r_{22} = 6.8(3.4); r_{51} = 32.6(28)$		$\lambda \approx 633 \text{ nm}$
KDP (KH <sub>2</sub> PO <sub>4</sub> )	Uniaxial	$n_o = 1.512$ $n_e = 1.470$	$r_{41} = 8.8; r_{63} = 10.3$		$\lambda \approx 546 \text{ nm}$
KD*P (KD <sub>2</sub> PO <sub>4</sub> )	Uniaxial	$n_o = 1.508$ $n_e = 1.468$	$r_{41} = 8.8; r_{63} = 26.8$		$\lambda \approx 546 \text{ nm}$
GaAs	Isotropic	$n_o = 3.43$	$r_{41} = 1.43$		$\lambda \approx 1.15 \mu\text{m}$
Glass	Isotropic	$n_o \approx 1.5$	0	$(1 - 20) \times 10^{-15}$	Typical values
Nitrobenzene	Isotropic	$n_o \approx 1.5$	0	$3 \times 10^{-12}$	

(Source: Data selectively extracted from A. Yariv and P. Yeh, *Photonics*, 6th Edition (Oxford University Press, 2007), Ch. 9, and other sources.)

**EXAMPLE 6.6.2 Kerr Effect Modulator**

Suppose that we have a glass rectangular block of thickness ( $d$ ) 100  $\mu\text{m}$  and length ( $L$ ) 20 mm and we wish to use the Kerr effect to implement a phase modulator in a fashion illustrated in Figure 6.26 (b). Note that  $d$  is the sample dimension along  $z$  and the applied field, and  $L$  is the sample length along  $y$ , the direction of light propagation. The input light has been polarized parallel to the applied field  $E_a$  direction, along the  $z$ -axis. Assume that the glass medium has a Kerr coefficient,  $K = 3 \times 10^{-15} \text{ m V}^{-2}$ . What is the applied voltage that induces a phase change of  $\pi$  (half-wavelength)?

**Solution**

The phase change  $\Delta\phi$  for the optical field  $E_z$  is

$$\Delta\phi = \frac{2\pi\Delta n}{\lambda}L = \frac{2\pi(\lambda KE_a^2)}{\lambda}L = \frac{2\pi LKV^2}{d^2}$$

For  $\Delta\phi = \pi$ ,  $V = V_{\lambda/2}$ ,

$$V_{\lambda/2} = \frac{d}{\sqrt{2LK}} = \frac{(100 \times 10^{-6})}{\sqrt{2(20 \times 10^{-3})(3 \times 10^{-15})}} = 9.1 \text{ kV!}$$

Although the Kerr effect is fast, it comes at a costly price. Notice that  $K$  depends on the wavelength and so does  $V_{\lambda/2}$ .

**6.7 INTEGRATED OPTICAL MODULATORS****A. Phase and Polarization Modulation**

**Integrated optics** refers to the integration of various optical devices and components on a single common substrate, for example lithium niobate, just as in integrated electronics all the necessary devices for a given function are integrated in the same semiconductor crystal substrate (chip). There is a distinct advantage to implementing various optically communicated devices, for example laser diodes, waveguides, splitters, modulators, and photodetectors on the same substrate, as it leads to miniaturization and also to an overall enhancement in performance and usability (typically).

One of the simplest examples is the polarization modulator shown in Figure 6.27 where an embedded waveguide has been fabricated by implanting an  $\text{LiNbO}_3$  substrate with Ti atoms, which increase the refractive index. Two coplanar strip electrodes run along the waveguide and enable the application of a transverse field  $E_a$  to the light propagation direction  $z$ . The external modulating voltage  $V(t)$  is applied between the coplanar drive electrodes and, by virtue of the Pockels effect, induces a change  $\Delta n$  in the refractive index and hence a voltage dependent phase shift through the device. We can represent light propagation along the guide in terms of two orthogonal modes,  $E_x$  along  $x$  and  $E_y$  along  $y$ . These two modes experience symmetrically opposite phase changes.<sup>12</sup> The phase shift  $\Delta\phi$  between the  $E_x$  and  $E_y$  polarized waves would normally be given by Eq. (6.6.5). However, in this case the applied (or induced) field is not uniform between the electrodes and, further, not all applied field lines are inside the waveguide.

<sup>12</sup>These are called transverse electric (TE) and transverse magnetic (TM) modes.

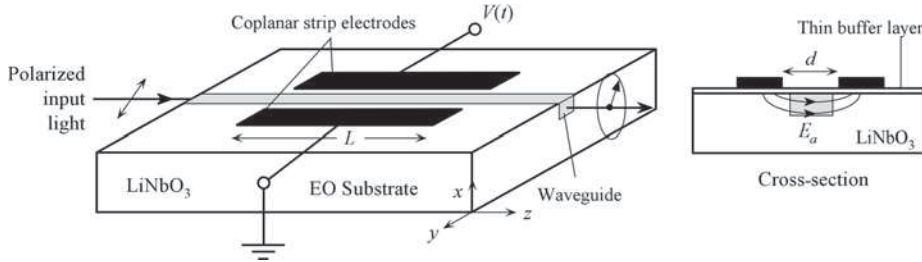


**FIGURE 6.27** Integrated transverse Pockels cell phase modulator in which a waveguide is diffused into an electro-optic (EO) substrate. Coplanar strip electrodes apply a transverse field  $E_a$  through the waveguide. The substrate is an  $x$ -cut  $\text{LiNbO}_3$  and typically there is a thin dielectric buffer layer (e.g.,  $\sim 200$  nm thick  $\text{SiO}_2$ ) between the surface electrodes and the substrate to separate the electrodes away from the waveguide.

The useful electro-optic effect takes place over the spatial overlap region between the applied field and the optical fields. This **spatial overlap efficiency** is represented by a coefficient  $\Gamma$ , and the phase shift  $\Delta\phi$  is written as

$$\Delta\phi = \Gamma \frac{2\pi}{\lambda} n_o^3 r_{22} \frac{L}{d} V \quad (6.7.1) \quad \text{Phase modulator}$$

where typically  $\Gamma \approx 0.5$ – $0.7$  for various integrated polarization modulators of this type. Since the phase shift depends on the product of  $V$  and  $L$ , a comparative device parameter would be the  $V \times L$  product for a phase shift of  $\pi$  (half-wavelength), i.e.,  $V_{\lambda/2}L$ . At  $\lambda = 1.5 \mu\text{m}$  for an  $x$ -cut  $\text{LiNbO}_3$  modulator as in Figure 6.27, with  $d \approx 10 \mu\text{m}$ ,  $V_{\lambda/2}L \approx 35 \text{ V cm}$ . For example, a modulator with  $L = 2 \text{ cm}$  has a half-wave voltage  $V_{\lambda/2} = 17.5 \text{ V}$ . By comparison, for a  $z$ -cut  $\text{LiNbO}_3$  plate, that is for light propagation along the  $y$ -direction and  $E_a$  along  $z$ , the relevant Pockels coefficients ( $r_{13}$  and  $r_{33}$ ) are much greater than  $r_{22}$  which leads to  $V_{\lambda/2}L \approx 5 \text{ V cm}$ .

## B. Mach-Zehnder Modulator

Induced phase shift by applied voltage can be converted to an amplitude variation by using an interferometer, a device that interferes two waves of the same frequency but different phase. Consider the structure shown in Figure 6.28 which has implanted single-mode waveguides in a  $\text{LiNbO}_3$  (or other electro-optic) substrate in the geometry shown. The waveguide at the input branches out at  $C$  to two arms  $A$  and  $B$ , and these arms are later combined at  $D$  to constitute the output.<sup>13</sup> The splitting operation at  $C$  and combining the waves at  $D$  involve simple Y-junction waveguides. In the ideal case, the power is equally split at  $C$  so that the field is scaled by a factor  $(2)^{1/2}$  going into each arm. The structure acts as an interferometer because the two waves traveling through the arms  $A$  and  $B$  interfere at the output port  $D$ , and the output amplitude depends on the phase difference (optical path difference) between the  $A$  and  $B$ -branches. Two back-to-back identical phase modulators enable the phase changes in  $A$  and  $B$  to be modulated. Notice that the applied field in branch  $A$  is in the opposite direction to that in branch  $B$ . The refractive index changes are therefore opposite, which means the phase changes in arms  $A$  and  $B$  are also opposite.

<sup>13</sup> For those who read Section 1.13 under Additional Topics, this is essentially the Mach-Zehnder interferometer explained in that section. The interferometer was named after Ludwig Mach and Ludwig Zehnder. (Ludwig Mach was the son of Ernst Mach.)

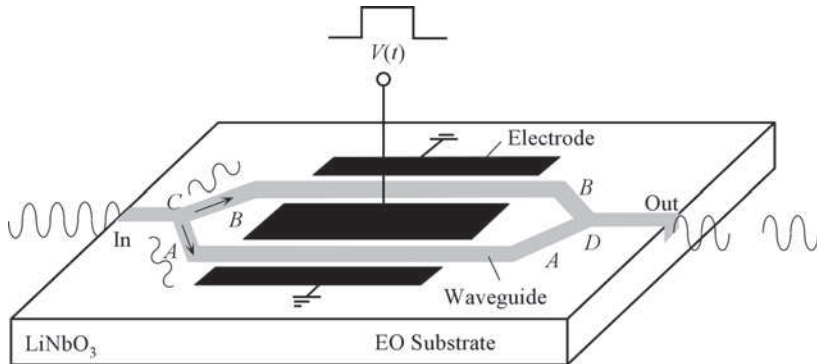
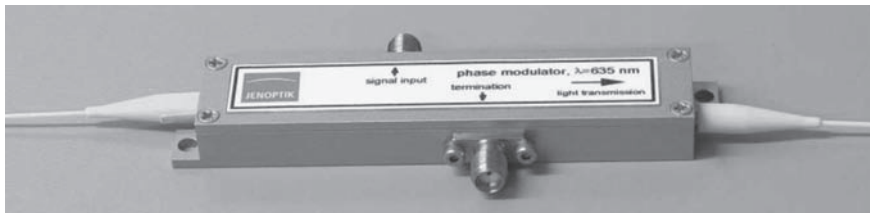


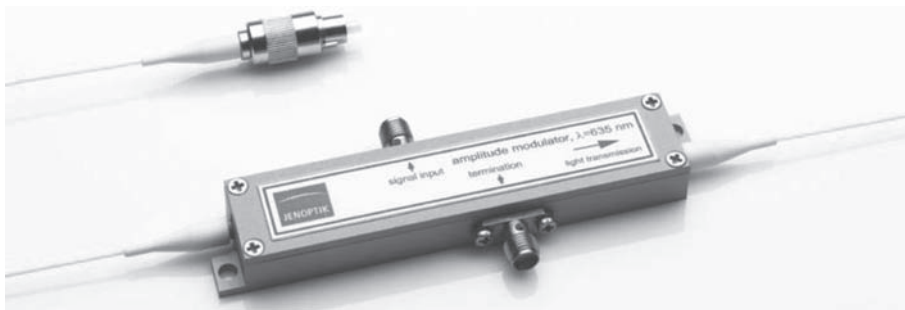
**FIGURE 6.28** An integrated Mach-Zehnder optical intensity modulator. The input light is split into two coherent waves A and B, which are phase shifted by the applied voltage, and then the two are combined again at the output.

For example, if the applied voltage induces a phase change of  $\pi/2$  in arm A, this will be  $-\pi/2$  in arm B so that A and B would be out of phase by  $\pi$ . These two waves will then interfere destructively and cancel each other at D. The output intensity would be zero. Since the applied voltage controls the phase difference between the two interfering waves A and B at the output, this voltage also controls the output light intensity, though the relationship is not linear.

It is apparent that the relative phase difference between the two waves A and B is therefore doubled with respect to a phase change  $\phi$  in a single arm. We can predict the output intensity by



An  $\text{LiNbO}_3$ -based phase modulator for use from the visible spectrum to telecom wavelengths, with modulation speeds up to 5 GHz. This particular model has  $V_{\lambda/2} = 10 \text{ V}$  at 1550 nm. (© JENOPTIK Optical System GmbH.)



An  $\text{LiNbO}_3$ -based Mach-Zehnder amplitude modulator for use from the visible spectrum to telecom wavelengths, with modulation frequencies up to 5 GHz. This particular model has  $V_{\lambda/2} = 5 \text{ V}$  at 1550 nm. (© JENOPTIK Optical System GmbH.)



adding waves  $A$  and  $B$  at  $D$ . If  $A$  is the amplitude of wave  $A$  and  $B$  (assumed equal power splitting at  $C$ ), the optical field at the output is

$$E_{\text{out}} \propto A \cos(\omega t + \phi) + A \cos(\omega t - \phi) = 2A \cos \phi \cos(\omega t)$$

The output power  $P_{\text{out}}$  is proportional to  $E_{\text{out}}^2$ , which is maximum when  $\phi = 0$ . Thus, at any phase difference  $\phi$ , we have

$$\frac{P_{\text{out}}(\phi)}{P_{\text{out}}(0)} = \cos^2 \phi \quad (6.7.2)$$

*Mach-Zehnder amplitude modulator*

Although the derivation is oversimplified,<sup>14</sup> it nonetheless represents approximately the right relationship between the power transfer and the induced phase  $\phi$  change per modulating arm. The power transfer is zero when  $\phi = \pi/2$  as expected. In practice, the Y-junction losses and uneven splitting result in less than ideal performance;  $A$  and  $B$  do not totally cancel out when  $\phi = \pi/2$ . Manufacturers often quote the extinction ratio, that is, the ratio between maximum and minimum power that can be transferred through the modulator by the application of a voltage  $V(t)$  in Figure 6.28. Another quantity of interest that is quoted is the half-voltage  $V_{\lambda/2}$ . In the case of an amplitude modulator, this half-wave voltage is the voltage needed to induce a phase difference of  $\pi$  between the two arms  $A$  and  $B$  and hence extinguish the output. Thus, the half-wave voltage  $V_{\lambda/2}$  is the voltage for switching the modulator from the on to the off state.

The output impedance of the driving circuit for the Mach-Zehnder modulator in Figure 6.28 has to be properly matched to the input impedance of the modulator to obtain the best frequency response. Commercially available high-end Mach-Zehnder modulators can handle digital modulation rates up to  $40 \text{ Gb s}^{-1}$  and beyond. The half-wave voltages are typically less than 10 V, with extinction ratios in the 30–40 dB range.

## C. Coupled Waveguide Modulators

When two parallel optical waveguides  $A$  and  $B$  are sufficiently close to each other, the electric fields associated with the propagation modes in  $A$  and  $B$  can overlap, as illustrated in Figure 6.29 (a). This implies that light can be coupled from one guide to another in a reminiscent way to frustrated total internal reflection (see Chapter 1). We can use qualitative arguments to understand the nature of light coupling between these two guides. Suppose that we launch a light wave into the guide  $A$  operating in single mode. Since the separation  $d$  of the two guides is small, some of the electric field in the evanescent wave of this mode extends into guide  $B$ , and therefore some electromagnetic energy will be transferred from guide  $A$  to  $B$ . This energy transfer will depend on the efficiency of coupling between the two guides and the nature of the modes in  $A$  and  $B$ , which in turn depend on the geometries and refractive indices of guides and the substrate (acting as a cladding).

As light in guide  $A$  travels along  $z$ , it leaks into  $B$  and, if the mode in  $B$  has the right phase, the transferred light waves build up along  $z$  as a propagating mode in  $B$ , as indicated in Figure 6.29 (b). By the same token, the light now traveling in  $B$  along  $z$  can be transferred back into  $A$  if the mode in  $A$  has the right phase. The efficient transfer of energy back and forth

<sup>14</sup> See R. Syms and J. Cozens, *Optical Guided Waves and Devices* (McGraw-Hill, 1992), Ch. 9.

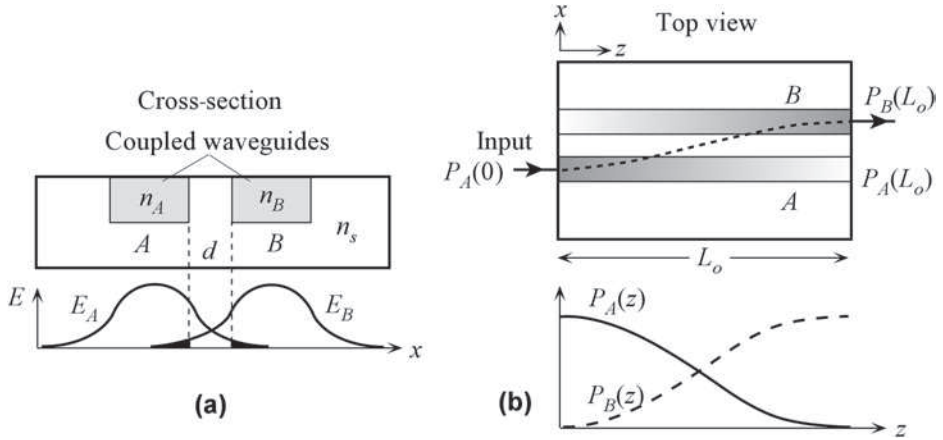


**FIGURE 6.29** (a) Cross-section of two closely spaced waveguides  $A$  and  $B$  (separated by  $d$ ) embedded in a substrate. The evanescent field from  $A$  extends into  $B$  and vice versa. *Note:*  $n_A$  and  $n_B > n_s$  ( $=$  substrate index). (b) Top view of the two guides  $A$  and  $B$  that are coupled along the  $z$ -direction. Light is fed into  $A$  at  $z = 0$ , and it is gradually transferred to  $B$  along  $z$ . At  $z = L_o$ , all the light has been transferred to  $B$ . Beyond this point, light begins to be transferred back to  $A$  in the same way.

between the two guides  $A$  and  $B$  requires that the two modes be in phase to allow the transferred amplitude to build up along  $z$ . If the two modes are out of phase, the waves transferred into a guide do not reinforce each other and the coupling efficiency is poor. Suppose that  $\beta_A$  and  $\beta_B$  are the propagation constants of the fundamental modes in  $A$  and  $B$ , then there is a phase mismatch per unit length along  $z$ , that is,  $\Delta\beta = \beta_A - \beta_B$ . The efficiency of energy transfer between the two guides depends on this phase mismatch. If the phase mismatch  $\Delta\beta = 0$ , then full transfer of power from  $A$  to  $B$  will require a certain coupling distance  $L_o$ , called the **transfer distance**, as shown in Figure 6.29 (b). This transfer distance depends on the efficiency of coupling  $C$  between the two guides  $A$  and  $B$ , which in turn depends on the refractive indices and geometries of the two guides.  $C$  depends on the extent of overlap of the mode fields  $E_A$  and  $E_B$  in Figure 6.29 (a). The transmission length  $L_o$  is inversely proportional to  $C$  (in fact, the theory shows that  $L_o = \pi/C$ ).

In the presence of no mismatch,  $\Delta\beta = 0$ , full transmission would occur over the distance  $L_o$ . However, if there is a mismatch  $\Delta\beta$ , then the transferred power ratio over the distance  $L_o$  becomes a function of  $\Delta\beta$ . Thus, if  $P_A(z)$  and  $P_B(z)$  represent the light power in the guides  $A$  and  $B$  at  $z$ , then

$$\frac{P_B(L_o)}{P_A(0)} = f(\Delta\beta) \quad (6.7.3)$$

where  $f$  is a function designation.  $P_B(L_o)/P_A(0)$  vs. phase mismatch  $\Delta\beta$  is shown in Figure 6.30, which has its maximum when  $\Delta\beta = 0$  (no mismatch) and then decays to zero at  $\Delta\beta = \pi\sqrt{3}/L_o$ . If we could induce a **phase mismatch** of  $\Delta\beta = \pi\sqrt{3}/L_o$  by applying an electric field, which modulates the refractive indices of the guides, we could then prevent the transmission of light power from  $A$  to  $B$ . The light in  $A$  is then *not* transferred to  $B$  at the applied voltage that induces the required phase change.

Figure 6.31 shows an integrated directional coupler where two implanted symmetrical guides  $A$  and  $B$  are coupled over a transmission length  $L_o$  and also have electrodes placed on

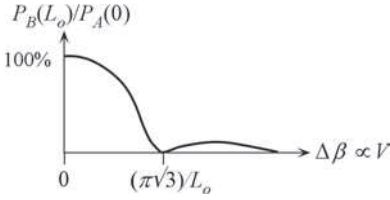


**FIGURE 6.30** Transmission power ratio from guide A to guide B over the transmission length  $L_o$  as a function of mismatch  $\Delta\beta$ .

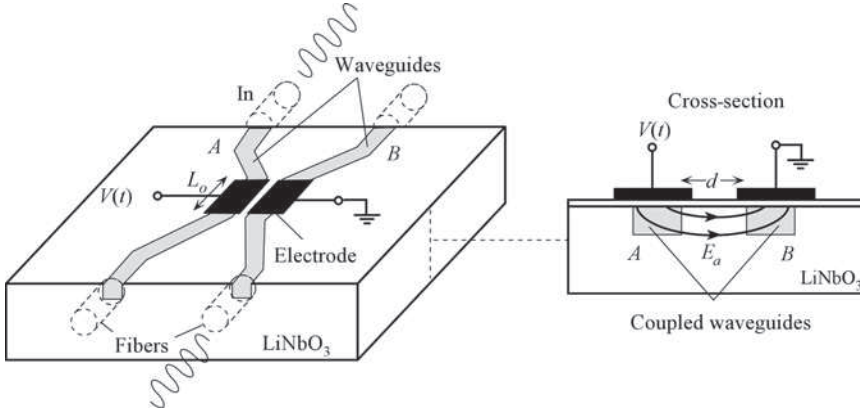


**FIGURE 6.31** An integrated directional coupler. The applied field  $E_a$  alters the refractive indices of the two guides (A and B) and therefore changes the strength of coupling.

them. In the absence of an applied field,  $\Delta\beta = 0$  (no mismatch) and there is a full transmission from guide A to B. If we apply a voltage between the electrodes, the two guides experience an applied field  $E_a$  in opposite directions, and hence experience opposite changes in their refractive indices. Suppose that  $n$  ( $= n_A = n_B$ ) is the refractive index of each guide, and  $\Delta n$  is the induced index change in each guide by the Pockels effect. The induced index difference  $\Delta n_{AB}$  between the guides is  $2\Delta n$ .

We can find  $\Delta n$  from the Pockels effect. The electric field, as a first approximation, can be written as  $E_a \approx V/d$ . However, we need to scale this field down because we need the effective field  $E_{\text{eff}}$  inside the crystal in the region of overlap with the optical mode that is propagating in guides A and B. This effective field  $E_{\text{eff}}$  is the field that modifies the refractive index, and can be written as  $\Gamma V/d$ , where  $\Gamma$ , called the **overlap factor**, is a factor that scales  $V/d$  to the right effective field for use in the Pockels effect; and represents the extent of overlap between the applied field and the optical mode that is propagating.<sup>15</sup> Typical values for  $\Gamma$  are 0.5–0.8. Thus, the mismatch  $\Delta\beta$  is

$$\Delta\beta = \Delta n_{AB} \left( \frac{2\pi}{\lambda} \right) \approx 2 \left( \frac{1}{2} n^3 r \Gamma \frac{V}{d} \right) \left( \frac{2\pi}{\lambda} \right) \quad (6.7.4)$$

Phase  
mismatch  
and  
voltage

<sup>15</sup>The calculation of  $\Gamma$  is actually quite difficult because the field is not uniform and we need to know what fraction of  $V/d$  appears in the optical mode region. Further, we need to average Pockels effect over this mode volume. In the present case, it will suffice to simply use a typical value for  $\Gamma$ .

where  $r$  is the appropriate Pockels coefficient. Setting  $\Delta\beta = \pi\sqrt{3}/L_o$  for the prevention of transfer, the corresponding switching voltage  $V_o$  is

Directional  
coupler  
switching  
voltage

$$V_o \approx \frac{\sqrt{3}\lambda d}{2\Gamma n^3 r L_o} \quad (6.7.5)$$

Since  $L_o$  depends inversely on the coupling efficiency  $C$ , for a given wavelength,  $V_o$  depends on the refractive indices, Pockels coefficient, and the geometry of the guides. Note that we simply used a magic factor  $\Gamma$  to represent the effective field that can be used in the Pockels effect to generate the right  $\Delta n$  that gives the right phase mismatch. The correct approach is to use coupled-wave theory, which is beyond the scope of this book. Equations (6.7.4) and (6.7.5) above are perfectly satisfactory for approximate calculations and clearly show the controlling factors.

### EXAMPLE 6.7.1 Modulated Directional Coupler

Suppose that two optical guides embedded in a substrate such as  $\text{LiNbO}_3$  are coupled as in Figure 6.31 to form a directional coupler, and the transmission length  $L_o = 10$  mm. The coupling separation  $d$  is  $10\text{ }\mu\text{m}$ ,  $\Gamma \approx 0.7$ , the operating wavelength is  $1.3\text{ }\mu\text{m}$  where Pockels coefficient  $r \approx 10 \times 10^{-12}\text{ m V}^{-1}$ , and  $n \approx 2.20$ . What is the switching voltage for this directional coupler?

#### Solution

Using Eq. (6.7.5), we can calculate the switching voltage

$$V_o \approx \frac{\sqrt{3}\lambda d}{2\Gamma n^3 r L_o} = \frac{\sqrt{3}(1.3 \times 10^{-6})(10 \times 10^{-6})}{2(0.7)(2.20)^3(10 \times 10^{-12})(10 \times 10^{-3})} = 15.1\text{ V}$$

## 6.8 ACOUSTO-OPTIC MODULATOR

### A. Photoelastic Effect and Principles

Experiments show that when we induce a strain ( $S$ ) in a crystal, its refractive index  $n$  changes. This change in  $n$  with  $S$  is called the **photoelastic effect**. The strain changes the density of the crystal and distorts the bonds (and hence the electron orbits) which lead to a change in the refractive index  $n$ . If we were to examine the change in  $1/n^2$  instead of  $n$ , then we would find that this is proportional to the induced strain  $S$ , and the proportionality constant is the **photoelastic coefficient**  $p$ , i.e.,

Photoelastic  
effect

$$\Delta\left(\frac{1}{n^2}\right) = pS \quad (6.8.1)$$

The relationship is not as simple as stated in Eq. (6.8.1) since we must consider the effect of a strain  $S$  along one direction in the crystal on the induced change in  $n$  for a particular light propagation direction and some specific polarization. Equation (6.8.1) in reality is a tensor relationship.<sup>16</sup>

<sup>16</sup>As in the case of Pockels effect, we will only use the appropriate photoelastic coefficient, which would be given for the particular problem at hand.

The photoelastic effect in Eq. (6.8.1) provides a convenient means to implement **acousto-optic (AO) modulators** to modulate light. The basic principle is illustrated in Figure 6.32. We can easily generate acoustic or ultrasonic waves in a suitable AO crystal by attaching an ultrasonic transducer, that is, a piezoelectric transducer to one of the crystal faces. The ultrasonic transducer has a piezoelectric crystal with two electrodes, which are driven by an RF source. The piezoelectric crystal vibrates and generates acoustic waves, which are coupled into the AO crystal. The acoustic waves then propagate along the crystal, as visualized in Figure 6.32. These acoustic waves in the crystal propagate by rarefactions and compressions of the crystal, which lead to a periodic variation in the strain and hence a periodic variation in the refractive index in synchronization with the acoustic wave amplitude. Put differently, the periodic variation in the strain  $S$  leads to a periodic variation in  $n$ , owing to the photoelastic effect in Eq. (6.8.1).

The periodic variation in the refractive index works just like a diffraction grating even though it is generated by an acoustic wave, which is moving. If light is incident on this periodic variation of refractive index, it becomes diffracted. There is a transmitted, or through beam and one or many diffracted beams, depending on the mode of operation of the AO modulator. There are essentially two modes of operation. In the **Raman–Nath regime**<sup>17</sup> of operation, as shown in Figure 6.33 (a), the width  $L$  of the diffraction grating is so small that the interaction of the incident light and the grating occurs almost along a line in the  $x$ -direction. The grating is a **thin grating**, and we can view this as the line grating we examined in Chapter 1. [See Figure 1.39 (a).] The thin grating diffracts the incident light into many diffracted beams as shown in Figure 6.33 (a).

On the other hand, in the **Bragg regime**, shown in Figure 6.33 (b), the width of the grating  $L$  is sufficiently large that we need to consider the interference of waves emanating from points along the width  $L$  or along  $z$ . The grating behaves like a **thick grating**, and the diffraction is not as straightforward as in the case of a single-line diffraction grating. For a given incident light wavelength  $\lambda$  and acoustic frequency  $f$ , or acoustic wavelength  $\Lambda$  in the crystal, there is a through (transmitted) beam and only one diffracted beam, corresponding to a first-order diffraction, if the angle of incidence is correct as shown in Figures 6.32 and 6.33 (b). Most practical

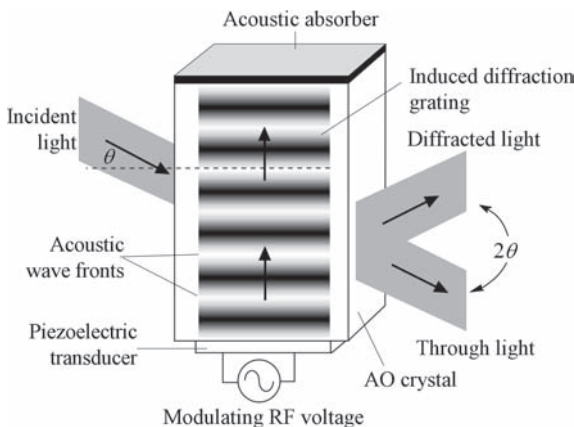


**FIGURE 6.32** A schematic illustration of the principle of the acousto-optic modulator.

<sup>17</sup>Also known as **Debye–Sears regime**.

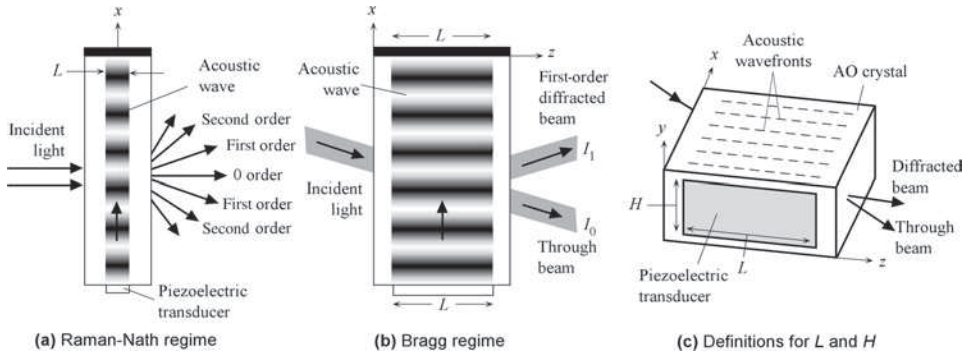


**FIGURE 6.33** Illustration of (a) Raman–Nath and (b) Bragg regimes of operation for an acousto-optic modulator. In the Raman regime, the diffraction occurs as if it were occurring from a line grating. In the Bragg regime, there is a through beam and only one diffracted beam. (c) Definitions of  $L$  and  $H$  based on the transducer and the AO modulator geometry used.

modulators operate in the Bragg regime. In both Figure 6.33 (a) and (b),  $L$  essentially represents the **interaction length** of the incident light with the acoustic grating, and is often called the **equivalent acoustic beam length**. The condition for the Bragg regime is that the interaction length  $L$  should satisfy

$$L \gg \frac{\Lambda^2}{\lambda} \quad (6.8.2)$$

in which  $\Lambda$  is the acoustic wavelength given by  $\Lambda = v_a/f$ , where  $v_a$  is the acoustic velocity and  $f$  is the acoustic frequency.

If  $L \ll \Lambda^2/\lambda$ , then we have the Raman–Nath regime. Suppose we take the light wavelength  $\lambda$  to be  $10^{-6}$  m, and generate 100 MHz acoustic waves in a  $\text{TeO}_2$  crystal (a common AO modulator crystal) in which  $v_a = 4.2 \times 10^3$  m s $^{-1}$ . The  $\Lambda^2/\lambda$  ratio in Eq. (6.8.2) is 1.8 mm. In most practical devices,  $L$  would be greater than this value and the AO modulator would be operating in the Bragg regime. In most cases, high operating acoustic frequencies (leading to shorter  $\Lambda$ ) lead to the Bragg regime and low frequencies (longer  $\Lambda$ ) to the Raman–Nath regime. The ultrasonic transducer attached to the AO crystal would have certain dimensions, which are represented as  $L \times H$  as shown in Figure 6.33 (c), where  $L$  is the length and  $H$  is the height of the transducer along  $x$  and  $y$ , respectively. The acoustic waves generated by this transducer would have a cross-section  $L \times H$ . We assume that this acoustic wave does not significantly diverge as it travels along  $x$ . In addition, we need the height  $H$  of the beam to be wider than the width (or size) of the incident beam along  $y$ , a condition that is easily satisfied in practice.

## B. Acousto-Optic Modulators

Consider the Bragg regime of operation. We can simplistically view the crystal region in which an acoustic wave is propagating as alternations in the refractive index from minimum  $n_{\min}$  to maximum  $n_{\max}$  as illustrated in Figure 6.34. We effectively have planes of layers with alternating indices  $n_{\min}$  and  $n_{\max}$ . The incident light interacts with these alternating planes of high and low refractive index. The acoustic wavelength  $\Lambda$  represents the separation of index boundaries. We can treat the incident optical beam as a stream of parallel coherent waves, two of which,  $A$  and  $B$ , are shown in Figure 6.34. These waves will be partially reflected at  $O$  and  $O_1$  by the

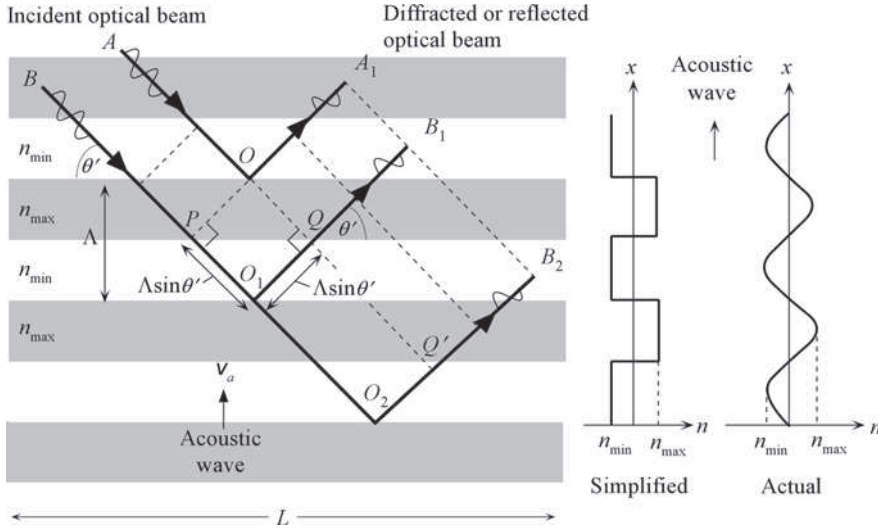


**FIGURE 6.34** Consider two coherent optical waves  $A$  and  $B$  being reflected from two adjacent identical acoustic wavefronts to become  $A_1$  and  $B_1$ . These reflected waves can only constitute the diffracted beam if they are in phase. The angle  $\theta'$  is exaggerated (typically, this is a few degrees).

index changes to become  $A_1$  and  $B_1$ . Further, as in ordinary reflection, we can take the angles of reflection and incidence to be the same. If the reflected waves  $A_1$  and  $B_1$  are in phase, then they would reinforce each other and thereby constitute a *diffracted beam*. Put differently, if there is a diffracted beam, then any two points on  $A_1$  and  $B_1$ , such as  $O$  and  $Q$ , must be on the same wavefront. Note also that the diffracted beam is essentially a *reflected beam*, though we will continue to use the term *diffracted beam*.

The points  $P$  and  $O$  on the incident beam ( $AB$ ) are on the same wavefront. If there is a diffracted beam, then  $O$  and  $Q$  must also be on the same wavefront after reflection. The angle  $\theta'$  represents the angle of the incident light with the acoustic wavefronts inside the crystal. The optical path difference from  $P$  to  $Q$  is  $PO_1Q$ , or  $2\Lambda \sin\theta'$ . This must be a whole optical wavelength in the medium for the diffracted beam to exist, *i.e.*,  $2\Lambda \sin\theta'$  must be  $\lambda/n$ , where  $\lambda$  is the free-space wavelength and  $n$  is the refractive index of the medium (normally taken as the unperturbed index). This condition is satisfied, and a diffracted beam is generated, only when the angle  $\theta'$  satisfies

$$2\Lambda \sin\theta' = \lambda/n; \quad \theta' = \theta'_B \quad (6.8.3)$$

*Bragg condition inside the crystal*

The angle  $\theta'$  that satisfies Eq. (6.8.3) is called the **Bragg angle**  $\theta'_B$ . As mentioned below, *there is only one angle and only one diffracted beam*, which is called the **first-order diffracted beam**. Note that  $\lambda$  is much smaller than  $\Lambda$ , so that  $\sin\theta'$  must be small, and we can use  $\sin\theta' \approx \theta'$  in Eq. (6.8.3). (Clearly, the diffraction shown in Figure 6.34 is highly exaggerated.)

Since the interaction length  $L$  of the grating is large, we also need to consider the partial reflections from different planes. For example, the wave  $B$  will also experience partial reflections from similar boundaries, one of which is  $O_2$  in Figure 6.34. We then need to examine the condition that will allow  $Q'$  on  $B_2$  to be in phase with  $Q$  on  $B_1$  if they are to be on the same wavefront. The examination of partial reflections from deeper planes in Figure 6.34 again leads to Eq. (6.8.3). The statement above that there is only one diffracted beam is not obvious in the



current discussion since any integer multiples of  $\lambda/n$  would also satisfy Eq. (6.8.2), and seemingly generate more diffraction angles. The existence of a single diffracted beam, which is a first-order beam, comes out if we carry out a proper treatment of the problem in which  $n$  varies sinusoidally.<sup>18</sup> In deriving Eq. (6.8.3) we assumed that the incident optical wave and the acoustic wave are both plane waves as shown in Figure 6.34. In practice, both the optical and the acoustic beams have finite sizes and their wavefronts are not perfect plane waves. Further, the interaction distance  $L$  is not infinite. Consequently, the peak diffraction still occurs at  $\theta = \theta_B$ , but there are angles over a small spread around  $\theta_B$  that can still yield some diffraction.

There is one further complication. In deriving Eq. (6.8.3) we assumed that the waves  $A$  and  $B$  were already inside the AO crystal. However, the light incident on the AO crystal is refracted into and then refracted out from the crystal. We are interested in the external angle of incidence and reflection  $\theta$  shown in Figure 6.32. At the surface of the crystal, Snell's law for refraction relates the external angle of incidence  $\theta$  and  $\theta'$  as  $\sin\theta = n\sin\theta'$  so that Eq. (6.8.3) becomes

$$2\Lambda\sin\theta = \lambda; \quad \theta = \theta_B \quad (6.8.4)$$

The frequency of the diffracted light is not the same as that of the incident light. Suppose that  $\omega$  is the angular frequency of the incident optical wave. The optical wave reflections occur from a moving diffraction pattern which moves with an acoustic velocity  $v_a$  as shown in Figure 6.34. As a result of the *Doppler effect*, the diffracted beam has either a slightly higher or slightly lower frequency depending on the direction of the traveling acoustic wave. If  $\Omega$  is the frequency of the acoustic wave, then the diffracted beam has a Doppler-shifted frequency given by

$$\omega' = \omega \pm \Omega \quad (6.8.5)$$

When the acoustic wave is traveling toward the incoming optical beam as in Figure 6.34, the diffracted optical beam frequency is up-shifted, *i.e.*,  $\omega' = \omega + \Omega$ . If the acoustic wave is traveling away from the incident optical beam, then the diffracted frequency is down-shifted,  $\omega' = \omega - \Omega$ . It is apparent that we can tune the frequency (wavelength) of the diffracted light beam by changing the frequency of the acoustic wave. (The diffraction angle is then also changed.)

Although the Bragg condition specifies the incidence angle  $\theta_B$  for beam deflection, it does not say anything about the diffracted optical intensity. As shown in Figure 6.34, there are many partial reflections from numerous planes of refractive index change in the interaction region. The proper analysis is quite complicated, but the final result is straightforward. The intensity of the diffracted (reflected) first-order beam  $I_1$  depends on the induced photoelastic change  $\Delta n$ , which depends on the amplitude and hence intensity of the acoustic waves. In the Bragg regime, the ratio of first-order diffracted (reflected) intensity  $I_1$  to intensity  $I_i$  of incident beam can be viewed as the diffraction (deflection) efficiency  $\eta_{DE}$  of the AO modulator.  $\eta_{DE}$  increases with the power  $P_a$  in the acoustic wave and the interaction length  $L$ , and depends on the material properties of the AO crystal,<sup>19</sup> *i.e.*,

$$\eta_{DE} = \frac{I_1}{I_i} = \sin^2 \left[ \frac{\pi}{\lambda} \left( \frac{L}{2H} M_2 P_a \right)^{1/2} \right] \quad (6.8.6)$$

<sup>18</sup>See, for example, B. E. A. Saleh and M. C. Teich, *Fundamentals of Photonics*, 2nd Edition (Wiley, 2007), Ch. 19.

<sup>19</sup>See, for example, I.-C. Chang, Ch. 6, "Acousto-Optic Modulators," in *The Handbook of Optics*, Vol. V, Ed. M. Bass *et al.*, (McGraw-Hill, 2010); or D. A. Pinnow, *IEEE J. Quantum Electron.*, QE6, 223, 1970.

Bragg  
condition  
with  
external  
angle

Doppler  
shift

Diffracted  
intensity



where  $P_a$  is the power in the acoustic wave,  $L$  is the acoustic beam length, and  $H$  the acoustic beam height, shown in Figure 6.33 (c), and  $M_2$  is a material dependent parameter that gauges the usefulness of the medium for AO modulation.  $M_2$  is called the **AO figure of merit** for the medium, and is defined by

$$M_2 = \frac{n^6 p^2}{\rho v_a^3} \quad (6.8.7) \quad \text{AO figure of merit}$$

where  $\rho$  is the density, and  $p$  is the appropriate photoelastic coefficient. The  $n^6$  in the numerator implies that the changes in  $n$  have the largest effect on the AO modulation efficiency. Table 6.3 summarizes the properties of a few selected useful AO materials. Notice how  $M_2$  can vary by a factor of about 100 from the lowest to the highest.

It should be apparent from Eq. (6.8.6) that the input RF power in the acoustic wave modulates the diffracted beam intensity,  $I_1$ . The through beam is also modulated since power is transferred from the zero-order to the first-order diffracted beam by the diffraction process. Thus, modulating the RF power applied to the piezoelectric transducer, we can modulate power in the acoustic wave and hence modulate both the through and the reflected beams. Figures 6.35 (a) and (b) illustrate how AO modulators can be used in analog and digital modulation. Note how both the diffracted ( $I_1$ ) and the through beam ( $I_0$ ) are modulated by the voltage applied to the transducer.

The modulation speed and hence the bandwidth of an AO are determined by the transit time of the acoustic waves across the light beam waist. If the optical beam has a waist (diameter)  $d$  in the modulator, then rise time (in digital modulation) is inversely proportional to  $d/v_a$ . Reducing  $d$  to increase the speed, however, results in the reduction of diffraction efficiency so there is a compromise between the speed of response and diffraction efficiency.

Acousto-optic modulators are used in a wide range of applications such as light deflectors, scanners, modulators, digital optical switches, frequency shifters,  $Q$ -switches, fiber attenuators, and various other applications. Although we attached a piezoelectric transducer to a crystal to generate acoustic waves, this is actually not necessary. If we use a piezoelectric crystal such as  $\text{LiNbO}_3$ , we can place periodic interdigital electrodes on the crystal surface at one end of

**TABLE 6.3 Properties and figures of merit  $M_2$  for various acousto-optic materials**

Material	$\text{LiNbO}_3$	$\text{TeO}_2$	Ge	GaAs	GaP	$\text{PbMoO}_4$	Fused silica	$\text{Ge}_{33}\text{Se}_{55}\text{As}_{12}$ glass
Useful $\lambda$ ( $\mu\text{m}$ )	0.6–4.5	0.4–5	2–20	1–11	0.6–10	0.4–1.2	0.2–4.5	1.0–14
$\rho$ ( $\text{g cm}^{-3}$ )	4.64	6.0	5.33	5.34	4.13	6.95	2.2	4.4
$n$	2.2	2.26	4	3.37	3.31	2.4	1.46	2.7
(at $\mu\text{m}$ )	(0.633)	(0.633)	(10.6)	(1.15)	(1.15)	(0.633)	(0.633)	
Maximum $p$	0.18	0.34	−0.07 <sup>a</sup>	−0.17 <sup>b</sup>	−0.151	0.3	0.27	0.21 <sup>c</sup>
(at 0.63 $\mu\text{m}$ )	( $p_{31}$ )	( $p_{13}$ )	( $p_{44}$ )	( $p_{11}$ )	( $p_{11}$ )	( $p_{33}$ )	( $p_{12}$ )	( $p_{11}, p_{12}$ )
$v_a$ ( $\text{km s}^{-1}$ )	6.6	4.2	5.5	5.3	6.3	3.7	6	2.5
$M_2$ ( $\text{s}^3 \text{kg}^{-1}$ ) $\times 10^{-15}$	7	35	181	104	45	36	1.5	248

(Source: Extracted from I.-C. Chang, Ch. 6, “Acousto-Optic Modulators” in *The Handbook of Optics*, Vol. V, Ed. M. Bass *et al.*, McGraw-Hill, 2010.)

Notes:  $n$  is the refractive index,  $v_a$  is the acoustic velocity, and  $p$  is the maximum photoelastic coefficient; the exact  $p_{ij}$  is shown in parantheses.  $M_2$  values must be multiplied by  $10^{-15}$ . <sup>a</sup> $\lambda = 2.0$ – $2.2 \mu\text{m}$ ; <sup>b</sup> $1.15 \mu\text{m}$ ; <sup>c</sup> $1.06 \mu\text{m}$ .

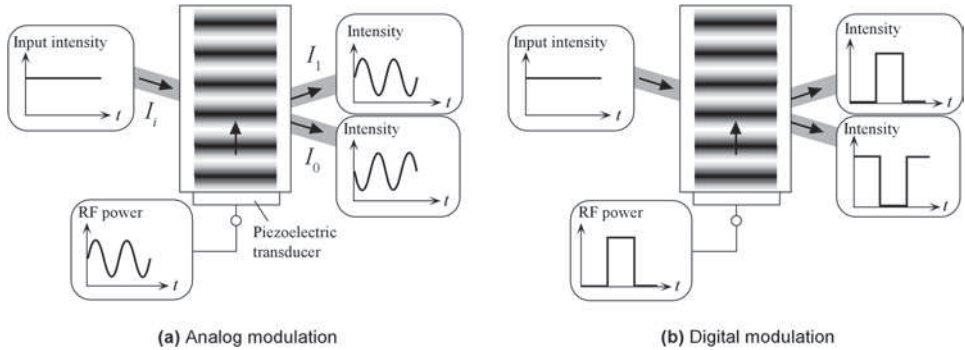


**FIGURE 6.35** (a) Analog modulation of an AO modulator.  $I_i$  is the input intensity,  $I_0$  is the zero-order diffraction, *i.e.*, the transmitted light, and  $I_1$  is the first-order diffracted (reflected) light. (b) Digital modulation of an AO modulator.

the crystal, and then apply the RF voltage to these electrodes as shown in Figure 6.36. Notice that the voltage polarity changes between two neighboring electrodes. The period of the interdigital electrodes (between two closest same-polarity electrodes) is chosen to be the same as the acoustic wave to be generated. The alternating voltage on the digital electrodes generates an alternating field inside the  $\text{LiNbO}_3$  crystal near the surface. Due to the piezoelectric effect, the oscillating RF field generates oscillating strains, that is, lattice vibrations. These lattice vibrations propagate along the surface of the  $\text{LiNbO}_3$  crystal, as shown in Figure 6.36, and are called **surface acoustic waves (SAWs)**. They travel along the surface of the  $\text{LiNbO}_3$  within a depth of about  $\Lambda$ , the acoustic wavelength, and give rise to the desired induced periodic variation in  $n$  through the photoelastic effect.

We need to increase the interaction of the light wave with the acoustic grating to obtain efficient diffraction. The surface region of  $\text{LiNbO}_3$  is doped (*e.g.*, with Ti) to increase its refractive index and hence create a thin planar dielectric waveguide at the surface of the  $\text{LiNbO}_3$  crystal. The light is fed into this thin waveguide where it is guided. This thin waveguide contains the SAW and hence the diffraction grating, from which the light becomes diffracted as illustrated in Figure 6.36.

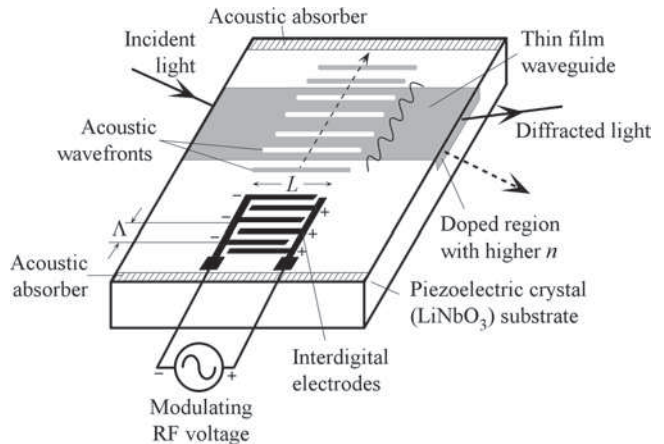


**FIGURE 6.36** A simplified and schematic illustration of a surface acoustic wave (SAW)-based waveguide AO modulator. The polarity of the electrodes shown is at one instant, since the applied voltage is from an AC (RF) source.

**EXAMPLE 6.8.1 AO Modulator**

Suppose that we generate 150 MHz acoustic waves in a TeO<sub>2</sub> crystal. The RF transducer has a length ( $L$ ) of 10 mm and a height ( $H$ ) of 5 mm. Consider modulating a red-laser beam from a He-Ne laser,  $\lambda = 632.8$  nm. Using the values in Table 6.3 for TeO<sub>2</sub>, calculate the acoustic wavelength and hence the Bragg deflection angle. What is the Doppler shift in the wavelength? What is the relative intensity in the first-order deflected beam if the RF acoustic power is 1.0 W?

**Solution**

If  $f$  is the frequency of the acoustic waves, and  $v_a$  is the acoustic velocity, then the acoustic wavelength  $\Lambda$  is

$$\Lambda = \frac{v_a}{f} = \frac{(4.2 \times 10^3 \text{ m s}^{-1})}{(150 \times 10^6 \text{ s}^{-1})} = 2.8 \times 10^{-5} \text{ m} = 28 \text{ } \mu\text{m}$$

Note that  $\Lambda^2/\lambda = (2.8 \times 10^{-5} \text{ m})^2/(0.6328 \times 10^{-6} \text{ m}) = 1.2 \text{ mm}$ . Since  $L (= 10 \text{ mm})$  is much longer than 1.2 mm, we can assume we are in the Bragg regime.

The external Bragg angle  $\theta$  is given by

$$\sin \theta = \frac{\lambda}{2\Lambda} = \frac{(632.8 \times 10^{-9} \text{ m})}{2(2.8 \times 10^{-5} \text{ m})} = 0.0113$$

so that  $\theta = 0.65^\circ$  or a deflection angle  $2\theta$  of  $1.3^\circ$ . Note that we could have easily used  $\sin \theta \approx \theta$ .

The Doppler shift in frequency from Eq. (6.8.5) is simply the acoustic frequency 150 MHz.

The diffraction efficiency into the first order can be found from Eq. (6.8.6)

$$\eta_{\text{DE}} = \sin^2 \left[ \frac{\pi}{(632.8 \times 10^{-9})} \left( \frac{10 \times 10^{-3}}{2(5 \times 10^{-3})} (35 \times 10^{-15})(1) \right)^{1/2} \right] = 0.64 \quad \text{or} \quad 64\%$$

where we have used  $M_2 = 35 \times 10^{-15} \text{ s}^3 \text{ kg}^{-1}$  from Table 6.3.

**6.9 FARADAY ROTATION AND OPTICAL ISOLATORS**

When an optically inactive material such as glass is placed in a strong magnetic field and then a plane polarized light is sent *along* the direction of the magnetic field, it is found that the emerging light's plane of polarization has been rotated. This magneto-optic phenomenon is called the **Faraday effect**, also known as the **Faraday rotation**, as originally observed by Michael Faraday (1845). The magnetic field can be applied, for example, by inserting the material into the core of a magnetic coil—a solenoid. Strong permanent magnets are also used. The induced specific rotatory power, rotation per unit length,  $\theta/L$ , has been found to be proportional to the magnitude of applied magnetic field,  $B$ . The amount of rotation  $\theta$  is given by

$$\theta = VBL \quad (6.9.1) \quad \text{Faraday effect}$$

where  $B$  is the magnetic field (flux density),  $L$  is the length of the medium, and  $V$  is the so-called **Verdet constant** or **coefficient**.<sup>20</sup> It depends on the material and the wavelength.

<sup>20</sup>The term *Verdet constant* is more common.

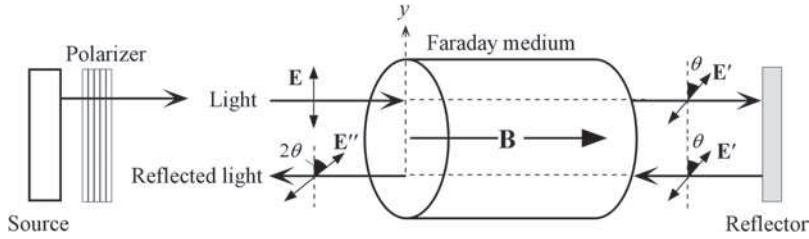


**FIGURE 6.37** The sense of rotation of the optical field  $\mathbf{E}$  depends only on the direction of the magnetic field for a given medium (given Verdet constant). If light is reflected back into the Faraday medium, the field rotates a further  $\theta$  in the same sense to come out as  $\mathbf{E}''$  with a  $2\theta$  rotation with respect to  $\mathbf{E}$ .

It seems to appear that an “optical activity” has been induced by the application of a strong magnetic field to an otherwise optically inactive material. There is, however, an important distinction between the natural optical activity in Figure 6.17 and the Faraday effect. The sense of rotation  $\theta$  in the Faraday effect, for a given material (Verdet constant), depends only on the direction of the magnetic field  $\mathbf{B}$ . If  $V$  is positive, for light propagating parallel to  $\mathbf{B}$ , the optical field  $\mathbf{E}$  rotates in the same sense as an advancing right-handed screw pointing in the direction of  $\mathbf{B}$ , as in Figure 6.37. The direction of light propagation, as in Figure 6.37, does not change the absolute sense of rotation of  $\theta$ . If we reflect the wave to pass through the medium again, the rotation increases to  $2\theta$ .

The Verdet constant depends not only on the wavelength  $\lambda$  but also on the material dispersion, that is,  $n$  vs.  $\lambda$ , through

Verdet  
constant

$$V = -\frac{(e/m_e)\lambda}{2c} \frac{dn}{d\lambda} \quad (6.9.2)$$

We know that near a polarization resonance,  $n$  changes rapidly with  $\lambda$ , and the change,  $dn/d\lambda$ , becomes small as we move away from this resonance peak, *e.g.*, as  $\lambda$  increases. Thus, the Verdet constant generally decreases with wavelength.

An **optical isolator** allows light to pass in one direction and not in the opposite direction. For example, the light source can be isolated from various reflections by placing a polarizer and a Faraday rotator that rotates the field by  $45^\circ$  as in Figure 6.37. The reflected light will have a  $2\theta = 90^\circ$  rotation and will not pass through the polarizer back to the source. The magnetic field is typically applied by enclosing the Faraday medium in a rare-earth magnet ring.

### EXAMPLE 6.9.1 Faraday rotation

Suppose we pass a polarized beam at 633 nm (from a He-Ne laser) through a 5 cm long SF57 dense flint glass rod. If the magnetic field along the rod is 0.7 T, what is the rotation of the optical field?

#### Solution

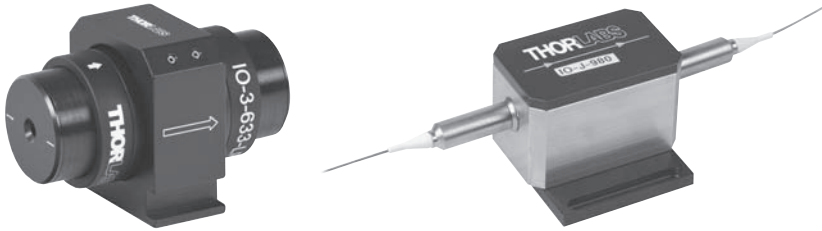
From Table 6.4, at 633 nm,  $V = 20 \text{ rad T}^{-1} \text{ m}^{-1}$  so that the rotation is

$$\theta = VBL = (20 \text{ rad T}^{-1} \text{ m}^{-1})(0.7 \text{ T})(0.05 \text{ m}) = 0.70 \text{ rad} \quad \text{or} \quad 40^\circ$$

**TABLE 6.4 Verdet constants of some selected materials at various wavelengths**

Material and the wavelength	Quartz 589 nm	Tb <sub>3</sub> Ga <sub>5</sub> O <sub>12</sub> 633 nm	ZnS 589 nm	ZnTe 633 nm	NaCl 589 nm	Crown glasses 633 nm	Dense flint glass (SF57) 633 nm
$V(\text{rad m}^{-1} \text{T}^{-1})$	4.0	-134	65.8	188	10	4-6	20

(Source: Data from various sources, including, M.J. Weber, *The Handbook of Optical Materials*, CRC Press, 2003.)



Optical isolators. Left: Free-space optical isolator for use at 633 nm up to 3 W. Right: Fiber-coupled optical isolator for use at 980 nm up to 2 W of optical power. (Courtesy of Thorlabs.)

## 6.10 NONLINEAR OPTICS AND SECOND HARMONIC GENERATION

The application of an electric field  $E$  to a dielectric material causes the constituent atoms and molecules to become polarized. The medium responds to the field  $E$  by developing a polarization  $P$  which represents the net induced dipole moment per unit volume. In a linear dielectric medium, the induced polarization  $P$  is proportional to the electric field  $E$  at that point and the two are related by  $P = \epsilon_0 \chi E$ , where  $\chi$  is the electric susceptibility. However, this linearity breaks down at high fields and the  $P$  vs.  $E$  behavior deviates from the linear relationship as shown in Figure 6.38 (a).  $P$  becomes a function of  $E$  which means that we can expand it in terms of increasing powers of  $E$ . It is customary to represent the induced polarization as

$$P = \epsilon_0 \chi_1 E + \epsilon_0 \chi_2 E^2 + \epsilon_0 \chi_3 E^3 \quad (6.10.1) \quad \text{Induced polarization}$$

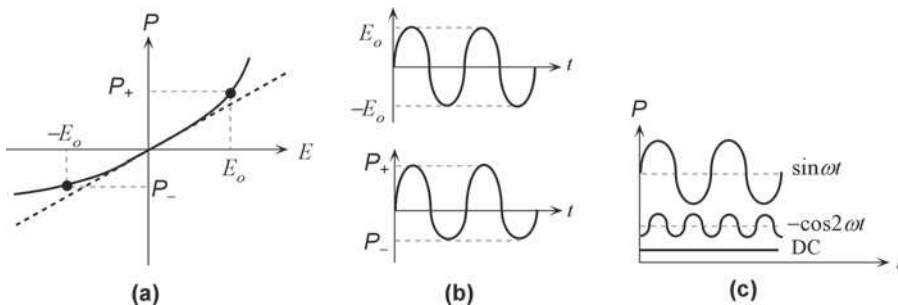


**FIGURE 6.38** (a) Induced polarization vs. optical field for a nonlinear medium. (b) Sinusoidal optical field oscillations between  $\pm E_o$  result in polarization oscillations between  $P_+$  and  $P_-$ . (c) The polarization oscillation can be represented by sinusoidal oscillations at angular frequencies  $\omega$  (fundamental),  $2\omega$  (second harmonic), and a small DC component.

where  $\chi_1$ ,  $\chi_2$ , and  $\chi_3$  are the **linear**, **second-order**, and **third-order susceptibilities**, respectively. The coefficients decrease rapidly for higher terms and are not shown in Eq. (6.10.1). The importance of the second and third terms, *i.e.*, nonlinear effects, depends on the field strength  $E$ . Nonlinear effects begin to become observable when fields are very large, *e.g.*,  $\sim 10^7 \text{ V m}^{-1}$ . Such high fields require light intensities ( $\sim 1000 \text{ kW cm}^{-2}$ ) that invariably require lasers. All materials, whether crystalline or noncrystalline, possess a finite  $\chi_3$  coefficient. However, only certain classes of crystals have a finite  $\chi_2$ , and the reason is the same as for the observation of the Pockels effect.<sup>21</sup> Only those crystals, such as quartz, that have no center of symmetry have nonzero  $\chi_2$  coefficient; these crystals are also piezoelectric. One of the most important consequences of the nonlinear effect is the **second harmonic generation (SHG)**,<sup>22</sup> when an intense light beam of frequency<sup>23</sup>  $\omega$  passing through an appropriate crystal (*e.g.*, quartz) generates a light beam of double the frequency,  $2\omega$ . SHG is based on a finite  $\chi_2$  coefficient in which the effect of  $\chi_3$  is negligible.

Consider a beam of monochromatic light, with a well-defined angular frequency  $\omega$ , passing through a medium. The optical field  $E$  at any point in the medium will polarize the medium at the same point in synchronization with the optical field oscillations. An oscillating dipole moment is well known as an electromagnetic emission source (just like an antenna). These secondary electromagnetic emissions from the dipoles in the medium interfere and constitute the actual wave traveling through the medium (Huygen's construction from secondary waves). Suppose that the optical field is oscillating sinusoidally between  $\pm E_o$  as shown in Figure 6.38 (b). In the linear regime, *i.e.*, under small fields,  $P$  oscillations will also be sinusoidal with a frequency  $\omega$ .

If the field strength is sufficiently large, the induced polarization will not be linear as indicated in Figure 6.38 (a), and will not oscillate in a simple sinusoidal fashion as shown in Figure 6.38 (b). The polarization now oscillates between  $P_+$  and  $P_-$  and is not symmetrical. The oscillations of the dipole moment  $P$  now emit waves not only at the frequency  $\omega$  but also at  $2\omega$ . In addition there is a DC component (light is said to be rectified, *i.e.*, it gives rise to a small permanent polarization). The *fundamental*  $\omega$  and the *second harmonic*,  $2\omega$ , components, along with the DC, are shown in Figure 6.38 (c).

If we write the optical field as  $E = E_o \sin(\omega t)$  and substitute this into Eq. (6.10.1), after some trigonometric manipulation,<sup>24</sup> and neglecting  $\chi_3$  terms, we would find the induced  $P$  as

$$P = \epsilon_o \chi_1 E_o \sin(\omega t) - \frac{1}{2} \epsilon_o \chi_2 E_o \cos(2\omega t) + \frac{1}{2} \epsilon_o \chi_2 E_o \quad (6.10.2)$$

The first term is the fundamental, the second is the second harmonic, and the third is the DC term (permanent polarization in the medium) as summarized in Figure 6.38 (c). The second harmonic ( $2\omega$ ) oscillation of local dipole moments generates secondary second harmonic ( $2\omega$ ) waves in the crystal. It may be thought that these secondary waves will interfere constructively and result in a second harmonic beam just as the fundamental ( $\omega$ ) secondary waves interfere and give rise to the propagating light beam. However, the crystal will normally possess

<sup>21</sup> See Section 6.6 B on the Pockels Effect.

<sup>22</sup> Second harmonic generation was first experimentally demonstrated by Peter A. Franken and coworkers at the University of Michigan (1961), where they focused a 3 kW pulse of red light (694.3 nm) from a ruby laser onto a quartz crystal and observed some ultraviolet light (347.15 nm) coming out. The conversion efficiency was  $1 \text{ in } 10^6$  [Eugene Hecht, *Optics*, 2nd Edition (Addison Wesley, 1987), p. 612].

<sup>23</sup> In this section, for brevity, the adjective *angular* is dropped from the frequency, though implied.

<sup>24</sup> That is,  $\sin^2(\omega t) = \frac{1}{2}[1 - \cos(2\omega t)]$ .

different refractive indices  $n(\omega)$  and  $n(2\omega)$  for frequencies  $\omega$  and  $2\omega$ , which means that the  $\omega$ - and  $2\omega$ -waves propagate with different phase velocities  $v_1$  and  $v_2$ , respectively. As the  $\omega$ -wave propagates in the crystal, it generates secondary  $2\omega$ -waves along its path, indicated as  $S_1$ ,  $S_2$ ,  $S_3$ , ... in Figure 6.39. When wave  $S_2$  is generated,  $S_1$  must arrive there in phase, which means  $S_2$  must travel with the same velocity as the fundamental wave, and so on as in Figure 6.39. It is apparent that only if these  $2\omega$ -waves are in phase, that is, they propagate with the same velocity as the  $\omega$ -wave, they can interfere constructively and constitute a second harmonic beam. Otherwise, the  $S_1$ ,  $S_2$ , and  $S_3$  will eventually fall out of phase and destroy each other, and there will be either no or very little second harmonic beam. The condition that the second harmonic waves must travel with the same phase velocity as the fundamental wave to constitute a second harmonic beam is called **phase matching** and requires  $n(\omega) = n(2\omega)$ . For most crystals, this is not possible as  $n$  is dispersive; that is, it depends on the wavelength.

SHG efficiency depends on the extent of phase matching,  $n(\omega) = n(2\omega)$ . One method is to use a birefringent crystal as these have two refractive indices: ordinary index  $n_o$  and extraordinary index  $n_e$ . Suppose that along a certain crystal direction at an angle  $\theta$  to the optic axis,  $n_e(2\omega)$  at the second harmonic is the same as  $n_o(\omega)$  at the fundamental frequency:  $n_e(2\omega) = n_o(\omega)$ . This is called **index matching** and the angle  $\theta$  is the **phase matching angle**. Thus, the fundamental would propagate as an ordinary wave and the second harmonic as an extraordinary wave and both would be in phase. This would maximize the conversion efficiency, though this would still be limited by the magnitude of the second term with respect to the first in Eq. (6.10.1). To separate the second harmonic beam from the fundamental beam, something like a diffraction grating, a prism or an optical filter will have to be used at the output as illustrated in Figure 6.40 (a). The phase matching angle  $\theta$  depends on the wavelength (or  $\omega$ ) and is sensitive to temperature.

Most green lasers, including many green laser pointers, use SHG in a similar way to that illustrated in Figure 6.40 (a). A diode-pumped  $\text{Nd}^{3+}$ -ion solid-state laser (e.g.,  $\text{Nd}^{3+}:\text{YVO}_4$  or  $\text{Nd}^{3+}:\text{YAG}$ ) produces a CW lasing emission at 1064 nm. This is a diode-pumped solid-state laser, and needs a laser diode emitting at 808 nm for pumping as shown in Figure 6.40 (b). The 1064 nm laser radiation from the  $\text{Nd}^{3+}:\text{YVO}_4$  is fed into the KTP crystal placed next it, and is often optically cemented to it. The 1064 nm laser intensity is sufficiently high to allow the SHG in KDP to produce a green radiation output beam. Most importantly, the  $\text{YVO}_4$  and KTP crystals are both placed *within* the optical cavity of the laser that is producing the  $\omega$ -radiation (the 1064 nm radiation), as shown in Figure 6.40 (b). Within the optical cavity, the  $\omega$ -radiation has high intensity, which enhances SHG, a distinct advantage. The cemented  $\text{YVO}_4$  and KTP crystals are typically a few millimeters in total thickness and come with the end-mirrors coated.

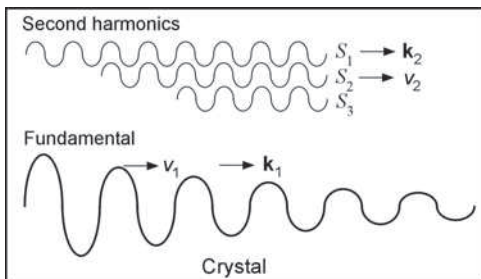


**FIGURE 6.39** As the fundamental wave propagates, it periodically generates second harmonic waves ( $S_1$ ,  $S_2$ ,  $S_3$ , ...) and if these are in phase then the amplitude of the second harmonic light builds up.



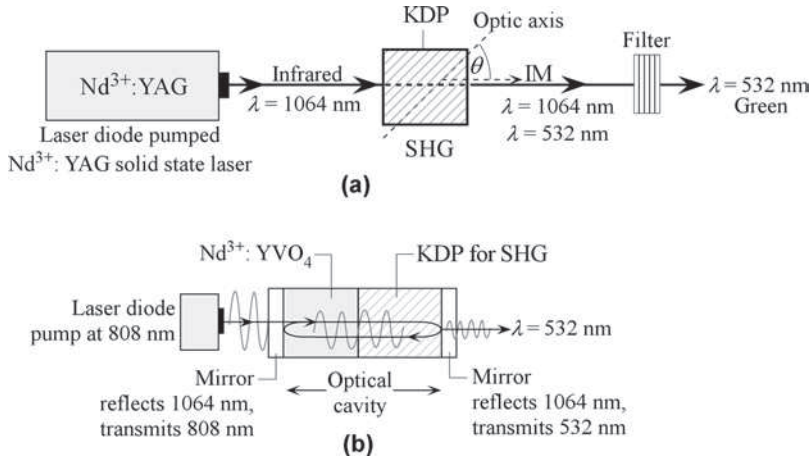


**FIGURE 6.40** (a) A simplified schematic illustration of optical frequency doubling using a KDP (potassium dihydrogen phosphate) crystal. IM is the index-matched direction at an angle  $\theta$  (about  $35^\circ$ ) to the optic axis. Along the IM direction,  $n_e(2\omega) = n_o(\omega)$ . The focusing of the laser beam onto the KDP crystal and the collimation of the light emerging from the crystal are not shown. (b) Typical SHG-based green laser principle. The KDP crystal is next to the  $\text{Nd}^{3+}:\text{YVO}_4$  crystal and both inside the laser optical cavity. The end mirrors reflect 1064 nm radiation and hence allow the 1064 nm radiation to build-up in the cavity.

It is instructive to consider the SHG process in terms of photon interactions inside the crystal, as shown in Figure 6.41. Two fundamental mode photons in the incident beam interact with the dipole moments in the crystal to produce a single second harmonic photon. From modern physics we know that the photon momentum is  $\hbar\mathbf{k}$  and its energy is  $\hbar\omega$ . Suppose that subscripts 1 and 2 refer to fundamental and second harmonic photons. In general terms, we can write the following two equations. Conservation of momentum requires that

$$\hbar\mathbf{k}_1 + \hbar\mathbf{k}_1 = \hbar\mathbf{k}_2 \quad (6.10.3)$$

The conservation of energy requires that

$$\hbar\omega_1 + \hbar\omega_1 = \hbar\omega_2 \quad (6.10.4)$$

We tacitly assumed that the interaction does not result in phonon (lattice vibration) generation or absorption. We can satisfy Eq. (6.10.4) by taking  $\omega_2 = 2\omega_1$ , so that the frequency of the second harmonic is indeed twice the fundamental. To satisfy Eq. (6.10.3) we need  $\mathbf{k}_2 = 2\mathbf{k}_1$ . The phase velocity  $v_2$  of the second harmonic waves is

$$v_2 = \frac{\omega_2}{k_2} = \frac{2\omega_1}{2k_1} = \frac{\omega_1}{k_1} = v_1$$

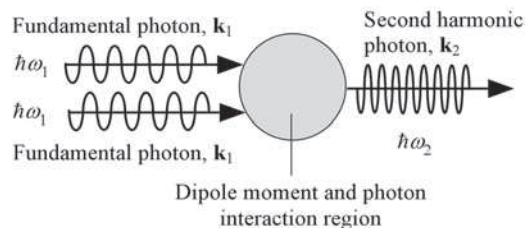


**FIGURE 6.41** Photonic interpretation of second harmonic generation.

Thus, the fundamental and second harmonic photons are required to have the same phase velocity, which is tantamount to the phase matching criterion developed above in terms of pure waves. If  $\mathbf{k}_2$  is not exactly  $2\mathbf{k}_1$ , *i.e.*,  $\Delta k = k_2 - 2k_1$  is not zero (there is a mismatch), then SHG is only effective over a limited length  $l_c$ , which can be shown to be given by  $l_c = \pi/\Delta k$ . This length  $l_c$  is essentially the *coherence length* of the second harmonic; depending on the index difference, this may be quite short, *e.g.*,  $l_c \approx 1 - 100 \mu\text{m}$ . If the crystal size is longer than this, the second harmonics will interfere randomly with each other and the SHG efficiency will be very poor, if not zero. Phase matching is therefore an essential requirement for SHG. The conversion efficiency depends on the intensity of exciting laser beam, the  $\chi_2$  coefficient of the material, and the extent of phase matching and can be substantial (as high as 70–80%) if well-engineered, for example, by placing the converting crystal into the cavity of the laser itself.

## Additional Topics

### 6.11 JONES VECTORS

We can represent the state of polarization of a light wave by using a matrix, called a **Jones matrix**<sup>25</sup> (or vector). Various operations on the polarization state of light then correspond to multiplying this matrix with another matrix that represents the optical operation. Consider a light wave traveling along  $z$  with field components  $E_x$  and  $E_y$  along  $x$  and  $y$ . These components are orthogonal and, in general, would be of different magnitudes and have a phase difference  $\phi$  between them. If we use the exponential notation then

$$E_x = E_{xo} \exp[j(\omega t - kz + \phi_x)] \quad \text{and} \quad E_y = E_{yo} \exp[j(\omega t - kz + \phi_y)]$$

**Jones matrix** is a column matrix whose elements are  $E_x$  and  $E_y$  without the common  $\exp j(\omega t - kz)$  factor

$$\mathbf{E} = \begin{bmatrix} E_x \\ E_y \end{bmatrix} = \begin{bmatrix} E_{xo} \exp(j\phi_x) \\ E_{yo} \exp(j\phi_y) \end{bmatrix} \quad (6.11.1)$$

Usually Eq. (6.11.1) is normalized by dividing by the total amplitude  $E_o = (E_{xo}^2 + E_{yo}^2)^{1/2}$ . We can factor out  $\exp(j\phi_x)$  to further simplify the matrix to obtain the **Jones matrix**

$$\mathbf{J} = \frac{1}{E_o} \begin{bmatrix} E_{xo} \\ E_{yo} \exp(j\phi) \end{bmatrix} \quad (6.11.2)$$

where  $\phi = \phi_y - \phi_x$ . For example, a light wave that is linearly polarized with the field at  $45^\circ$  to the  $x$ -axis can be conveniently written as

$$\mathbf{J} = \frac{1}{\sqrt{2}} \begin{bmatrix} 1 \\ 1 \end{bmatrix}$$

<sup>25</sup>R. Clark Jones introduced these matrices circa 1941.

**TABLE 6.5** Examples of Jones vectors

<b>Jones vector <math>\mathbf{J}_{in}</math></b>	$\begin{bmatrix} 1 \\ 0 \end{bmatrix}$	$\frac{1}{\sqrt{2}} \begin{bmatrix} 1 \\ 1 \end{bmatrix}$	$\begin{bmatrix} \cos \theta \\ \sin \theta \end{bmatrix}$	$\frac{1}{\sqrt{2}} \begin{bmatrix} 1 \\ j \end{bmatrix}$	$\frac{1}{\sqrt{2}} \begin{bmatrix} 1 \\ -j \end{bmatrix}$
<b>Polarization</b>	Linear; horizontal $\mathbf{E}$	Linear; $\mathbf{E}$ at $45^\circ$ to $x$ -axis	Linear; $\mathbf{E}$ at $\theta$ to $x$ -axis	Right circularly polarized	Left circularly polarized
<b>Transmission matrix <math>\mathbf{T}</math></b>	$\begin{bmatrix} 1 & 0 \\ 0 & 0 \end{bmatrix}$	$\begin{bmatrix} e^{j\phi} & 0 \\ 0 & e^{j\phi} \end{bmatrix}$	$\begin{bmatrix} 1 & 0 \\ 0 & j \end{bmatrix}$	$\begin{bmatrix} 1 & 0 \\ 0 & -1 \end{bmatrix}$	$\begin{bmatrix} 1 & 0 \\ 0 & e^{-j\Gamma} \end{bmatrix}$
<b>Optical operation</b>	Linear polarizer; horizontal transmission axis	Isotropic phase changer	Quarter-wave plate	Half-wave plate	Wave retarder; fast axis along $x$

Table 6.5 shows Jones vectors for various polarizations. Note that right and left circularly polarized waves have matrices with complex numbers. In this case  $\pm j$  for the bottom matrix element, by virtue of Eq. (6.11.2), implies that  $E_y$  is  $\pm 90^\circ$  out of phase with  $E_x$ , which results in a circularly polarized light.

If we pass a wave of given Jones vector  $\mathbf{J}_{in}$  through an optical device, then this operation would be multiplying  $\mathbf{J}_{in}$  by the **transmission matrix  $\mathbf{T}$**  of the device. If  $\mathbf{J}_{out}$  is the Jones vector for the output light through the device, then

$$\mathbf{J}_{out} = \mathbf{T} \mathbf{J}_{in} \quad (6.11.3)$$

For example, the transmission matrix for **quarter-wave operation** would be

$$\mathbf{T} = \begin{bmatrix} 1 & 0 \\ 0 & j \end{bmatrix}$$

The output will be

$$\mathbf{J}_{out} = \mathbf{T} \mathbf{J}_{in} = \begin{bmatrix} 1 & 0 \\ 0 & j \end{bmatrix} \begin{bmatrix} 1 \\ 1 \end{bmatrix} = \begin{bmatrix} 1 \\ j \end{bmatrix}$$

which represents a wave that has  $E_y$  and  $E_x$  out of phase by  $\pi/2$ , and hence corresponds to a right circularly polarized light as given in Table 6.5. We can represent a chain of optical manipulations by multiplying Jones matrices and eventually find the output light. Various optical operations are also shown in Table 6.5.

## Questions and Problems

**6.1 Polarization** Suppose that we write the  $E_y$  and  $E_x$  components of a light wave generally as

$$E_x = E_{xo} \cos(\omega t - kz) \quad \text{and} \quad E_y = E_{yo} \cos(\omega t - kz + \phi)$$

Show that at any instant  $E_x$  and  $E_y$  satisfy the ellipse equation on the  $E_y$  vs.  $E_x$  coordinate system:

$$\left( \frac{E_x}{E_{xo}} \right)^2 + \left( \frac{E_y}{E_{yo}} \right)^2 - 2 \left( \frac{E_x}{E_{xo}} \right) \left( \frac{E_y}{E_{yo}} \right) \cos \phi = \sin^2 \phi$$

Sketch schematically what this ellipse looks like assuming  $E_{xo} = 2E_{yo}$ . When would this ellipse form (a) an ellipse with its major axis on the  $x$ -axis, (b) a linearly polarized light at  $45^\circ$ , (c) right and left circularly polarized light?

- 6.2 Linear and circular polarization** Show that a linearly polarized light wave can be represented by two circularly polarized light waves with opposite rotations. Consider the simplest case of a wave linearly polarized along the  $y$ -axis. What is your conclusion?
- 6.3 Wire-grid polarizer** Figure 6.42 shows a wire-grid polarizer which consists of closely spaced parallel thin conducting wires. The light beam passing through the wire grid is observed to be linearly polarized at right angles to the wires. Can you explain the operation of this polarizer?

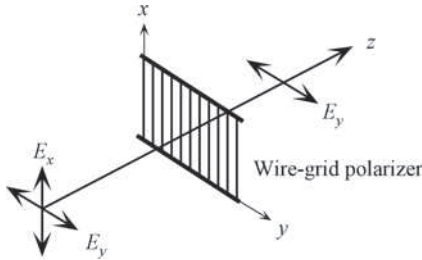


**FIGURE 6.42** The wire grid acts as a polarizer.

- 6.4 Anisotropic scattering and polarization** It is well known that an oscillating electric dipole emits electromagnetic radiation. Figure 6.43 (a) shows a snapshot of the electric field pattern around an oscillating electric dipole moment  $p(t)$  parallel to the  $y$ -axis. There is no field radiation along the dipole axis  $y$ . The irradiance  $I$  of the radiation along a direction at an angle  $\theta$  perpendicular to the dipole axis is proportional to  $\cos^2\theta$ . Sketch the relative radiation intensity pattern around the oscillating dipole. Suppose that the electric field in an incoming electromagnetic wave induces dipole oscillations in a molecule of the medium. Explain how scattering of an incident unpolarized electromagnetic wave by this molecule leads to waves with different polarizations along the  $x$ - and  $y$ -axes in Figure 6.43 (b).

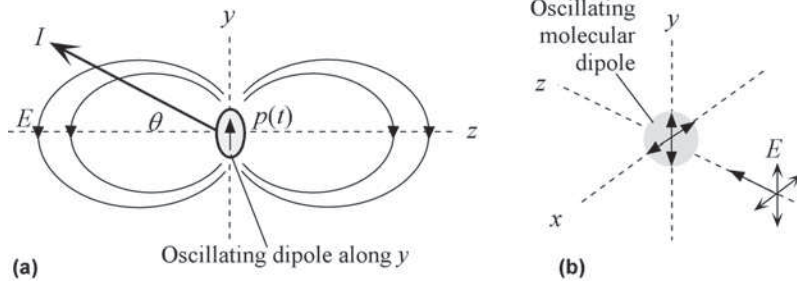


**FIGURE 6.43** (a) A snapshot of the field pattern around an oscillating dipole moment in the  $y$ -direction. Maximum electromagnetic radiation is perpendicular to the dipole axis and there is no radiation along the dipole axis. (b) Scattering of electromagnetic waves from induced molecular dipole oscillations is anisotropic.

- 6.5 Malus's law** Find the angle between the transmission axes of two polarizers for the transmitted light intensity through both polarizers to be 60%, and 30%.
- 6.6 Modulation by Malus's law** Suppose that a linearly polarized light is passed through a polarizer placed with its transmission axis at an angle  $\pi/4$  (or  $45^\circ$ ) to the incoming optical field. Suppose now that we *rotationally modulate* the transmission axis of the polarizer by small amounts  $\phi$  about  $\pi/4$  (by using a suitable piezoelectric actuator). Show that the changes in the transmission intensity is

$$\Delta I \propto -\phi + \frac{2}{3}\phi^3 - \dots$$

where  $\phi$  is in radians. What is the extent of change (in degrees) in  $\phi$  so that the second term is only 1% of the first term? What is your conclusion?

- 6.7 Birefringence** Consider a negative uniaxial crystal such as calcite ( $n_e < n_o$ ) plate that has the optic axis (taken along  $z$ ) parallel to the plate face. Suppose that a linearly polarized wave is incident at normal incidence on a plate face. If the optical field is at an angle  $45^\circ$  to the optic axis, sketch the rays through the calcite plate.
- 6.8 Wave plates** A quarter-wave plate is rotated between two crossed polaroids. If an unpolarized beam is incident on the first polaroid, describe the variation of intensity of the emergent beam as the quarter-wave plate is rotated. What would happen if we have a half-wave plate in place of the quarter-wave plate?
- 6.9 Soleil Compensator** Consider a Soleil compensator as shown in Figure 6.15 that uses a quartz crystal. Given a light wave with a wavelength  $\lambda \approx 633$  nm, a lower plate thickness of 6 mm, calculate the range of  $d$  values in Figure 6.15 that provide a retardation from 0 to  $\pi/2$  (quarter-wavelength).
- 6.10 Quartz Wollaston prism** Draw a quartz Wollaston prism and clearly show and identify the directions of orthogonally polarized waves traveling through the prisms. How would you test the polarization states of the emerging rays? Consider two identical Wollaston prisms, one from calcite and the other from quartz. Which will have a greater beam-splitting ability? Explain.
- 6.11 Glan–Foucault prism** Figure 6.44 shows the cross-section of a Glan–Foucault prism which is made of two right angle calcite prisms with a prism angle of  $38.5^\circ$ . Both have their optic axes parallel to each other and to the block faces as in the figure. Explain the operation of the prisms and show that the  $o$ -wave does indeed experience total internal reflection.

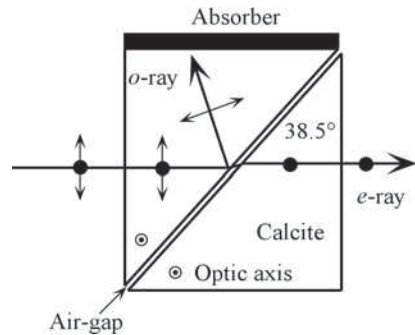


**FIGURE 6.44** The Glan–Foucault prism provides linearly polarized light.

### 6.12 Optical activity

- (a) Consider an optically active medium. The experimenter *A* (Alan) sends a vertically polarized light into this medium as shown in Figure 6.17. The light that emerges from the back of the crystal is received by an experimenter *B* (Barbara). *B* observes that the optical field  $\mathbf{E}$  has been rotated to  $\mathbf{E}'$  counterclockwise. She reflects the wave back into the medium so that *A* can receive it. Describe the observations of *A* and *B*. What is your conclusion?
- (b) Figure 6.45 shows a simplified version of the Fresnel prism that converts an incoming unpolarized light into two divergent beams that have opposite circular polarizations. Explain the principle of operation.

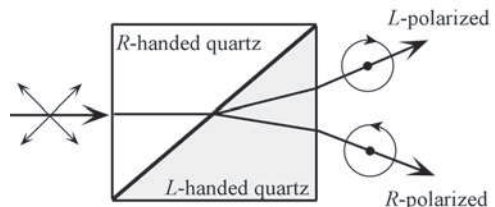


**FIGURE 6.45** The Fresnel prism for separating unpolarized light into two divergent beams with opposite circular polarizations ( $R$  = right,  $L$  = left; divergence is exaggerated).

### 6.13 Liquid crystal display

Consider the LCD display shown in Figure 6.20.

- (a) The LCD display shown in Figure 6.20 would be one of the pixels on an LCD display. Based on Chapter 5, how would you use an active matrix array technology to drive the pixels on an LCD screen?
- (b) Sketch how you would construct an LCD cell that is normally black and becomes bright upon the application of an AC voltage.

- 6.14 Liquid crystal display** The LCD characterization measurements of M. Schadt and W. Helfrich reported in their paper in *Applied Physics Letters* in 1971 (18, 127, 1971) are summarized in Table 6.6.  $\Phi$  is the rotation of the linearly polarized light through the liquid crystal and  $V_{\text{rms}}$  is the rms voltage of the 1 kHz AC voltage used to drive the LCD. The normalized transmittance  $T' = T(V_{\text{rms}})/T_{\text{max}}$  is the measured transmittance divided by the maximum transmittance. Their LCD cell was 10  $\mu\text{m}$  in thickness, whereas most LCDs in modern displays have a thickness of about 5  $\mu\text{m}$  or less. (a) Plot  $\Phi$  vs.  $V_{\text{rms}}$ . (b) Plot  $T'$  vs.  $V_{\text{rms}}$ . (c) What are the threshold and saturation voltages?

**TABLE 6.6** Data obtained by M. Schadt and W. Helfrich on a twisted nematic liquid crystal cell. The normalized transmission  $T'$  is the measured transmittance divided by the maximum transmittance, i.e.,  $T(V_{\text{rms}})/T_{\text{max}}$

$V_{\text{rms}}$ (V)	0.17	0.98	3.00	3.57	3.97	4.49	4.90	5.30	5.99	6.99		
$\Phi$	89.4°	89.2°	89.6°	84.5°	71.7°	52.3°	34.6°	16.9°	8.84°	2.75°		
$V_{\text{rms}}$ (V)	0.20	1.50	3.00	3.39	3.71	4.01	4.50	5.00	5.46	6.00	6.97	7.72
$T'$ (%)	3.41	3.41	3.41	6.83	15.1	30.1	60.0	80.1	91.8	96.2	99.6	100

(Source: Data extracted from Figure 2 in the original paper.)

- 6.15 LiNbO<sub>3</sub> phase modulator** What should be the aspect ratio  $d/L$  for the transverse LiNbO<sub>3</sub> phase modulator in Figure 6.24 that will operate at a free-space wavelength of 1.3  $\mu\text{m}$  and will provide a phase shift  $\Delta\phi$  of  $\pi$  (half wavelength) between the two orthogonal field components propagating through the crystal for an applied voltage of 12 V?

We cannot arbitrarily set  $d/L$  to any ratio we like for the simple reason that when  $d$  becomes too small, the light will suffer diffraction effects that will prevent it from passing through the device. Consideration of diffraction effects leads to<sup>26</sup>

$$d \approx 2 \left( \frac{\lambda L}{n_o \pi} \right)^{1/2}$$

Taking the crystal length  $L \approx 20$  mm, calculate  $d$  and hence the new aspect ratio.

- 6.16 Transverse Pockels cell with LiNbO<sub>3</sub>** Suppose that instead of the configuration in Figure 6.25, the field is applied along the  $z$ -axis of the crystal and the light propagates along the  $y$ -axis. The  $z$ -axis is the polarization of the ordinary wave and  $x$ -axis that of the extraordinary wave. Light propagates through as  $o$ - and  $e$ -waves. Given that  $E_a = V/d$ , where  $d$  is the crystal length along  $z$  (crystal thickness), the indices are

$$n'_o \approx n_o + \frac{1}{2} n_o^3 r_{13} E_a \quad \text{and} \quad n'_e \approx n_e + \frac{1}{2} n_e^3 r_{33} E_a$$

Show that the phase difference between the  $o$ - and  $e$ -waves emerging from the crystal is

$$\Delta\phi = \phi_e - \phi_o = \frac{2\pi L}{\lambda} (n_e - n_o) + \frac{2\pi L}{\lambda} \left[ \frac{1}{2} (n_e^3 r_{33} - n_o^3 r_{13}) \right] \frac{V}{d}$$

where  $L$  is the crystal length along the  $y$ -axis.

Explain the first and second terms. How would you use two such Pockels cells to cancel the first terms in the total phase shift for the two cells?

If the light beam entering the crystal is linearly polarized in the  $z$ -direction, show that

$$\Delta\phi = \frac{2\pi n_e L}{\lambda} + \frac{2\pi L}{\lambda} \left[ \frac{n_e^3 r_{33}}{2} \right] \frac{V}{d}$$

Consider a nearly monochromatic light beam of the free-space wavelength  $\lambda = 633$  nm and polarization along  $z$ -axis. Calculate the voltage  $V_\pi$  needed to *change* the output phase  $\Delta\phi$  by  $\pi$  given a LiNbO<sub>3</sub> crystal with  $d/L = 0.01$  (see Table 6.2).

<sup>26</sup>A. K. Ghatak and K. Thyagarajan, *Optical Electronics* (Cambridge University Press, 1989), pp. 477–479.

**6.17 Longitudinal Pockels cell**

- (a) Sketch schematically the structure of a longitudinal Pockels cell in which the applied field is along the direction of light propagation, both parallel to the  $z$ -axis (optic axis). Suggest schemes that would allow light to enter the crystal along the applied field direction.
- (b) Suppose that an  $\text{LiNbO}_3$  crystal is used.  $\text{LiNbO}_3$  is uniaxial and  $n_1 = n_2 = n_o$  (polarizations parallel to  $x$  and  $y$ ) and  $n_3 = n_e$  (polarization parallel to  $z$ ). Neglecting the rotation of the axes (same principal axes in the presence of an applied field), the new ordinary refractive index is

$$n'_o \approx n_o + \frac{1}{2}n_o^3 r_{13} E_a$$

Calculate the half-wave voltage required to induce a retardation of  $\pi$  between the emerging and incident waves if the free-space wavelength is  $1\text{ }\mu\text{m}$ . What are their polarizations? (Note: For  $\text{LiNbO}_3$  at  $633\text{ nm}$ ,  $n_o \approx 2.28$  and  $r_{13} \approx 9 \times 10^{-12}\text{ m V}^{-1}$ .)

- (c) Suppose that a KDP crystal is used. KDP is uniaxial and  $n_1 = n_2 = n_o$  (polarizations parallel to  $x$  and  $y$ ) and  $n_3 = n_e$  (polarization parallel to  $z$ ). The principal axes  $x$  and  $y$  are rotated by  $45^\circ$  to become  $x'$  and  $y'$  as in Figure 6.23 and

$$n'_1 \approx n_o - \frac{1}{2}n_o^3 r_{63} E_a \quad n'_2 \approx n_o + \frac{1}{2}n_o^3 r_{63} E_a \quad \text{and} \quad n'_3 = n_3 = n_e$$

Calculate the half-wave voltage required to induce a retardation of  $\pi$  between the emerging components of the electric field for free-space wavelength of  $633\text{ nm}$  if, for KDP at this wavelength,  $n_o \approx 1.51$  and  $r_{63} \approx 10.3 \times 10^{-12}\text{ m V}^{-1}$ .

- 6.18 Response time and bandwidth of an EO phase modulator** Consider the electro-optic modulator in Figure 6.46 (a). Suppose that we suddenly apply a step-voltage from a supply with an output resistance  $R_s = 50\text{ }\Omega$  (or this may be the impedance of a coaxial cable bringing in the pulse). The EO crystal between the electrodes is a dielectric with a relative permittivity  $\epsilon_r$ . The time required to charge (and discharge) the capacitance between the electrodes is determined by the time constant of the electric circuit,  $\tau = R_s C_{\text{EO}}$ , where  $C_{\text{EO}}$  is the capacitance of the EO crystal. On the other hand, light has to propagate through the length  $L$  of the EO crystal. This transit time  $\tau_{\text{light}}$  of light is determined by the length  $L$  and the refractive index  $n$ . Thus,

$$\tau = \frac{R_s L W \epsilon_o \epsilon_r}{D} \quad \text{and} \quad \tau_{\text{light}} = \frac{L}{c/n}$$

- (a) Calculate these characteristic times for a GaAs crystal assuming an operation at  $\lambda = 1.3\text{ }\mu\text{m}$ , length  $L = 20\text{ mm}$ , width  $W = 2\text{ mm}$ , and thickness  $D = 2\text{ mm}$  given that  $\epsilon_r \approx 12$  and  $n \approx 3.6$ .
- (b) Consider Figure 6.46 (b) in which a step voltage is applied to an integrated modulator. The effective capacitance between the electrodes is  $C_{\text{eff}} = g L W \epsilon_o \epsilon_r / d$ , where  $g$  is a numerical geometric factor that accounts for the fact that field lines have to bend from one electrode to the other. Consider a  $\text{LiNbO}_3$  crystal based modulator. Take length  $L \approx 10\text{ mm}$ , width  $W \approx 10\text{ }\mu\text{m}$ , electrode separation  $d \approx 10\text{ }\mu\text{m}$ ,  $g \approx 0.6$ ,  $n \approx 2.2$ ,  $\epsilon_r \approx 5$  (high frequency), and calculate  $\tau$  and  $\tau_{\text{light}}$ .

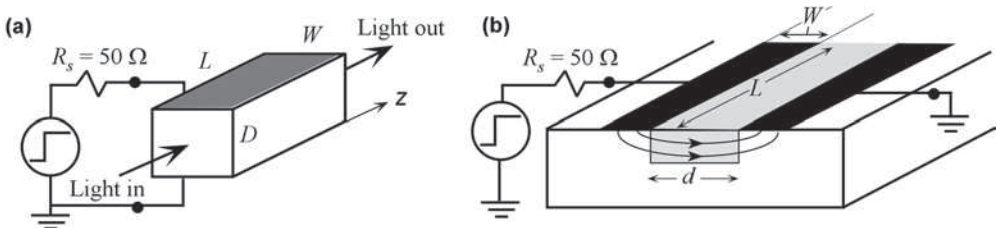


**FIGURE 6.46** (a) A step voltage is suddenly applied to an EO modulator.  $L$  = length,  $W$  = width,  $D$  = thickness or depth. (b) A step voltage is applied to an integrated phase modulator.  $L$  = electrode length,  $W$  = width of electrode,  $d$  = separation of electrodes.



- 6.19 Acousto-optic figure of merit.** Using the values for  $n$ ,  $p$ ,  $\rho$ , and  $v_a$  in Table 6.3, calculate the AO figure of merit for  $\text{LiNbO}_3$  and  $\text{GaP}$ .
- 6.20 Acousto-Optic Modulator** A  $\text{TeO}_2$  crystal is used to generate 220 MHz acoustic waves. The RF transducer has a length ( $L$ ) of 8 mm and a height ( $H$ ) of 8 mm. Calculate the acoustic wavelength, and hence the Bragg deflection angle. What is the Doppler shift in the wavelength? What is the relative intensity in the first order reflected beam for RF acoustic powers 1 W, and 7 W?
- 6.21 Acousto-Optic Modulator Comparison** An AO modulator operating at  $1.55 \mu\text{m}$  can switch the through beam to the deflected beam with 90% efficiency, that is,  $I_1/I_i$  is 90% when we apply an RF voltage to the piezoelectric transducer. Assume that  $L/H$  is roughly 1. Calculate the required acoustic power for an AO modulator using  $\text{TeO}_2$  and a chalcogenide glass based AO modulator using the values in Table 6.3.
- 6.22  $\text{LiNbO}_3$  SAW AO modulator** A SAW AO modulator is shown in Figure 6.36 and operates at a wavelength of  $1.5 \mu\text{m}$ . The interdigital electrodes are driven from a 500 MHz RF source. What should be the periodicity of the interdigital electrodes? What is the deflection angle? If the length  $L$  of the transducer is 5 mm, and the power in the acoustic wave is 200 mW, estimate the diffraction efficiency.
- 6.23 Bragg acousto-optic modulator and diffraction** Consider the acousto-optic modulator in Figure 6.32. We can represent the incident and diffracted optical waves in terms of their wave vectors  $\mathbf{k}$  and  $\mathbf{k}'$ . The incident and the diffracted photons will have energies  $\hbar\omega$  and  $\hbar\omega'$  and momenta  $\hbar\mathbf{k}$  and  $\hbar\mathbf{k}'$ . An acoustic wave consists of **lattice vibrations** (vibrations of the crystal atoms) and these vibrations are quantized just like electromagnetic waves are quantized in terms of photons. A quantum of lattice vibration is called a **phonon**. A traveling lattice wave is essentially a strain wave and can be represented by  $S = S_o \cos(\Omega t - Kx)$  where  $S$  is the instantaneous strain at  $x$ ,  $\Omega$  is the angular acoustic frequency,  $K$  is the wave vector,  $K = 2\pi/\Lambda$ ,  $S_o$  is the amplitude of the strain wave, and  $\Lambda$  is the wavelength of the lattice vibration. A phonon has an energy  $\hbar\Omega$  and a momentum  $\hbar K$ . When an incoming photon is diffracted, it does so by interacting with a phonon; it can absorb or generate a phonon. We can treat the interactions as we do between any two particles; they must obey the conservation of momentum and energy rules:

$$\begin{aligned}\hbar\mathbf{k}' &= \hbar\mathbf{k} \pm \hbar\mathbf{K} \\ \hbar\omega' &= \hbar\omega \pm \hbar\Omega\end{aligned}$$

The positive sign case is illustrated in Figure 6.47 which involves absorbing a phonon. Since the acoustic frequencies are orders of magnitude smaller than optical frequencies ( $\Omega \ll \omega$ ), we can assume that, in magnitude,  $k' \approx k$ . Hence using the above rules, which correspond to Figure 6.47, derive the Bragg diffraction condition.

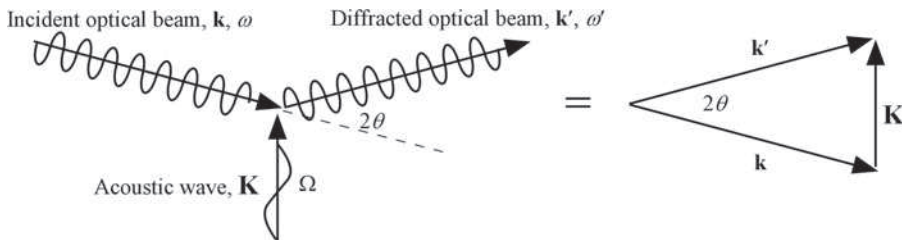


**FIGURE 6.47** Wave vectors for the incident and diffracted optical waves and the acoustic wave.

- 6.24 Faraday effect** Given that glass and  $\text{ZnTe}$  have Verdet constants of about 5 and  $190 \text{ rad T}^{-1} \text{ m}^{-1}$ , respectively, for sodium light having wavelength 593 nm, calculate the necessary magnetic field for a rotation of  $2^\circ$  over a length 20 mm. What is the rotation per unit magnetic field for a medium of length 15 cm?
- 6.25 Faraday effect** Consider a  $\text{ZnTe}$  crystal which rotates the optical field of the 633 nm polarized laser beam from a He-Ne laser. If the crystal length is 2 cm, and the magnetic field is 0.9 T, what is the rotation of the optical field?
- 6.26 Verdet constant** Silica-germania ( $\text{SiO}_2\text{-}13.5\%\text{GeO}_2$ ) glass has a refractive index of 1.4698 at 800 nm. The group index  $N_g$  at this wavelength is 1.4890. What is its Verdet constant?
- 6.27 Magneto-optic modulator and isolator**
- Sketch schematically how you would construct a light intensity modulator using the Faraday effect. What would be its advantages and disadvantages?
  - Sketch schematically how you would construct an optical isolator, using a Faraday rotator and two polarizers, that allows light to travel in one direction but not in the opposite direction.

- 6.28 SHG** The mismatch between  $k_2$  for the second harmonic wave vector and  $k_1$  for the fundamental wave is defined by  $\Delta k = k_2 - 2k_1$ . Perfect match means  $k_2 = 2k_1$  and  $\Delta k = 0$ . When  $\Delta k \neq 0$ , then the coherence length  $l_c$  is given by  $l_c = \pi/(\Delta k)$ . Show that

$$l_c = \frac{\lambda}{4(n_2 - n_1)}$$

where  $\lambda$  is the free-space wavelength of the fundamental wave. Suppose that a light with wavelength 1000 nm is passed through a KDP crystal along its optic axis. Given that  $n_o = 1.509$  at  $\lambda = 1000$  nm and  $n_o = 1.530$  nm at  $2\lambda$ , what is the coherence length  $l_c$ ? Find the percentage difference between  $n_2$  and  $n_1$  for a coherence length of 2 mm.

- 6.29 Optical Kerr effect** Consider a material in which the polarization does not have the second-order term:

$$P = \epsilon_o \chi_1 E + \epsilon_o \chi_3 E^3 \quad \text{or} \quad P/(\epsilon_o E) = \chi_1 + \chi_3 E^2$$

The first term with the electric susceptibility  $\chi_1$  corresponds to the relative permittivity  $\epsilon_r$  and hence to the refractive index  $n_o$  of the medium in the absence of the third-order term, *i.e.*, under low fields. The  $E^2$  term represents the irradiance  $I$  of the beam. Thus, the refractive index depends on the intensity of the light beam, a phenomenon called the optical Kerr effect:

$$n = n_o + n_2 I \quad \text{and} \quad n_2 = \frac{3\eta\chi_3}{4n_o^2}$$

where  $\eta = (\mu_o/\epsilon_o)^{1/2} = 120\pi = 37 \Omega$ , is the impedance of free space.

- (a) Typically, for many glasses,  $\chi_3 \approx 10^{-21} \text{ m}^2 \text{ W}^{-1}$ ; for many doped glasses,  $\chi_3 \approx 10^{-18} \text{ m}^2 \text{ W}^{-1}$ ; for many organic substances,  $\chi_3 \approx 10^{-17} \text{ m}^2 \text{ W}^{-1}$ ; for semiconductors,  $\chi_3 \approx 10^{-14} \text{ m}^2 \text{ W}^{-1}$ . Calculate  $n_2$  and the intensity of light needed to change  $n$  by  $10^{-3}$  for each case.
- (b) The phase  $\phi$  at a point  $z$  is given by

$$\phi = \omega_o t - \frac{2\pi n}{\lambda} z = \omega_o t - \frac{2\pi(n_o + n_2 I)}{\lambda} z$$

It is clear that the phase depends on the light intensity  $I$  and the change in the phase along  $\Delta z$  due to light intensity alone is

$$\Delta\phi = \frac{2\pi n_2 I}{\lambda} \Delta z$$

As the light intensity modulates the phase of the wave, this is called **self-phase modulation**. Obviously light is controlling light. When the light intensity is small  $n_2 I \ll n_o$ , the instantaneous frequency

$$\omega = \partial\phi/\partial t = \omega_o$$

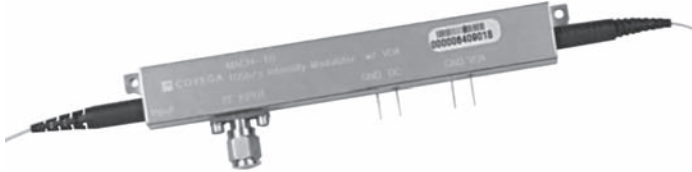
Suppose we have an intense beam and the intensity  $I$  is time dependent,  $I = I(t)$ . Consider a pulse of light traveling along the  $z$ -direction and the light intensity vs.  $t$  shape is a “Gaussian” (this is approximately so when a light pulse propagates in an optical fiber, for example). Find the instantaneous frequency  $\omega$ . Is this still  $\omega_o$ ? How does the frequency change with “time,” or across the light pulse? The change in the frequency over the pulse is called **chirping**. Self-phase modulation therefore changes the frequency spectrum of the light pulse during propagation. What is the significance of this result?

- (c) Consider a Gaussian beam in which the intensity across the beam cross-section falls with radial distance in a Gaussian fashion. Suppose that the beam is made to pass through a plate of nonlinear medium. Explain how the beam can become **self-focused**. Can you envisage a situation where diffraction effects trying to impose divergence are just balanced by self-focusing effects?

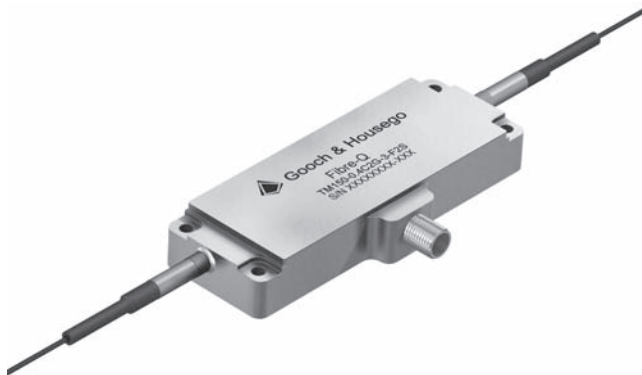
- 6.30. Jones vector** Consider a light wave that has the Jones vector  $\mathbf{J}_{\text{in}}$ , and is put through an optical modulation that has a transfer matrix  $\mathbf{T}$ ,

$$\mathbf{J}_{\text{in}} = \begin{bmatrix} 0 \\ 1 \end{bmatrix} \quad \text{and} \quad \mathbf{T} = \begin{bmatrix} j & 0 \\ 0 & 1 \end{bmatrix}$$

What do these represent, and what is the output Jones vector  $\mathbf{J}_{\text{out}}$ ? If we take the output and put it through another optical modulation that has the same transmission matrix, what is the output Jones vector?



Twenty GHz analog Mach-Zehnder intensity modulator for use at 1550 nm, with half-wave voltage of 3.5 V. The modulator uses titanium-diffused Z-cut LiNbO<sub>3</sub>. (Courtesy of Thorlabs.)



Fiber-coupled acousto-optic modulator. (Courtesy of Gooch & Housego.)

# APPENDIX A

## Gaussian Distribution

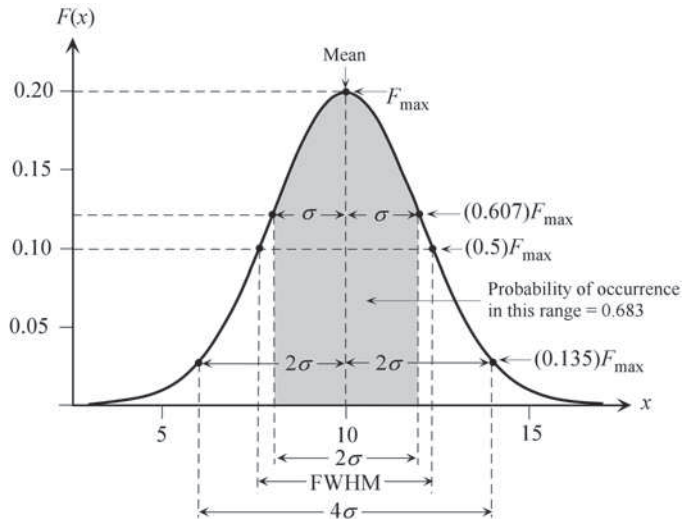
The **Gaussian distribution** refers to the *normal distribution* found in statistics; that is, it is a particular probability density function, denoted  $F(x)$ , of a variable  $x$  such that  $F(x)$  is continuous and has a symmetrical shape about a mean value  $\bar{x}$  with the functional form given by

$$F(x) = \frac{1}{\sigma\sqrt{2\pi}} \exp\left[-\frac{(x - \bar{x})^2}{2\sigma^2}\right]$$

in which  $\sigma^2$  is the **variance**, *i.e.*, the mean value of  $(x - \bar{x})^2$  found by integrating  $(x - \bar{x})^2 F(x)$  over all  $x$  (from  $-\infty$  to  $+\infty$ );  $\sigma$  is the **standard deviation**.  $F(x)$  is called the **Gaussian function**. The integral of  $F(x)$  over all  $x$  is unity, *i.e.*,  $\int F(x) dx = 1$ . Suppose that we observe a property  $x$  of a process or a phenomenon that has a Gaussian probability density function, then we can find the total probability  $\Delta P$  of the occurrence of  $x$  in an interval  $\Delta x$  from  $x_1$  to  $x_2$  from

$$\Delta P = \int_{x_1}^{x_2} F(x) dx$$

Put differently, the probability  $dP$  of observing  $x$  with a value in  $x$  to  $x + dx$  is  $F(x)dx$ . The Gaussian function is widely used in representing many observable quantities. For example, the output spectrum from gas lasers usually has a Gaussian distribution. The maximum of the Gaussian distribution is  $F_{\max} = F(\bar{x}) = 0.399/\sigma$ . When  $x = \sigma$ , one standard deviation away from the peak,  $F(\sigma) = 0.242/\sigma$ , and  $F(\sigma)/F_{\max} = 0.607$ . In moving  $2\sigma$  from the peak, the Gaussian drops from its maximum by a factor of 0.135. The full width at half maximum, FWHM, is the width  $\Delta x = |x_2 - x_1|$ , where  $F(x_1) = F(x_2) = (1/2)F_{\max}$ , and  $\text{FWHM} = \sigma 2\sqrt{2 \ln(2)} = 2.355\sigma$ , or  $\sigma = 0.425\Delta x$ .



The Gaussian distribution that has  $\bar{x} = 10$  and  $\sigma = 2$ . The shaded area is the integration from  $x = \bar{x} - \sigma$  to  $x = \bar{x} + \sigma$  and has a probability of 0.683.

**Selected Elementary Properties of the Gaussian Distribution**

Mean	$\bar{x}$	Total area	1
Variance	$\sigma^2$	Probability in $\bar{x} \pm \sigma$	0.683
Maximum, $F_{\max}$	$(\sigma\sqrt{2\pi})^{-1}$	Probability in $\bar{x} \pm 2\sigma$	0.955
$F(\sigma)$	$0.607F_{\max}$	FWHM	$\sigma 2\sqrt{2 \ln(2)} = 2.355\sigma$



A UV LED that emits at 315 nm. (Courtesy of Chris Collins.)

# APPENDIX B

## Solid Angles

The **solid angle** is an angle  $\Omega$  in three dimensions that an area  $S$  on a sphere subtends at the center of the sphere whose magnitude is given by  $\Omega = S/r^2$ , as illustrated in Figure B.1. More rigorously, the solid angle is defined in terms of an **element of solid angle**  $d\Omega$ , defined by

$$d\Omega = \frac{dS}{r^2}$$

where  $dS$  is the elemental area on a sphere of radius  $r$  as shown in Figure B.2 (a). The units for the solid angle are **steradians**, abbreviated to sr. Steradians are essentially *square radians*. The solid angle is a dimensionless quantity.

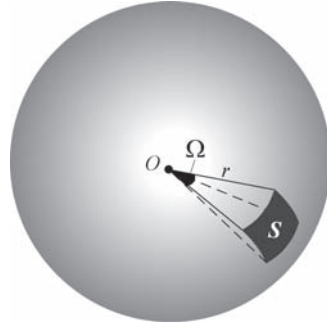


**FIGURE B.1** The definition of the solid angle  $\Omega$  in terms of the area  $S$  on a sphere of radius  $r$ .

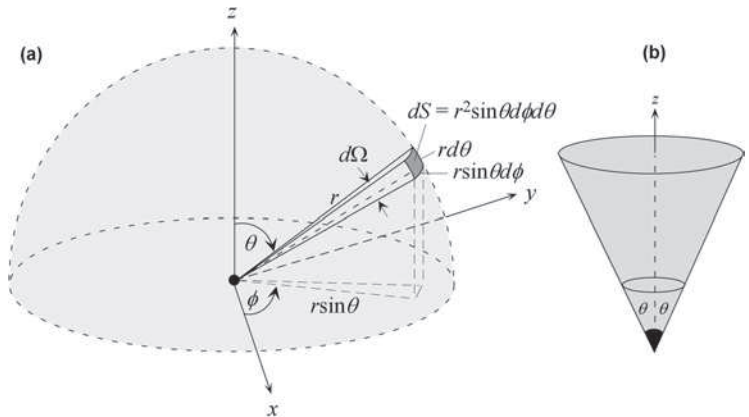


**FIGURE B.2** (a) The definition of the elemental solid angle  $d\Omega$  in terms of spherical coordinates  $r$ ,  $\theta$ , and  $\phi$ . (b) The solid angle of a cone with an apex angle  $2\theta$ .

It is useful to express the differential solid angle  $d\Omega$  in spherical coordinates. The area  $dS = r^2 \sin\theta d\phi d\theta$  so that

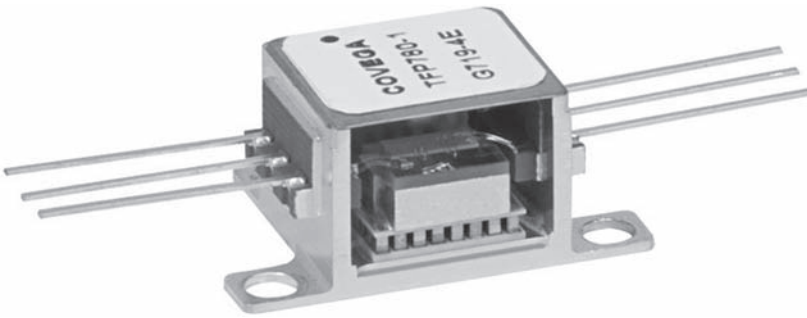
$$d\Omega = \sin\theta d\phi d\theta$$

For a whole sphere,  $S = 4\pi r^2$  so that  $\Omega = 4\pi$  sr, and for a hemisphere  $\Omega$  is  $2\pi$  sr. The surface area  $S$  for 1 sr is about 8% of the total spherical surface area.

The solid angle that corresponds to a cone of apex angle  $2\theta$  is of particular importance, especially when LED emission distribution is considered as in Figure B.2 (b). In this case, light is emitted from a point into a cone centered around the  $z$ -axis, and the angle between the  $z$ -axis and the side of the cone is  $\theta$ . Integrating  $d\Omega$  above, we find

$$\Omega = \int_0^{2\pi} \int_0^\theta \sin\theta d\phi d\theta = 2\pi(1 - \cos\theta) \approx \pi\theta^2$$

where the approximate sign is for small angles only ( $\theta$  in radians). A cone of apex angle  $2\theta$  subtends a solid angle  $\Omega$  given by the above expression. Thus, 1 sr is equivalent to an apex angle of  $65.5^\circ$ . The definitions of many radiometric and photometric quantities involve a solid angle.



Covega Fabry-Perot semiconductor optical gain chip for use in external cavity tunable diode laser applications in the 750–790 nm range. The package has a thermoelectric (TE) cooler and a thermistor for temperature control of the chip. (Courtesy of Thorlabs.)



# APPENDIX C

## Basic Radiometry and Photometry

The science of radiation measurement—for example, the measurement of emitted, absorbed, reflected, and transmitted radiation energy—is called **radiometry**; radiation is understood to mean electromagnetic energy in the optical frequency range (ultraviolet, visible, and infrared). **Photometry**, on the other hand, is a subset of radiometry in which radiation is measured with respect to the spectral responsivity of the eye, that is, over the visible spectrum and by taking into account the spectral visual sensitivity of the eye under normal light-adapted conditions, *i.e.*, *photopic* conditions.

The **flux** ( $\Phi$ ) in radiometry has three related definitions—**radiant**, **luminous**, and **photon flux**—which correspond to the rate of flow of radiation energy, perceptible visual energy, and photons. (Notice that, in radiometry, these fluxes are not defined in terms of flow *per unit area*.) For example, **radiant flux** is the energy flow per unit time in the units of Watts. Radiometric quantities, such as radiant flux,  $\Phi_e$  (radiant energy flow per unit time), usually have a subscript *e*, and invariably involve energy or power. Radiometric *spectral* quantities, such as **spectral radiant flux**  $\Phi_\lambda$ , refer to the radiometric quantity per unit wavelength, *i.e.*,  $\Phi_\lambda = d\Phi_e/d\lambda$  is the radiant flux per unit wavelength.

The radiant flux  $\Phi_e$  is simply referred to as the **optical power**  $P_o$  in many textbooks on optoelectronics due to the common use of *P* in representing power.

The **luminous flux** or **photometric flux**  $\Phi_v$ , is the visual “brightness” of a source as observed by an average daylight-adapted eye, and is proportional to the radiant flux (radiation power emitted) of the source and the efficiency of the eye in detecting the spectrum of the emitted radiation.<sup>1</sup> While the eye can see a red color source, it cannot see an infrared source and the luminous flux of the infrared source would be zero. Similarly, the eye is less efficient in the violet than in the green region, and less radiant flux is needed to have a green source at the same luminous flux as the violet source. Luminous flux  $\Phi_v$  is measured in **lumens** (lm) (also defined in Chapter 3), and at a particular wavelength it is given by

Luminous  
flux

$$\Phi_v = \Phi_e \times K \times V(\lambda) \quad (\text{C.1.1})$$

where  $\Phi_e$  is the radiant flux (in watts), *K* is a conversion constant (standardized to be 683 lm W<sup>-1</sup>), and *V*( $\lambda$ ) is the **luminous efficiency** (sometimes also called the *luminous efficacy*) of the daylight-adapted eye, which is unity at 555 nm. The luminous efficiency of the eye is written as *V*( $\lambda$ ) to highlight its dependence on the wavelength. *V*( $\lambda$ ) is also called the **visibility function**. The dependence of *V*( $\lambda$ ) on  $\lambda$  is shown in Figure 3.41.

By definition, a 1 W light source emitting at 555 nm (amber green, where *V* = 1) emits a luminous flux of 683 lm. The same 1 W light source at 650 nm (red), where *V* = 0.11, emits only 70 lm. When we buy a light bulb, we are essentially paying for lumens because it is luminous flux that the eye perceives. A typical 100 W incandescent lamp provides roughly 1700 lm. Fluorescent tubes provide more luminous flux output than incandescent lamps for the same electrical power input as they have more spectral emission in the visible region and make better use of the eye’s spectral sensitivity.

<sup>1</sup>The subscript *v* represents *visible*.

The **radiant intensity** is the radiant flux (radiant energy flowing per unit time) per unit solid angle; it is a radiometric quantity with the units of  $\text{W sr}^{-1}$ . It is a particularly useful quantity for point sources. If  $d\Phi_e$  is the radiant flux within a solid angle  $d\Omega$  in a particular direction  $\theta, \phi$ , with respect to spherical coordinates placed at the source, as in Figure C.1 (a), then

$$I_e = \frac{d\Phi_e}{d\Omega} = r^2 \frac{d\Phi_e}{dS} \quad (\text{C.1.2}) \quad \text{Radiant intensity}$$

The **luminous intensity** is the luminous flux per unit solid angle along a particular direction, and measures the visual **brightness** of radiation as observed by a daylight-adapted eye within a unit solid angle. If  $d\Phi_v$  is the luminous flux within a solid angle  $d\Omega$  for a direction  $\theta, \phi$ , as in Figure C.1 (a), then luminous intensity is defined as

$$I_v = \frac{d\Phi_v}{d\Omega} = r^2 \frac{d\Phi_v}{dS} \quad (\text{C.1.3}) \quad \text{Luminous intensity}$$

The units for the luminous intensity are lumens per steradian or **candela** (cd). Both the radiant and luminous intensity,  $I_e$  and  $I_v$ , usually depend on the angles  $\theta$  and  $\phi$ . Suppose that a source emits over  $4\pi$  steradians and emits equally in all directions. This would be a point source. If the source has a luminous flux of 1 lm, then its luminous intensity is  $1/(4\pi)$  cd. A **1 candela** point source emits  $4\pi$  lumens into space in all directions. It is important to note that the candela is a visual photometric unit (an SI unit) for measuring the light intensity of a source which emits a luminous flux of 1 lm in a particular direction within one unit of solid angle, *i.e.*,  $1 \text{ cd} = 1 \text{ lm sr}^{-1}$ , at a reference frequency  $\nu = 540 \times 10^{12} \text{ Hz}$  ( $\lambda \approx 555 \text{ nm}$ ).<sup>2</sup> Thus,

$$1 \text{ cd} = \left( \frac{1}{683} \right) \text{W sr}^{-1} \quad (\text{C.1.4}) \quad \text{One candela}$$

Conventionally, the intensity is plotted on a polar plot, as illustrated in Figure C.1 (b). A point on this plot has an angle  $\theta$  with respect to  $z$ , which is usually taken along the maximum intensity. The distance from the origin is either  $I_v$  or proportional to  $I_v$ . Such polar plots represent

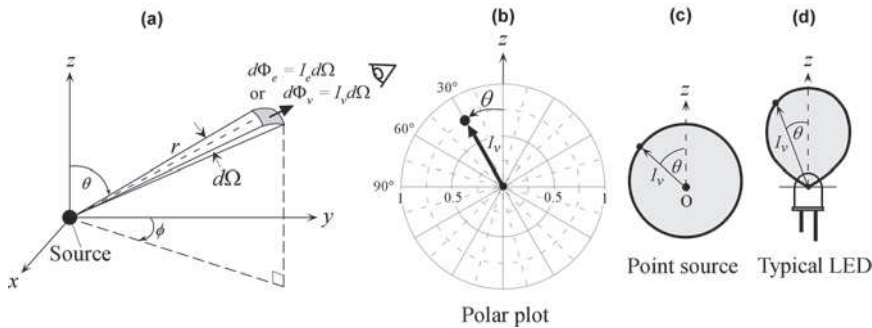


**FIGURE C.1** (a) Radiant or luminous flux that is within an elemental solid angle  $d\Omega$  and the definition of radiant or luminous intensity. (b) Representation of luminous intensity in polar coordinates. The point shown has a luminous intensity of 0.75 cd at an angle of  $30^\circ$  to  $z$ . (c) Isotropic emitter. (d) Typical angular dependence of luminous intensity from a single LED.

<sup>2</sup>Definition by the 16th Conférence Générale des Poids et Mesures—General Conference on Weights and Measures, 1979.

the angular distribution of intensity from a source. For a **point source**,  $I_v(\theta)$  is a circle, as illustrated in Figure C.1 (c), that is  $I_v(\theta) = \text{constant}$ . An isotropic source emits luminous intensity that is the same in all directions as mentioned above. For a **Lambertian source**, the intensity depends on  $\theta$  as

Lambertian  
source

$$I_v(\theta) = I_v(0)\cos\theta \quad (\text{C.1.5})$$

For an exponential intensity source,  $I_v$  falls exponentially (very rapidly) with  $\theta$ , and can be approximated by using

$$I_v(\theta) = I_v(0)(\cos\theta)^n$$

where  $n$  is usually greater than unity. If  $I_v(\theta) = I_v(0)(1/2)$  when  $\theta = \theta_{1/2}$ , then  $n = \ln(0.5)/\ln[\cos(\theta_{1/2})]$ . Figure C.1 (d) shows a typical example on the angular dependence of the luminous intensity from a single LED device.

The radiant intensity can also be a function of wavelength but, in this case, we must use spectral radiant intensity to represent the distribution of intensity over wavelengths. The **spectral radiant intensity**  $I_{e\lambda}$  is defined by

Spectral  
radiant  
intensity

$$I_{e\lambda} = \frac{dI_e}{d\lambda} \quad (\text{C.1.6})$$

Similarly, the **spectral luminous intensity**  $I_{v\lambda}$  is defined by

Spectral  
luminous  
intensity

$$I_{v\lambda} = \frac{dI_v}{d\lambda} \quad (\text{C.1.7})$$

Clearly, if we integrate the spectral intensity  $I_{e\lambda}$  (or  $I_{v\lambda}$ ) over all wavelengths, we would get the total intensity  $I_e$  (or  $I_v$ ), which is sometimes called the integrated intensity. An integration of spectral intensity over a limited wavelength range  $\Delta\lambda$  would, of course, only give the total intensity within  $\Delta\lambda$ .



Piezoelectric transducer controlled Fabry-Perot etalons. Left has a 70 mm and the right has a 50 mm clear aperture. The piezoelectric controller maintains the reflecting plates parallel while the cavity separation is scanned. (The left etalon has a reflection of interference fringes on its surface plate that are actually on the adjacent computer display; not shown.) (Courtesy of IC Optical Systems Ltd.)

# APPENDIX D

## Useful Mathematical Formulae

### QUADRATIC EQUATION

$$ax^2 + bx + c = 0$$

$$x = \frac{-b \pm \sqrt{b^2 - 4ac}}{2a}$$

### COMPLEX NUMBERS

$$j = (-1)^{1/2}$$

$$\exp(j\theta) = \cos \theta + j \sin \theta$$

$$Z = a + jb = re^{j\theta}$$

$$Z^* = a - jb = re^{-j\theta}$$

$$\text{Magnitude}^2 = |Z|^2 = ZZ^* = a^2 + b^2$$

$$\cos \theta = \frac{1}{2}[e^{j\theta} + e^{-j\theta}]$$

$$j^2 = -1$$

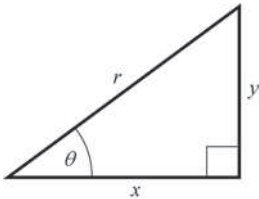
$$r = (a^2 + b^2)^{1/2} \quad \tan \theta = b/a$$

$$\text{Re}(Z) = a \quad \text{Im}(Z) = b$$

$$\text{Argument} = \theta = \arctan(b/a)$$

$$\sin \theta = \frac{1}{2j}[e^{j\theta} - e^{-j\theta}]$$

### TRIGONOMETRY



$$\sin \theta = y/r$$

$$\cos \theta = x/r$$

$$\tan \theta = y/x = \sin \theta / \cos \theta$$

$$r^2 = x^2 + y^2$$

$$\sin(\pi/2 \pm \theta) = \cos \theta$$

$$\sin 2\theta = 2 \sin \theta \cos \theta$$

$$\sin(A + B) = \sin A \cos B + \cos A \sin B$$

$$\sin A + \sin B = 2 \sin\left[\frac{1}{2}(A + B)\right] \cos\left[\frac{1}{2}(A - B)\right]$$

$$\sin^2 \theta + \cos^2 \theta = 1$$

$$\cos 2\theta = 1 - 2 \sin^2 \theta = 2 \cos^2 \theta - 1$$

$$\cos(A + B) = \cos A \cos B - \sin A \sin B$$

$$\cos A + \cos B = 2 \cos\left[\frac{1}{2}(A + B)\right] \cos\left[\frac{1}{2}(A - B)\right]$$

### EXPANSIONS

$$e^x = 1 + x + \frac{1}{2!}x^2 + \frac{1}{3!}x^3 + \dots$$

$$(1 + x)^n = 1 + nx + \frac{n(n-1)}{2!}x^2 + \frac{n(n-1)(n-2)}{3!}x^3 + \dots$$

$$f(x_o + \Delta x) = f(x_o) + \Delta x \left[ \frac{df}{dx} \right]_{x_o} + \frac{(\Delta x)^2}{2} \left[ \frac{d^2f}{dx^2} \right]_{x_o} + \dots$$

Small  $x$        $(1 + x)^n \approx 1 + nx$        $\sin x \approx x$        $\tan x \approx x$        $\cos x \approx 1$

Small  $\Delta x$  in  $x = x_o + \Delta x$ ,       $f(x) \approx f(x_o) + \Delta x \left[ \frac{df}{dx} \right]_{x_o}$

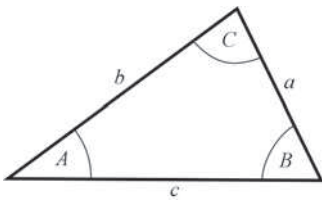
## GEOMETRY

Area of a circle =  $\pi r^2$

Circumference of a circle =  $2\pi r$

Surface area of a sphere =  $4\pi r^2$

Volume of a sphere =  $(4/3)\pi r^3$



$$a^2 = b^2 + c^2 - 2bc \cos A$$

$$\frac{a}{\sin A} = \frac{b}{\sin B} = \frac{c}{\sin C}$$

## USEFUL RELATIONSHIPS

$\ln x = 2.303 \log x$

$\log x = 0.434 \ln x$

$a^x = e^{(\ln a)x}$

## HYPERBOLIC FUNCTIONS

$\sinh x = (e^x - e^{-x})/2$

$\cosh x = (e^x + e^{-x})/2$

$\tanh x = (e^x - e^{-x})/(e^x + e^{-x})$

$\tanh x = \sinh x / \cosh x$